A MICROSCOPIC ANALYSIS OF THE PLUMULACEOUS FEATHER CHARACTERISTICS OF ACCIPITRIFORMES WITH EXPLORATION OF SPECTROPHOTOMETRY TO SUPPLEMENT FEATHER IDENTIFICATION

by

Charles Coddington

A Thesis
Submitted to the
Graduate Faculty
of
George Mason University
in Partial Fulfillment of
The Requirements for the Degree
of
Master of Science
Biology

Committee:

_____	Dr. Larry Rockwood, Thesis Director
_____	Dr. David Luther, Committee Member
_____	Dr. Carla J. Dove, Committee Member
_____	Dr. Ancha Baranova, Committee Member
_____	Dr. Iosif Vaisman, Director, School of Systems Biology
_____	Dr. Donna Fox, Associate Dean, Office of Student Affairs & Special Programs, College of Science
_____	Dr. Peggy Agouris, Dean, College of Science
Date: _____	Summer Semester 2018 George Mason University Fairfax, VA

A Microscopic Analysis of the Plumulaceous Feather Characteristics of Accipitriformes with Exploration of Spectrophotometry to Supplement Feather Identification

A Thesis submitted in partial fulfillment of the requirements for the degree of Master of Science at George Mason University

by

Charles Coddington
Bachelor of Arts
Connecticut College 2013

Director: Larry Rockwood, Professor/Chair
Department of Biology

Summer Semester 2019
George Mason University
Fairfax, VA

Copyright 2018 Charles Coddington
All Rights Reserved

DEDICATION

This thesis is dedicated to Carla Dove, Marcy Heacker-Skeans, James Whatton, and Nor Faridah Dahlan of the Feather Identification Lab, Smithsonian Institution, National Museum of Natural History. Their continued mentorship, patience, and support fueled my inspiration for this thesis.

.

ACKNOWLEDGEMENTS

This study was conducted at the Smithsonian Institution (SI), National Museum of Natural History (USNM), Division of Birds, Washington D.C. I would like to thank the following Smithsonian staff: Dr. Gary Graves, Curator, Division of Birds, for his advice on experimental design and statistical analysis. Dr. Sarah Luttrell, Research Assistant, Feather Identification Lab, for her advice on spectrophotometry experimental design and statistical analysis. Marcy Heacker-Skeans, James Whatton, Nor Faridah Dahlan, Research Assistants, Feather Identification Lab, for their comments on the manuscript and figures. Chris Milensky, Collections Manager, Division of Birds, for his advice on sampling technique and access to research collections. Dr. Jonathan Coddington, Director Global Genome Initiative, for his comments on the manuscript. Committee members Dr. Larry Rockwood, George Mason University and Dr. Ancha Baranova, George Mason University for their time and consideration. Jonathan Clark, Graduate Student, George Mason University, for his assistance with statistical coding. Thanks to George Mason University for providing funding for my degree through a Graduate Teaching Assistantship.

Special acknowledgement and gratitude goes to Dr. Carla Dove, Program Director, Feather Identification Laboratory, and Dr. David Luther, George Mason University for all their patience, advice and support during this project.

TABLE OF CONTENTS

LIST OF TABLES

LIST OF FIGURES

LIST OF ABBREVIATIONS AND SYMBOLS

Mean ..... $\bar{x}$
Standard Deviation..... σ
Range ..... R
Coefficient of Variation CV
Analysis of Variance..... ANOVA
Subpennaceous Length ..... SPL
Barbule Length (Base) ..... BLB
Basal Cell (Base)..... BCB
Basal Internodal Distance (Base)..... BIDB
Basal Internodal Distance (Mid)..... BIDM
Basal Internodal Distance (Distal)..... BIDD
Nodal Abundance (Base) ..... NAB
Basal Nodal Width (Base) ..... BNWB
Basal Nodal Width (Mid)..... BNWM
Basal Nodal Width (Distal)..... BNWD
Barbule Length (Mid) ..... BLM
Basal Cell (Mid)..... BCM
Mid Internodal Distance (Base)..... MIDB
Mid Internodal Distance (Mid) ..... MIDM
Mid Internodal Distance (Distal) ..... MIDD
Nodal Abundance (Mid) ..... NAM
Mid Nodal Width (Base)..... MNWB
Mid Nodal Width (Mid)..... MNWM
Mid Nodal Width (Distal)..... MNWD
Barbule Length (Distal) ..... BLD
Basal Cell (Distal)..... BCD
Distal Internodal Distance (Base) ..... DIDB
Distal Internodal Distance (Mid) ..... DIDM
Distal Internodal Distance (Distal) ..... DIDD
Nodal Abundance (Distal) ..... NAD
Distal Nodal Width (Base)..... DNWB
Distal Nodal Width (Mid)..... DNWM
Distal Nodal Width (Distal)..... DNWD
Average Number of Nodes/Barbule..... NA/BL
Turkey Vulture (*Cathartes aura*)..... TUVU
Black Vulture (*Coragyps atratus*) ..... BLVU

Western Osprey (*Pandion haliaetus*).....OSPR
Red-tailed Hawk (*Buteo jamaicensis*) .....RTHA
Swainson's Hawk (*Buteo swainsoni*).....SWHA
Cooper's Hawk (*Accipiter cooperii*)..... COHA
Sharp-shinned Hawk (*Accipiter striatus*)..... SSHA
Common Black-Hawk (*Buteogallus anthracinus*)..... CBHA
Harris's Hawk (*Parabuteo unicinctus*) .....HRSH
Northern Harrier (*Circus cyaneus*) .....NOHA
Bald Eagle (*Haliaeetus leucocephalus*) .....BAEA
Golden Eagle (*Aquila chrysaetos*) ..... GOEA
Mississippi Kite (*Ictinia mississippiensis*)..... MIKI
Swallow-tailed Kite (*Elanoides forficatus*) .....STKI
White-tailed Kite (*Elanus leucurus*) .....WTKI
Snail Kite (*Rostrhamus sociabilis*) ..... SNKI
Peregrine Falcon (*Falco peregrinus*).....PEFA
American Kestrel (*Falco sparverius*) .....AMKE
Crested Caracara (*Caracara cheriway*) .....CRCA
Monk Parakeet (*Myopsitta monachus*) .....MOPA
Dark Primary Feathers ..... PD
Light Primary Feathers .....PL
Dark Secondary Feathers ..... SD
Light Secondary Feathers .....SL

ABSTRACT

A MICROSCOPIC ANALYSIS OF THE PLUMULACEOUS FEATHER CHARACTERISTICS OF ACCIPITRIFORMES WITH EXPLORATION OF SPECTROPHOTOMETRY TO SUPPLEMENT FEATHER IDENTIFICATION

Charles Coddington M.S.

George Mason University, 2019

Thesis Director: Dr. Larry Rockwood

Microscopic feather structures can reveal conserved traits that may be used to identify taxonomic groups of birds based on mere fragments of feathers. Analyzing microscopic feather structure has many practical applications including: criminal investigations, food contamination cases, anthropological artifact analysis, prey remains analysis, and identification of bird species involved in aircraft collisions. This thesis research investigates specialized microscopic feather identification techniques by surveying pigmentation patterns and intensity, basic morphology, spinal distribution, and by using statistical analysis and spectrophotometry to examine the variation within feather characters of Accipitriformes representing 16 species from 3 different taxonomic families (Cathartidae, Accipitridae, Pandionidae) that occur in the United States. Further, feather micro-structure of some Falconiformes (Falconidae) were compared with Psittacidae (parrots) to test recent hypotheses of the evolutionary relationships of these groups.

Significant differences were found among some microscopic characters of the avian families Cathartidae, Accipitridae and, Pandionidae. Falconidae and Psittacidae are visually more similar to each other than to any Accipitriformes based on pigmentation patterns and plumulaceous feather structure. Differences were discovered between family, and genera in pigmentation pattern and spine distribution along the downy barbules of vultures, eagles, kites, *Accipiter* hawks and *Buteo* hawks. Significant differences in quantitative and qualitative feather characters between species within the same genera were seldom observed.

Spectrophotometry was investigated as a potential new method of identifying fragmentary feathers of species by generating quantitative measurements of the color of the primary and secondary feathers of select species. Significant differences in spectrophotometry reflectance peaks were found between species pairs that had visually distinguishable coloration, but species that had similar coloration showed no significant differences suggesting that spectrophotometry may not be an effective method for melanin-based feather fragment analysis in the species studied here.

The results of this study indicate that microscopic plumulaceous feather characters of Accipitriformes contain quantifiable, and basic morphological differences that may aid in separation of distinct groups based on micromorphology if similar feather types and feather barbs are compared. Additionally, feather characters studied here support recent taxonomic organization of previously unrelated taxa such as falcons and parrots. This study of plumulaceous microstructure of Accipitriformes and Falconiformes enhances our knowledge of these biological structures and provides additional justification that feather

microstructure is indeed useful for the practical applications of forensic feather identification and for taxonomic studies.

CHAPTER ONE - MICROSTRUCTURE

Introduction

The taxonomic significance of microscopic feather structures has been a subject of scientific importance since Chandler's (1916) pioneering research, in which he observed differences in plumulaceous or downy barbules and suggested that these microscopic structures could be used for taxonomic identifications. The combination of Chandler's research along with other major works (Lucas and Stettenheim 1972; Brom 1991; Dove 2000) have demonstrated that both microscopic and macroscopic feather structures can be utilized to aid in the identification of fragmentary feather remains. Using macroscopic and microscopic feather characters to identify species of birds has many applications including: criminal investigations (Davies 1970; Trail 2003; Dove and Koch 2011), food contamination cases (Olsen 1981), anthropological artifact analyses (Messinger 1965; Dove and Peurach 2002; Robertson 2002; Rogers et al. 2002; Dove et al. 2005; Dove and Wickler 2016), ecological studies of prey remains identification (Day 1966; Gilbert and Nancekivell 1982; Griffin et al. 1982; Ward and Laybourne 1985; Boonseub et al. 2012; Dove and Coddington 2015), invasive species impact analysis (Dove et al. 2011), and the identification of fossilized feathers in amber (Laybourne et al. 1994; Thomas et al 2014). Birdstrike (bird/aircraft collisions) identification is he application of this technique that is currently in most demand (Manville 1963; Laybourne 1974; Brom 1991; Dove 2000).

While it is clear that there are many useful applications to this field of research, we are just beginning to describe the morphological differences at various taxonomic levels

within Aves. Dove and Agreda (2007) investigated the differences in plumulaceous microstructure between dabbling (*Anatinae sp.*) and diving ducks (*Aythyini sp.*; *Mergini sp.*) and found differences in nodal size and distribution along barbules. These findings suggest that taxonomic identifications are possible at sub-familial taxonomic levels. Few thorough investigations into differences in feather microstructures have been conducted, and only Charadriiformes (Dove 1997, Dove 2000) and Anseriformes (Heacker-Skeans 2002) have generated quantitative data to distinguish higher level taxonomic differences.

Accipitriformes (hawks, eagles, kites, and vultures) are of significant interest for further study as they are often involved in aircraft collisions and are responsible for over $30,000 in damage per strike (Dolbeer et al. 2016; United States Air Force 2015). There is a large amount of overlap in observations of microscopic feather characters of Accipitriformes species, and accurate identification at the family or generic level is often challenging but important to several areas of study. It is important to accurately identify this group of birds when involved in birdstrikes to properly implement effective wildlife management strategies on airfields to reduce risks and lower damaging costs. Feathers from this order of birds are frequently used in anthropological artifacts and the accurate identification is of importance to cultural and Native American studies (De Meo 1994). Accipitriform feathers are also among the most popular items found in illegally imported tourist trade items (Trail 2003; Sweeney 2016). Providing a detailed descriptive and quantitative analysis of the ultra-structure within these orders further validates microscopic analysis for the practical applications and may initiate future interest in these characters for taxonomic studies. This study describes the general feather microstructure characteristics

of a subset of Accipitriformes that occur in the United States and seeks to determine if feather microstructure alone can be used to distinguish lower taxonomic groups within this order.

Materials and Methods

Accipitriformes in the United States comprise a subset of 28 species within 3 families (Sibley 2014). For this study of feather microstructure, phylogenetic organization follows Jarvis et al. (2014) and includes Accipitridae, Pandionidae, and Cathartidae as families of Accipitriformes. Traditional phylogenies have included Falconidae within Accipitriformes but recent revisions based on genomic sequencing (Hackett et al. 2008; Jarvis et al. 2014; Prum et al. 2015), elevate Falconidae to ordinal status (Falconiformes) and document a close relationship to parrots (Psittaciformes) which were formally considered distant relatives of Accipitriformes.

Because previous phylogenetic analyses of feather microstructure have shown that species level differentiation is unlikely using microstructure alone (Dove 1997, Dove 2000, Heacker-Skeans 2002), two species within representative accipitriform genera (*Buteo* and *Accipiter*) that occur in the United States were selected for this study. Falconidae and Psittacidae are included in this study to investigate feather characters in these recently determined related families (Hackett et al. 2008; Jarvis et al. 2014; Prum et al. 2015).

Sampling and Microslide Preparation

Feather barbs were sampled from museum study skins at The National Museum of Natural History, Smithsonian Institution (USNM), Washington, D.C. Barbs were sampled from vouchered study skins collected within similar geographic regions and during the same calendar season. An effort was made to sample only male individuals to ensure

consistency but due to specimen availability constraints, females were sampled if insufficient male specimens were available. To minimize destructive sampling damage to museum specimens, plumulaceous barbs (Figure 1) were removed from the right vane of a single attached feather at 4 separate sections (Figure 2) of upper-left breast feathers (pectoral tract) from three individual specimens for each species studied within Accipitriformes, Falconiformes and Psittaciformes (Appendix 1). Destructive sampling labels including researcher name and institution, were attached to all museum specimens sampled for this study.

Microslides were prepared following Laybourne and Dove (1994) using two to three drops of xylenes ($C_6H_4(CH_3)_2$) on pre-cleaned microslides (75 x 25 mm) to facilitate barb arrangement and allow barbules to separate for easier visual study. For this study, barbs were placed on the microslide in pairs with the basal-most barb positioned on the top portion of the slide. After the xylenes evaporated the barbs were firmly attached and permanent microslides were created using three to four drops of Flo-Tex® (Lerner Laboratories, Thermo Fisher Scientific, Waltham, MA, USA) and mounted with coverslips (25 x 50 mm). Each microslide was labeled with the species name, catalogue number, and the plumulaceous region from where the barb originated (i.e. basal, basal-mid, mid-distal, distal; Figure 2). Microslides dried for a minimum of 24 hours before examination. The permanent microslides are stored in the reference slide collection in the Feather Identification Lab, USNM.

Quantitative Analysis

Microslides were studied using a Leica© DM750 (Leica Microsystems, Wetzlar, Germany) comparison light microscope provided by the Smithsonian Institution at 50x, 100x, 200x, and 400x. Photomicrographs of barbules were taken with a Leica© DFC290 HD camera (Leica Microsystems, Wetzlar, Germany) to measure qualitative differences in nodal structures, pigmentation patterns and general barbule lengths. Measurements (μm) were made on each photomicrograph using the 'Manual Measurements' module in Leica Application Suite© (version 4.12.0, Leica Microsystems, Wetzlar, Germany). Subpennaceous length (Figure 3) was measured on each barb, and nodal abundance was manually counted on basal, mid and distal barbules. The following measurements were made from the basal, mid and distal sections of each barbule: basal cell length, barbule length, internodal distance, and nodal width (Figure 3, Figure 4, Table 2). A total of 40 measurements were made on each of the 12 barbs for each of the 20 species, for a grand total of 240 barbs and 9,600 measurements.

Principal component analysis (PCA) was conducted on microscopic characters at the family, genus and species level using R© statistical software (R Foundation for Statistical Computing, Vienna, Austria) to determine if significant differences existed in the variation of microscopic characters studied. Barbules from all barbs sampled from each species were analyzed for minimum, maximum and standard deviation from the mean for each measurement. Characters were tested for significance using analysis of variance (ANOVA), with P values adjusted using a Holm-Bonferroni stat correction to reduce type

1 error. A Tukey's test was used for comparisons with more than two groups to identify which groups were significantly different from each other.

Qualitative Analysis

Statistical analyses were not performed for pigmentation patterns because this character was deemed difficult to quantify with morphometrics in Accipitriformes. Pigmentation was subjectively described and characterized separately here because the patterns and intensity are too variable for consistent measurements across all groups of Accipitriformes. Pigment patterns and intensity of plumulaceous barbules were qualitatively examined using a Leica© DM750 comparison light microscope (Leica Microsystems, Wetzlar, Germany) provided by the Smithsonian Institution at 50x, 100x, 200x and 400x. Barbule pigmentation patterns were described within the internode and node as stippled, spotted or nodal (Figure 5), at basal, mid and distal barbules of each barb. Pigment patterns were defined qualitatively by examining the amount of internodal pigment observed in various parts of the barbule and scoring as light, medium or heavy (Figure 6). Pigment intensity was described on a scale of 0-4 (Figure 7).

Spines located at cell junctions (nodes) on barbules (Figure 3) were noted on many species in this study and were scored on a scale of 0-4; 0 = no spines; 1 = spines on 0-25% of each barbule; 2 = spines on 25-50% of each barbule; 3 = spines on 50-75% of each barbule; 4 = spines on 75-100% of each barbule.

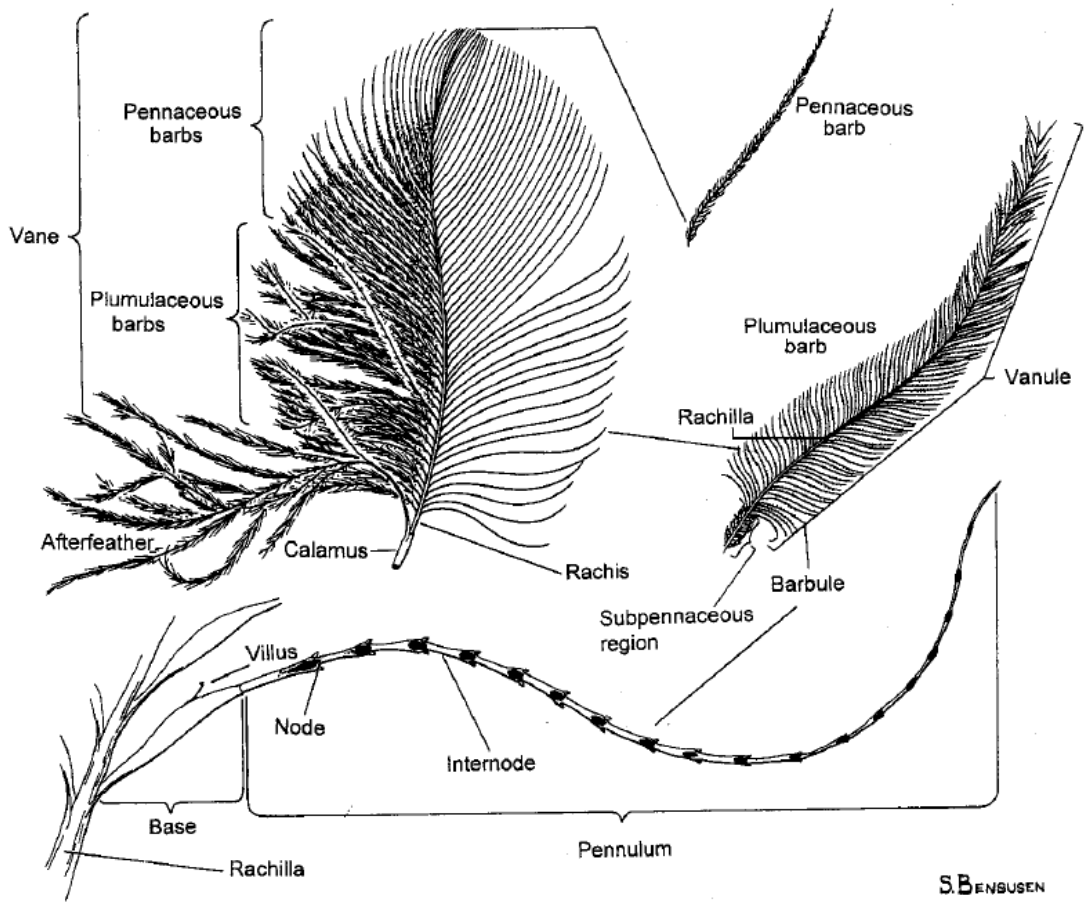

Figure 1: Topography of a contour feather (from figure 1 in Dove 1997).

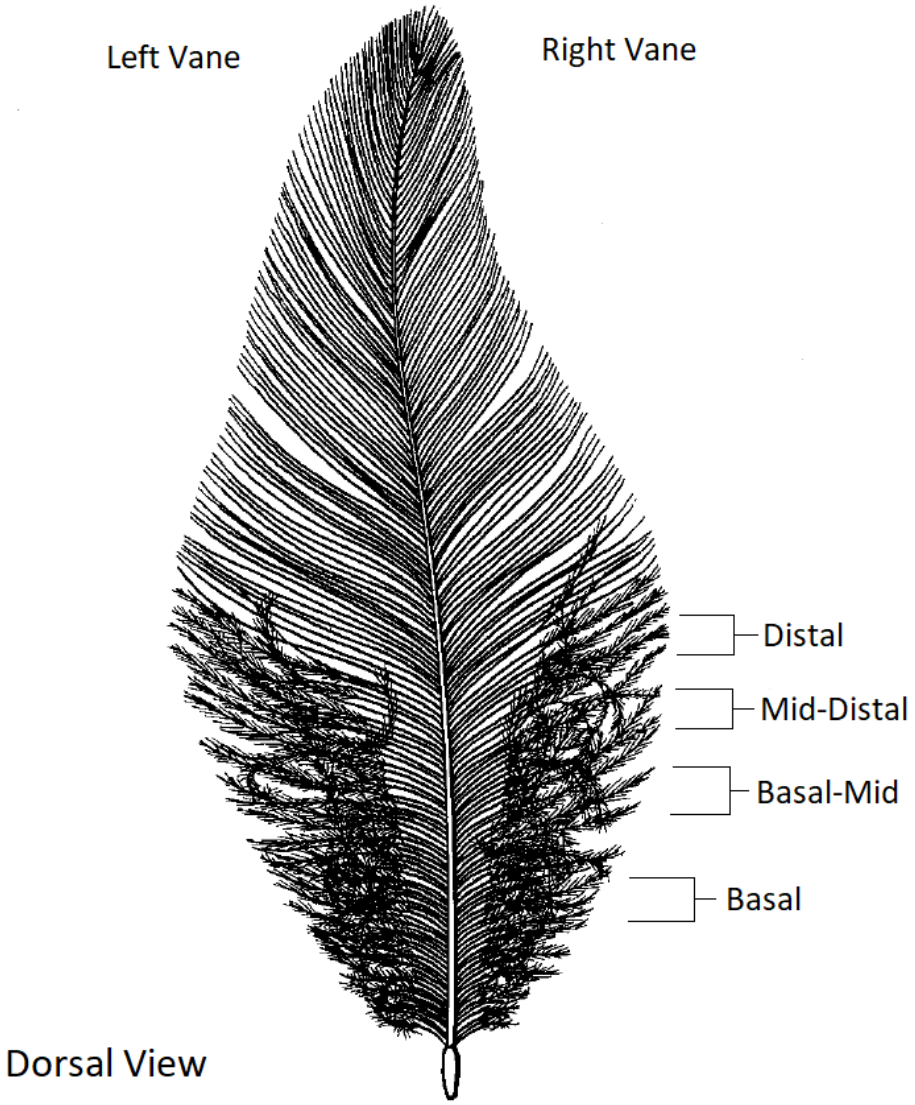

Figure 2: The four plumulaceous regions of a contour feather examined in this study include basal, basal-mid, mid-distal and distal. Barbs were removed from the right vane of a single upper left breast feather of three individuals for each species selected for this study (Original figure by Trudy Nicholson).

Table 1: Twenty species selected from five families of Accipitriformes, Falconiformes and Psittaciformes were examined in this study. Phylogeny follows Jarvis et al. (2014), so species within Accipitriformes and Falconiformes were analyzed separately, and one species of Psittaciformes was included with Falconiformes.

Order	Family	Species
Accipitriformes	New World Vultures (Carthartidae)	Turkey Vulture (*Cathartes aura*) Black Vulture (*Coragyps atratus*)
Accipitriformes	Osprey (Pandionidae)	Western Osprey (*Pandion haliaetus*)
Accipitriformes	Hawks, Eagles, Kites, Harriers (Accipitridae)	Red-tailed Hawk (*Buteo jamaicensis*) Swainson's Hawk (*Buteo swainsoni*) Cooper's Hawk (*Accipiter cooperii*) Sharp-shinned Hawk (*Accipiter striatus*) Common Black-Hawk (*Buteogallus anthracinus*) Harris's Hawk (*Parabuteo unicinctus*) Northern Harrier (*Circus cyaneus*) Bald Eagle (*Haliaeetus leucocephalus*) Golden Eagle (*Aquila chrysaetos*) Mississippi Kite (*Ictinia mississippiensis*) Swallow-tailed Kite (*Elanoides forficatus*) White-tailed Kite (*Elanus leucurus*) Snail Kite (*Rostrhamus sociabilis*)
Falconiformes	Falcons (Falconidae)	Peregrine Falcon (*Falco peregrinus*) American Kestrel (*Falco sparverius*) Crested Caracara (*Caracara cheriway*)
Psittaciformes	Parrots (Psittacidae)	Monk Parakeet (*Myopsitta monachus*)

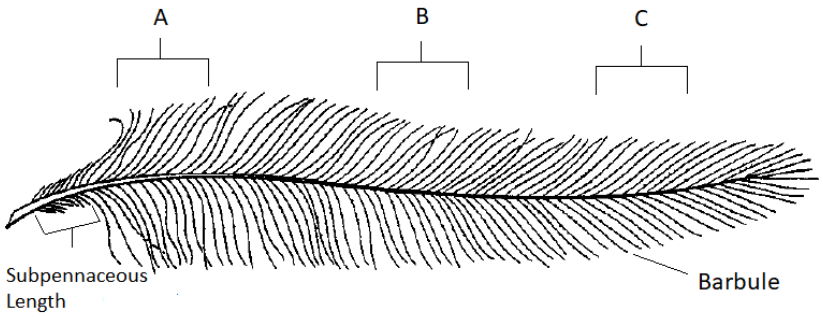

Barb - Subpennaceous length. Barb section: Basal (A), Mid (B), and Distal (C).

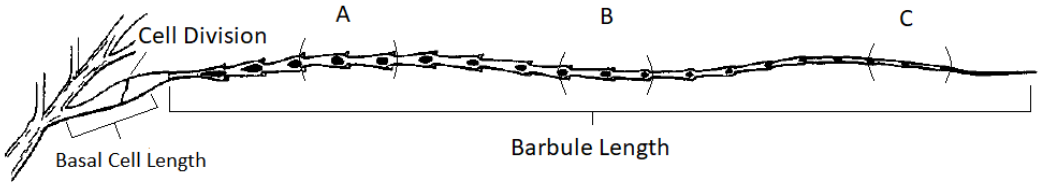

Barbule - Barbule length, Basal cell length, Barbule sections: Basal (A), Mid (B), and Distal (C).

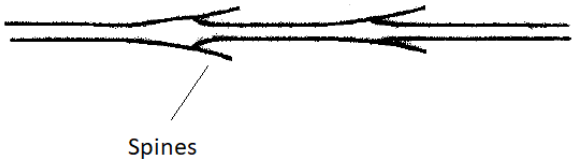

Figure 3: Sections of plumulaceous barbs and barbules measured for this study. Spines at nodes on barbules were recorded as a percentage of total distribution along the barbule (Original figure by Trudy Nicholson).

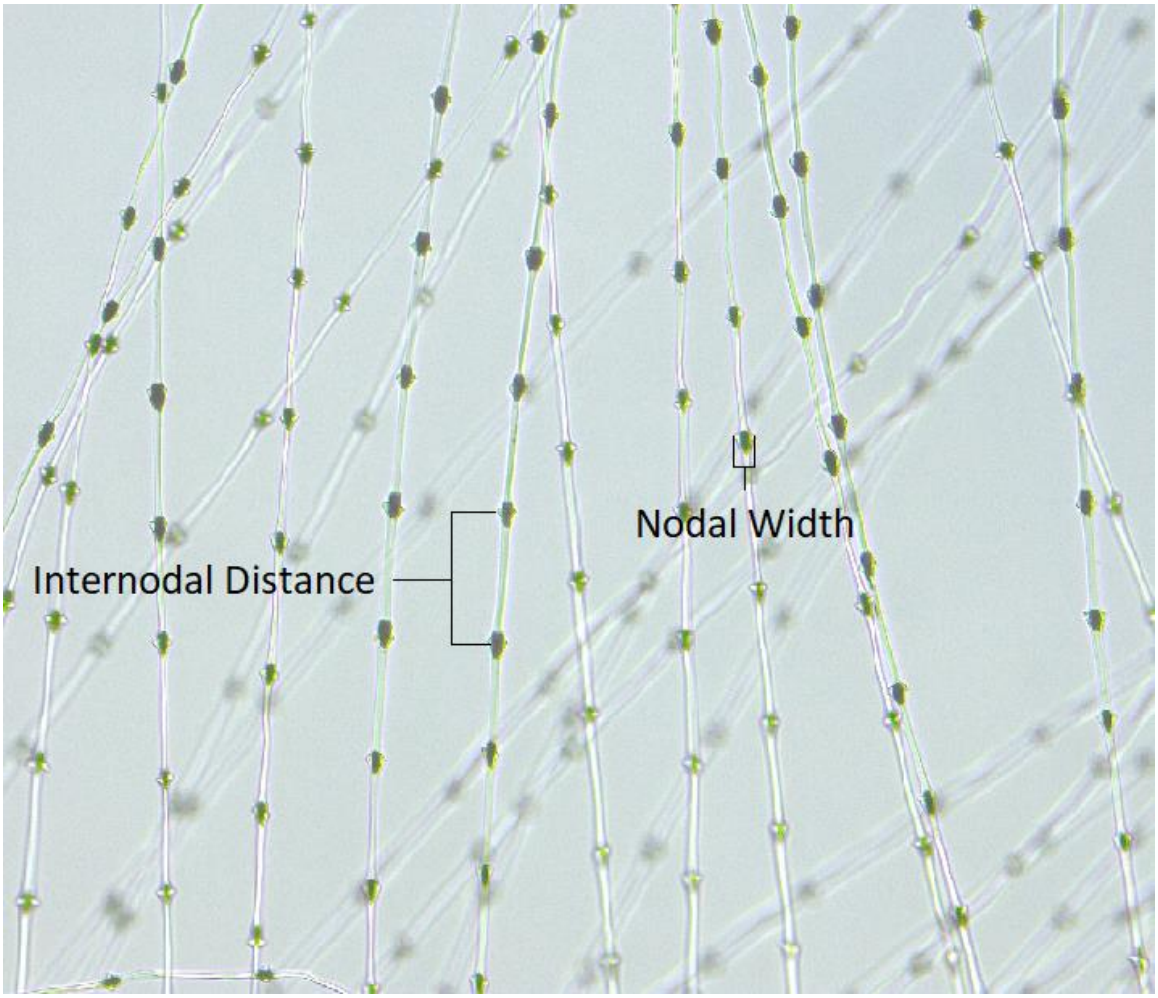

Figure 4: Quantifiable characters of internodal distance and nodal width measured at 200x (e.g. American Kestrel (*Falco sparverius*)) on basal, mid and distal sections of barbules (Photo by Charles Coddington).

Table 2: Definitions of measurements selected for quantitative analysis made on each of four barbs per species. Measurements made at low (50x), medium (100x) or high power (200x) on barbs of three different individuals.

Character	Definition	Measurement
Subpennaceous Length	Total length of this region measured from the attachment point at rachilla distally to the point where normal downy barbules occur (Figure 3).	Once at the base of each barb (Figure 3).
Basal Cell Length	Total length of the flattened first cell (or cells) on the barbule (Figure 3).	Measured on 3 separate barbules, from the basal, mid and distal sections of each barb (Figure 3).
Barbule Length	Total length of barbule. Measured from the attachment of base cell to tip of the distal end of the barbule (Figure 3).	Measured on 3 separate barbules from the basal, mid and distal sections of each barb (Figure 3).
Internodal Distance	Area between nodal structures on barbules. Measured from the mid-point of node at widest point to mid-point of adjacent distal node at widest point (Figure 4).	Measured at 3 points on the basal, mid and distal sections of each barbule on 3 separate barbules from the basal, mid and distal sections of the barb (Figure 3).
Nodal Abundance	Number of nodes counted along the barbule.	Nodes were counted on 3 separate barbules from the basal, mid and distal sections of the barb.
Nodal Width	Width of node at its widest point (Figure 4).	Measured at 3 points on the basal, mid and distal sections of each barbule on 3 separate barbules from the basal, mid and distal sections of the barb (Figure 3).
Average Nodes/Barbule	Average nodal abundance divided by average barbule length.	Calculated by dividing the average nodal abundance of 3 separate barbules from the basal, mid and distal sections of the barb and dividing by the average length of 3 separate barbules from the basal, mid and distal sections of each barb.

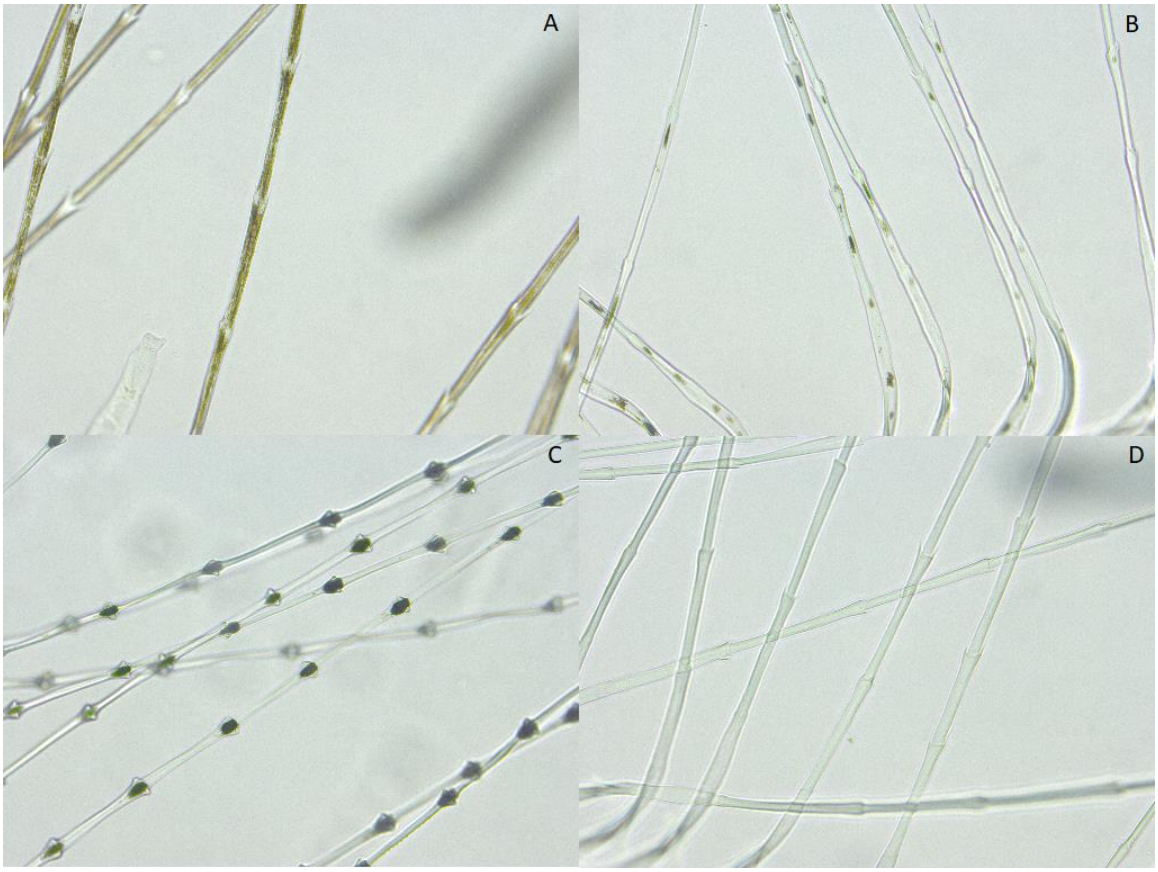

Figure 5: Pigment patterns of barbules were defined as: Stippled - e.g. Common Black Hawk (*Buteogallus anthracinus*) (A), Spotted – e.g. White-tailed Kite (*Elanus leucurus*) (B), Nodal – e.g. American Kestrel (*Falco sparverius*) (C), and Absent – e.g. Swallow-tailed Kite (*Elanoides forficatus*) (D). Photomicrographs taken at 400x (Photo by Charles Coddington).

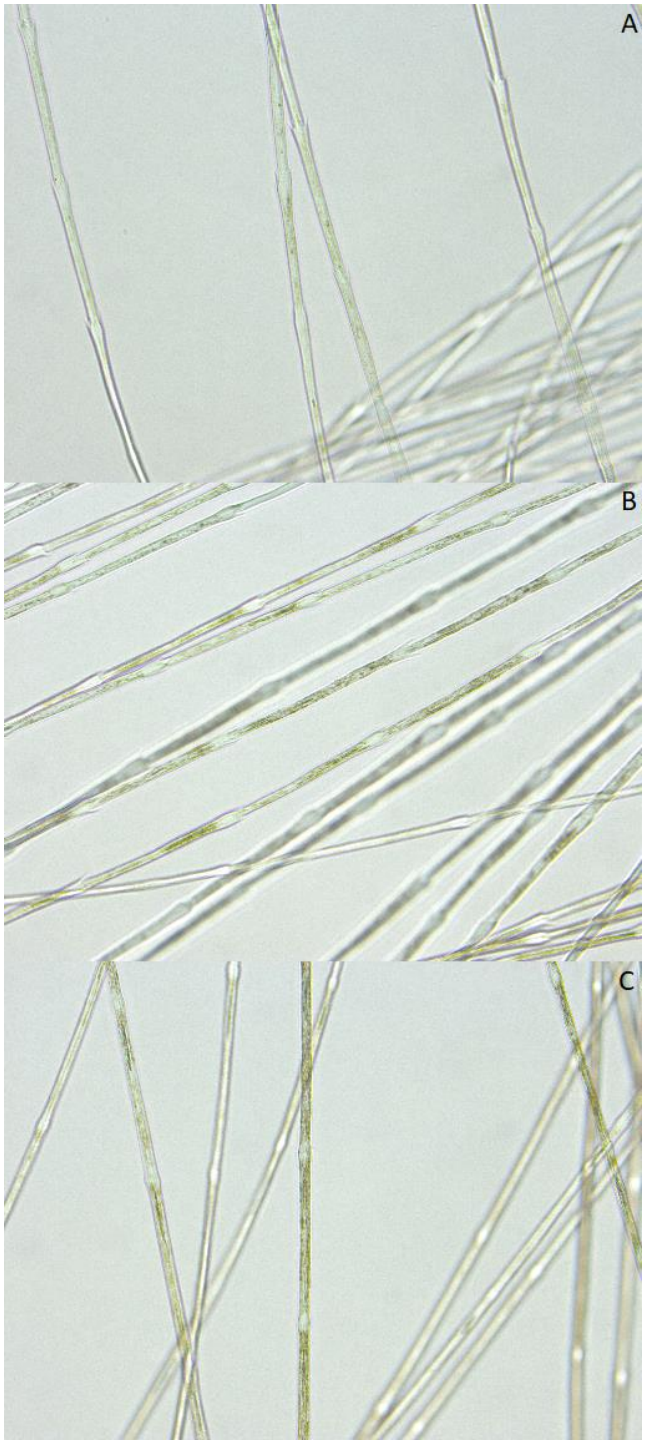

Figure 6: Internodal pigmentation was described among Accipitriformes as: Light – Red-tailed Hawk *(Buteo jamaicensis*) (A), Medium – Swainson's Hawk (*Buteo swainsoni*) (B), and Heavy – Bald Eagle (*Haliaetus leucocephalus*) (C) (Photo by Charles Coddington).

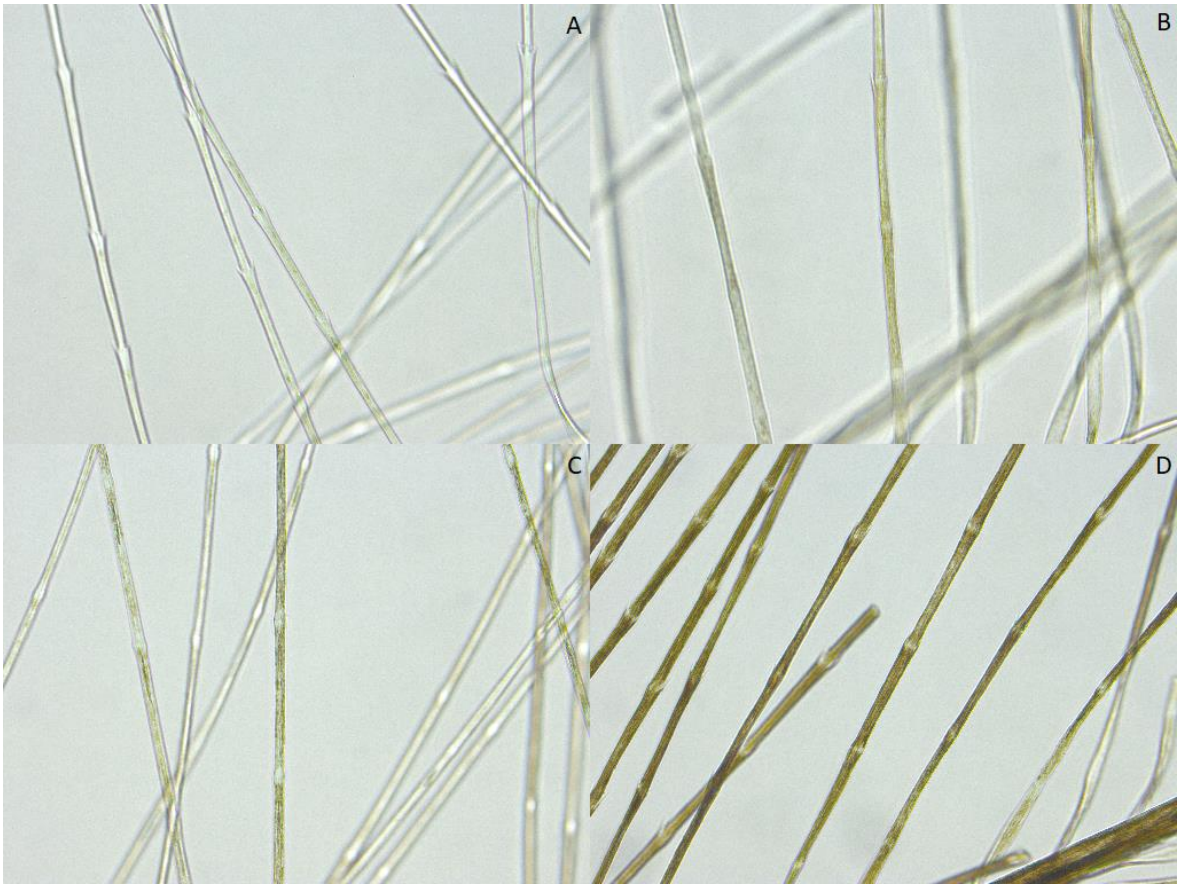

Figure 7: Pigment intensity was scored on a scale of 1-4 (A = 1 (0-25% of light absorbed), B = 2 (25-50% of light absorbed), C = 3 (50-75% of light absorbed), D = 4(75-100% of light absorbed)) (Photo by Charles Coddington).

Results

Quantitative Results: Accipitriformes

Of the 40 initial measurements examined in this study, 12 measurements were determined to be insignificant based on repetitiveness or lack of sampling consistency and were excluded from further analysis. In this study of Accipitriformes, 28 measurements of 7 characters were selected for further examination (Table 2). Measurements of all characters were checked for normal distributions prior to ANOVA. The PCA for all Accipitriformes species identified two principal components (PCs) with eigenvalues greater than 1 that accounted for 41.66% of the observed interspecific variation (Table 3). Measurements with eigenvectors weighting greater than 0.30 were considered important (Quinn and Keough 2002). PC1 was negatively weighted with average nodes/barbule, nodal width of basal and mid barbules, nodal abundance on basal barbules, internodal distance of basal barbules, and subpennaceous length; and positively weighted with barbule length of basal, mid and distal barbules (Table 3). PC2 was positively weighted with nodal abundance of basal and mid barbules, subpennaceous length, and nodal abundance and nodal width on distal barbules (Table 3).

Both PCs were significant in separating various Accipitriformes taxa via ANOVA tests, and significant comparisons were isolated with Tukey's honest significant difference test (Table 4). Accipitriformes ANOVA tests revealed that both PC1 ($P < 0.001$, $F = 27.05$, $DF = 5$) and PC2 ($P < 0.001$, $F = 45.99$, $DF = 5$) significantly separated the Accipitriformes clades (Figure 8). Tukey's honest significant difference test showed PC1 significantly separated the means of Harriers from Eagles ($P < 0.001$), Hawks ($P < 0.001$), Kites ($P <$

0.001), Osprey ($P < 0.001$), and Vultures ($P < 0.001$). It also separated the means of Osprey from Eagles ($P = 0.007$), Hawks ($P < 0.001$), Kites ($P < 0.001$), Harrier ($P < 0.001$), and Vultures ($P < 0.001$). PC2 significantly separated Eagles ($P < 0.001$) from all other groups of Accipitriformes; Harriers were significantly separated from Hawks ($P = 0.012$), Kites ($P = 0.036$), Vultures ($P < 0.001$), and Osprey ($P = 0.039$); Osprey were also significantly separated from Hawks ($P < 0.001$), Kites ($P < 0.001$) and Vultures ($P < 0.001$).

Analyses between different hawk genera revealed that both PC1 ($P < 0.001$, $F = 18.47$, $DF = 4$) and PC2 ($P < 0.001$, $F = 10.71$, $DF = 4$) significantly separated the means of characters for hawk genera (Figure 9). Tukey's honest significant difference test showed PC1 significantly separated *Accipiter* from *Buteo* ($P < 0.001$), *Buteogallus* ($P = 0.002$), *Parabuteo* ($P < 0.001$) and *Circus* ($P < 0.001$); *Circus* was significantly separated from *Buteo* ($P = 0.001$), *Buteogallus* ($P = 0.002$) and *Parabuteo* ($P = 0.003$). PC2 significantly separated *Accipiter* from *Buteo* ($P = 0.002$) and *Buteogallus* ($P < 0.001$); *Circus* from *Buteo* ($P < 0.001$) and *Buteogallus* ($P < 0.001$); and *Parabuteo* from *Buteogallus* ($P = 0.03$). Comparisons between species in the same genera revealed many observable differences. PC1 ($P = 0.009$, $F = 11.11$, $DF = 1$) and PC2 ($P = 0.006$, $F = 12.52$, $DF = 1$) for *Buteo* hawks significantly separated *Buteo jamaicensis* from *Buteo swainsoni* (Figure 10). PC2 was important for *Accipiter* hawks ($P < 0.001$, $F = 43.06$, $DF = 1$) (Figure 11) as they significantly separated *Accipiter cooperii* and *Accipiter striatus*. Species in the kite genera studied were significantly separated by means of PC1 ($P < 0.001$, $F = 28.1$, $DF = 3$) (Figure 12). Tukey's honest significant difference test showed PC1 significantly separated *Elanus*

from all other kite genera ($P < 0.001$) but overlap is noted in the range of character measurements.

Comparisons between the two vulture genera revealed PC1 ($P = 0.001$, $F = 17.05$, $DF = 1$) and PC2 ($P = 0.006$, $F = 12.26$, $DF = 1$) (Figure 13) significantly separated the means of characters for *Cathartes aura* and *Coragyps atratus*. Analyses between the different eagle genera showed PC2 ($P < 0.001$, $F = 16.83$, $DF = 1$) (Figure 14) significantly separated the means of characters for *Haliaeetus leucocephalus* and *Aquila chrysaetos* but there is a large degree of overlap in individual character measurements.

Table 3: Variable loadings in each significant PC for Hawks. PC's are labeled with their eigenvalue and % of variance explained. Loadings are arranged in order of significance for the respective principle component and labeled with PC loading weight in bold.

PC1 – **24.64%** Eigenvalue: **2.67**	PC2 – **17.02%** Eigenvalue: **2.22**
Average # Nodes/Barbule = **-0.919** Barbule Length (Mid) = **0.817** Basal Nodal Width (Distal) = **-0.775** Basal Nodal Width (Mid) = **-0.730** Barbule Length (Base) = **0.698** Mid Internodal Distance (Mid) = **0.683** Barbule Length (Distal) = **0.682** Distal Internodal Distance (Mid) = **0.631** Nodal Abundance (Base) = **-0.617** Basal Internodal Distance (Distal) = **-0.560** Basal Internodal Distance (Mid) = **-0.512** Distal Internodal Distance (Distal) = **0.505** Mid Nodal Width (Distal) = **-0.473** Subpennaceous Length = **-0.445** Nodal Abundance (Distal) = **0.424** Distal Internodal Distance (Base) = **0.389** Basal Internodal Distance (Base) = **0.381** Mid Internodal Distance (Distal) = **0.369** Mid Nodal Width (Base) = **0.361** Mid Nodal Width (Mid) = **-0.319**	Nodal Abundance (Mid) = **0.676** Nodal Abundance (Base) = **0.645** Subpennaceous Length = **0.576** Mid Nodal Width (Distal) = **0.550** Nodal Abundance (Distal) = **0.424** Basal Nodal Width (Base) = **0.515** Barbule Length (Distal) = **0.510** Mid Nodal Width (Mid) = **0.509** Basal Nodal Width (Mid) = **0.495** Basal Internodal Distance (Mid) = **0.477** Basal Nodal Width (Distal) = **0.404** Distal Nodal Width (Base) = **0.403** Barbule Length (Mid) = **0.402** Distal Nodal Width (Mid) = **0.377** Distal Internodal Distance (Base) = **0.366** Barbule Length (Base) = **0.364**

Table 4: Accipitriformes microstructure PCA ANOVA Results – P Values mark with * are significant (P < 0.05). P values are adjusted with a Holm-Bonferroni stat correction test. Tukey's test results show significant comparisons (P < 0.05) between means of all Accipitriformes taxa measurements with multiple groups and relevant principal components.

Group	Principal Component	Adjusted P Value	F Value	Degrees of Freedom	Comparison	Tukey's P Value
All Accipitriformes	1	< 0.001*	27.05	5	Harrier-Eagle	< 0.001*
					Harrier-Hawk	< 0.001*
					Harrier-Kite	< 0.001*
					Harrier-Osprey	< 0.001*
					Harrier-Vulture	< 0.001*
					Osprey-Eagle	0.007*
					Osprey-Hawk	< 0.001*
					Osprey-Kite	< 0.001*
					Osprey-Vulture	0.002*
					Eagle-Hawk	0.036*
					Eagle-Kite	0.015*
					Vulture-Kite	0.047*
	2	< 0.001*	45.99	5	Eagle-Harrier	< 0.001*
					Eagle-Hawk	< 0.001*
					Eagle-Kite	< 0.001*
					Eagle-Osprey	< 0.001*
					Eagle-Vulture	< 0.001*
					Harrier-Hawk	0.012*
					Harrier-Kite	0.036*
					Harrier-Vulture	< 0.001*
					Harrier-Osprey	0.039*
					Osprey-Hawk	< 0.001*
					Osprey-Kite	< 0.001*
					Osprey-Vulture	< 0.001*
All Hawk Genera	1	< 0.001*	18.47	4	Accipiter-Buteo	< 0.001*
					Accipiter-Buteogallus	0.002*
					Accipiter-Circus	< 0.001*
					Accipiter-Parabuteo	< 0.001*
					Circus-Buteo	0.001*
					Circus-Buteogallus	0.002*
					Circus-Parabuteo	0.003*
	2	< 0.001*	10.71	4	Accipiter-Buteo	0.002*
					Accipiter-Buteogallus	< 0.001*
					Circus-Buteo	< 0.001*
					Circus-Buteogallus	< 0.001*
					Parabuteo-Buteogallus	0.03*
Buteo Species	1	0.009*	11.11	1	NA	NA
	2	0.006*	12.52	1	NA	NA
Accipiter Species	1	1	0.18	1	NA	NA
	2	< 0.001*	43.06	1	NA	NA
All Kite Genera	1	< 0.001*	28.1	3	Elanus-Elanoides	< 0.001*
					Elanus-Ictina	< 0.001*
					Elanus-Rostrhamus	< 0.001*
	2	1	0.513	3	NA	NA
Vulture Genera	1	0.001*	17.05	1	NA	NA
	2	0.006*	12.26	1	NA	NA
Eagle Genera	1	0.219	3.549	1	NA	NA
	2	0.001*	16.83	1	NA	NA

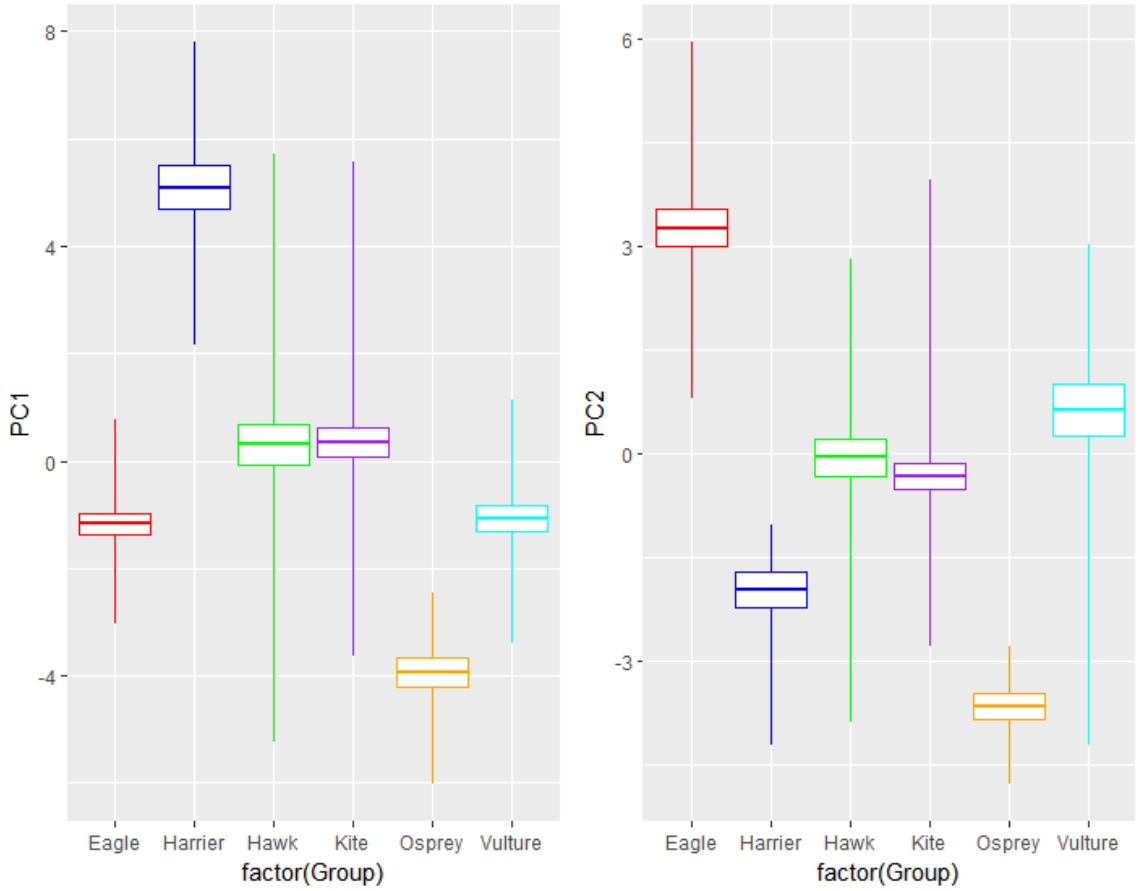

Figure 8: The separation of all groups of Accipitriformes via principal components 1 (left) and 2 (right). Plots show mean (middle horizontal line), +1 standard error measurement (top horizontal line), -1 standard error measurement (bottom horizontal line), max value (top vertical line), min value (bottom vertical line). PC1 is negatively weighted with average nodes/barbule, width of nodes on the basal barbule, basal nodal abundance, and basal internodal distance; and positively weighted with barbule length of all barbules measured. PC2 is positively weighted with nodal abundance of basal and mid barbules, subpennaceous length, and nodal abundance and nodal width on the distal barbule. Harriers have the longest barbules and Osprey the shortest barbules. Eagles have the highest average nodal abundance, and Harriers and Osprey have lower nodal abundances than all other groups studied. Overlap is noted in ranges of most measurements.

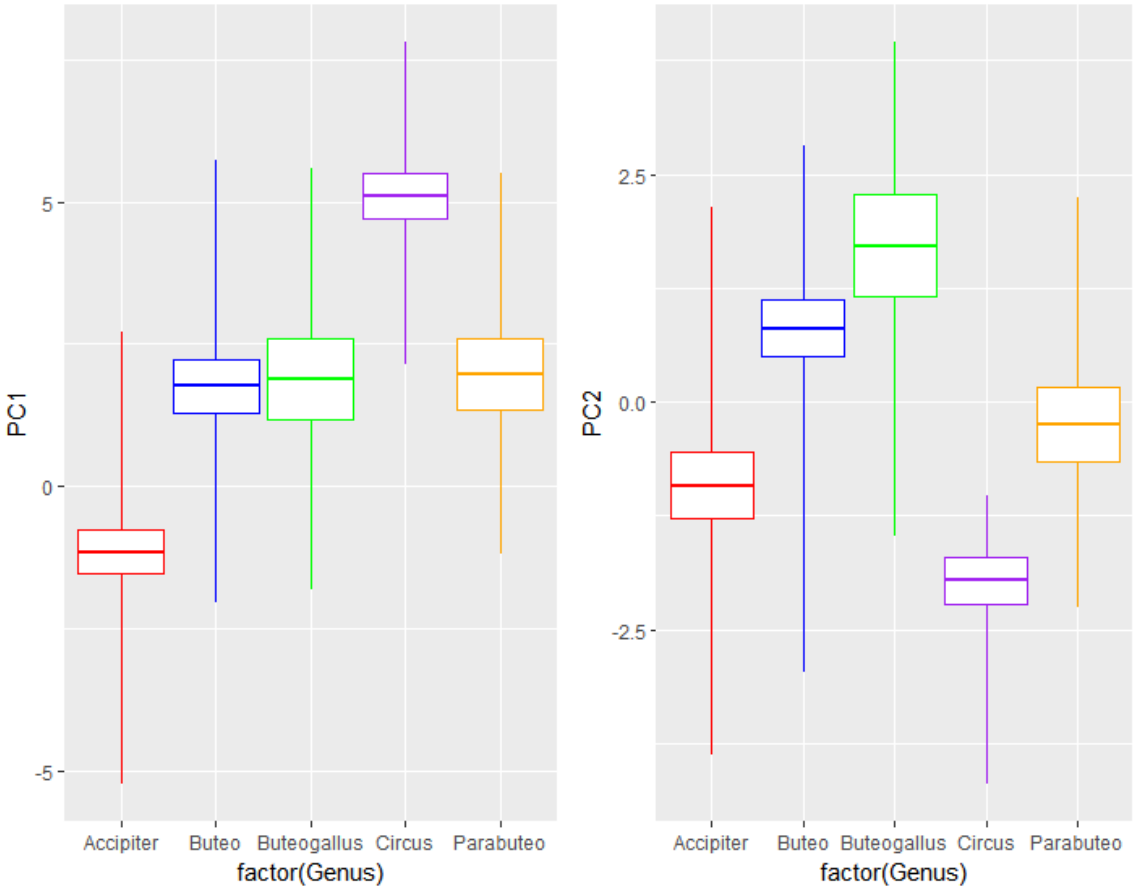

Figure 9: The separation of hawk genera via principal components 1 (left) and 2 (right). Boxplots show mean (middle horizontal line), +1 standard error measurement (top horizontal line), -1 standard error measurement (bottom horizontal line), max value (top vertical line), min value (bottom vertical line). PC1 is negatively weighted with average nodes/barbule, width of nodes on the basal barbule, basal barbule nodal abundance, and basal barbule internodal distance; and positively weighted with barbule length of basal, mid and distal barbules. PC2 is positively weighted with nodal abundance of basal and mid barbules, subpennaceous length, and nodal abundance and nodal width on the distal barbule. *Circus* had the longest barbules of all hawk genera studied. *Accipiter* had the highest average nodal abundance/barbule length of any of the hawk genera, and *Circus* had the lowest. Overlap is noted in ranges of most measurements.

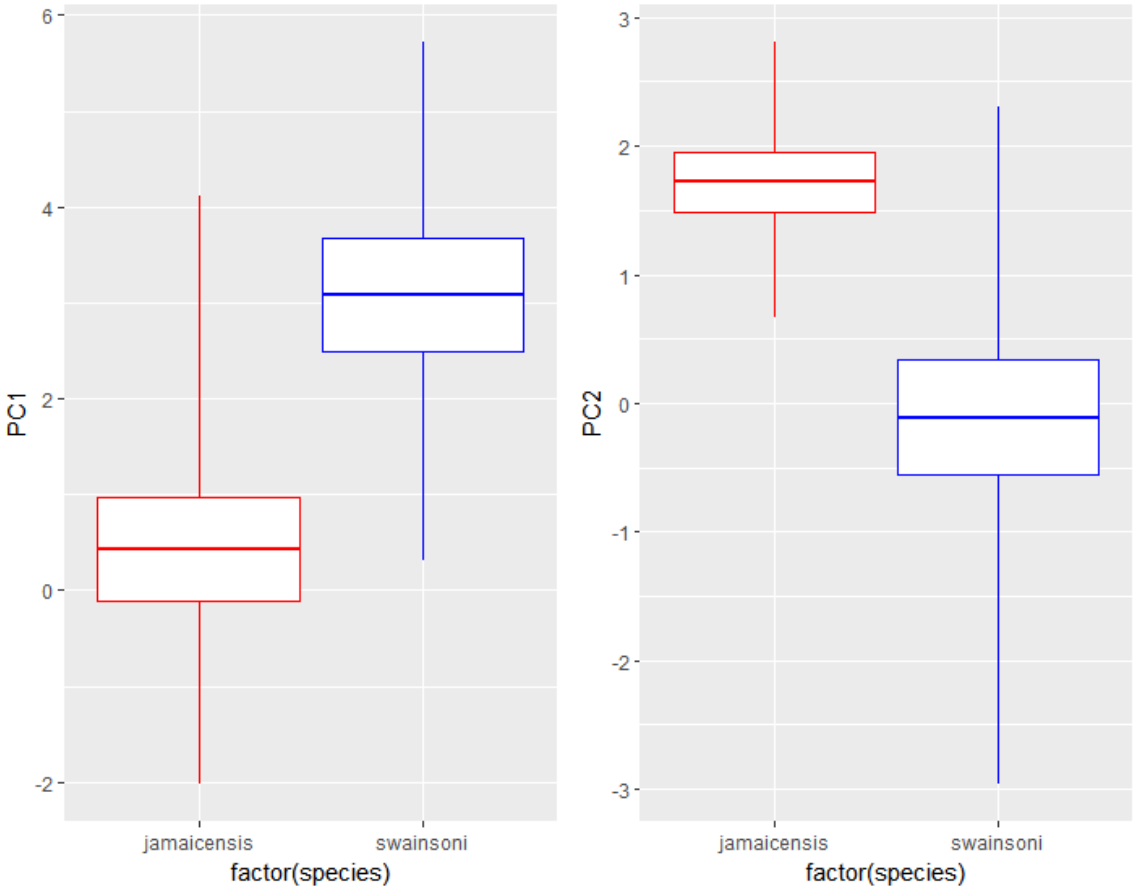

Figure 10: Pair comparisons of *Buteo* hawks at the species level via principal components 1 (left) and 2 (right) show overlap of these closely related species. Boxplots show mean (middle horizontal line), +1 standard error measurement (top horizontal line), -1 standard error measurement (bottom horizontal line), max value (top vertical line), min value (bottom vertical line). PC1 is negatively weighted with average nodes/barbule, width of nodes on the basal barbule, basal barbule nodal abundance, and basal barbule internodal distance; and positively weighted with barbule length of basal, mid and distal barbules. PC2 is positively weighted with nodal abundance of basal and mid barbules, subpennaceous length, and nodal abundance and nodal width on the distal barbule. *B. jamaicensis* had a significantly higher average nodes/barbule length, basal nodal abundance, and a longer subpennaceous length than *B. swainsoni*. Overlap is noted in ranges of most measurements.

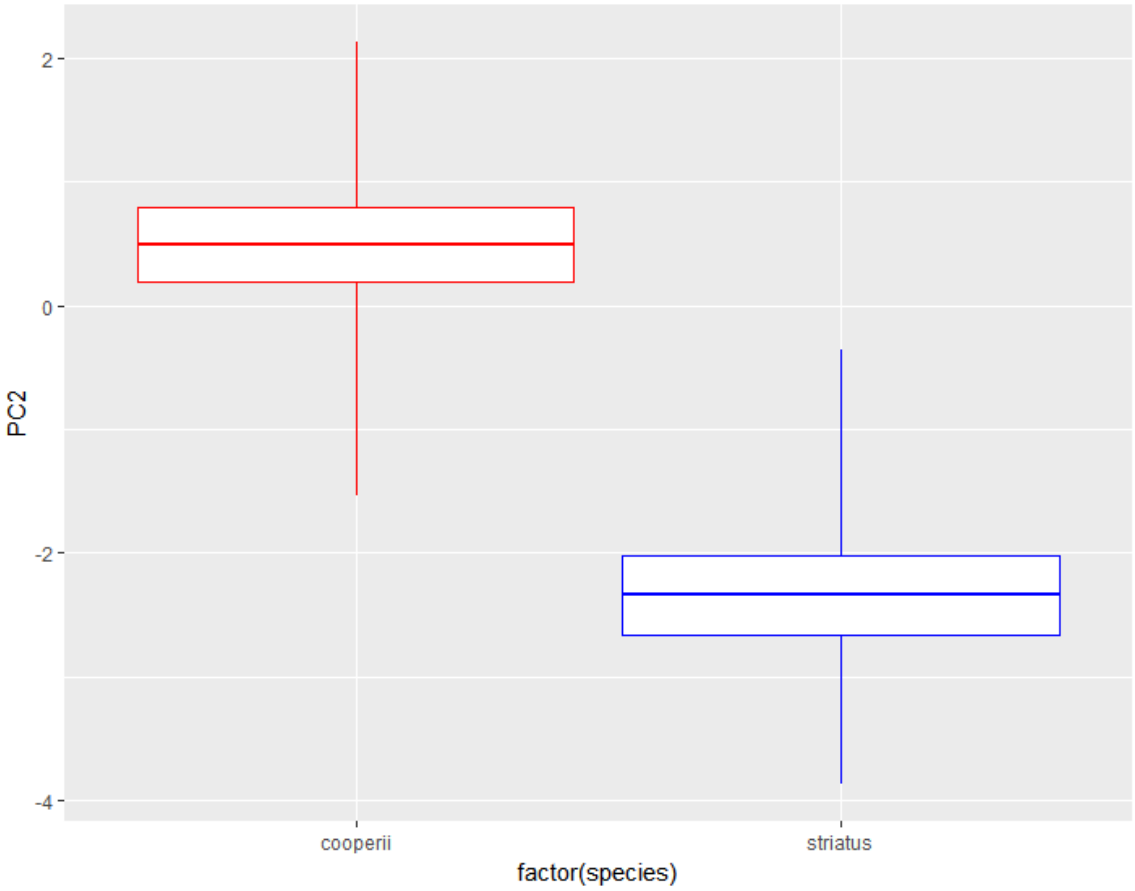

Figure 11: The separation of *Accipiter* species studied here via principal component 2. Boxplots show mean (middle horizontal line), +1 standard error measurement (top horizontal line), -1 standard error measurement (bottom horizontal line), max value (top vertical line), min value (bottom vertical line). PC2 is positively weighted with nodal abundance of basal and mid barbules, subpennaceous length, and nodal abundance and nodal width on the distal barbule. *A. cooperii*, on average, had a higher nodal abundance on the basal and mid barbules, and a longer subpennaceous length than *A. striatus*. Overlap is noted in ranges of most measurements

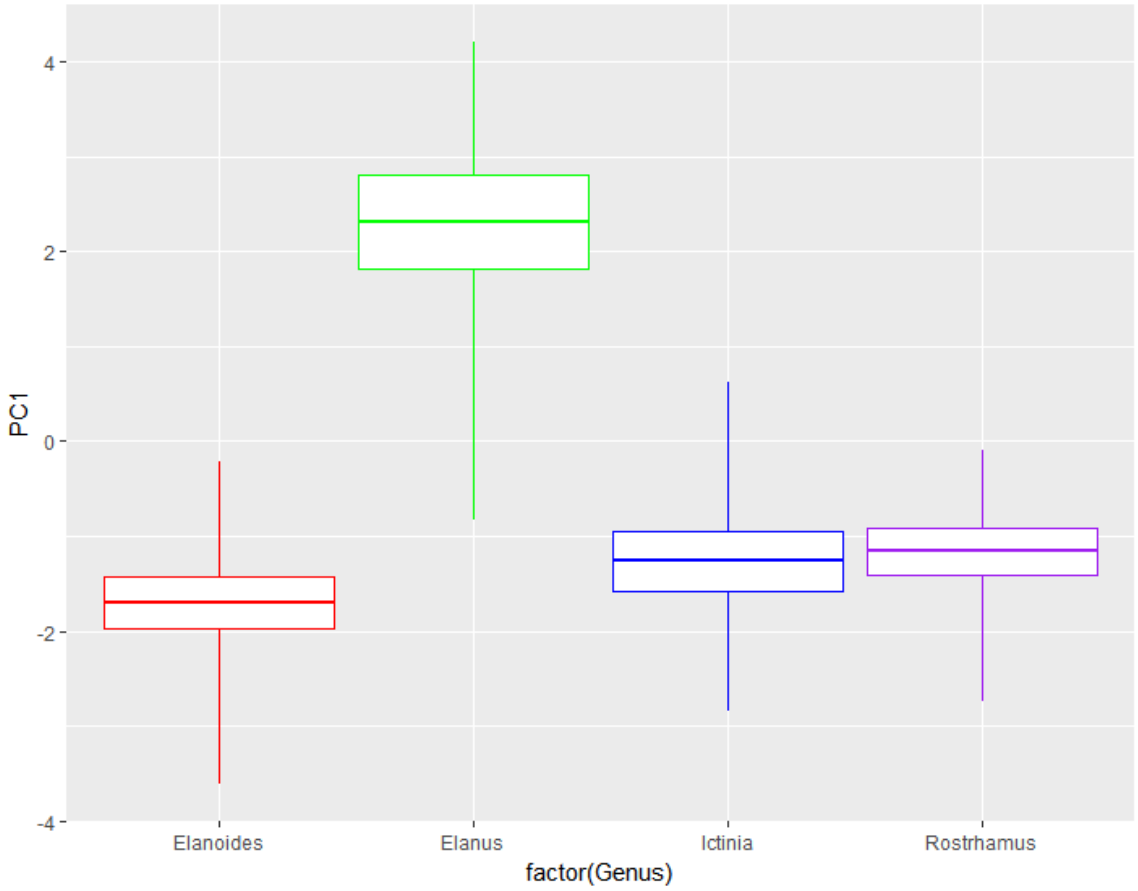

Figure 12: The separation of all kite genera via principal component 1. Boxplots show mean (middle horizontal line), +1 standard error measurement (top horizontal line), -1 standard error measurement (bottom horizontal line), max value (top vertical line), min value (bottom vertical line). PC1 is negatively weighted with average nodes/barbule, width of nodes on the basal barbule, basal barbule nodal abundance, and basal barbule internodal distance; and positively weighted with barbule length of basal, mid and distal barbules. *Elanus* generally had the longest basal, mid and distal barbules of any kite genera studied. Overlap is noted in ranges of most measurements.

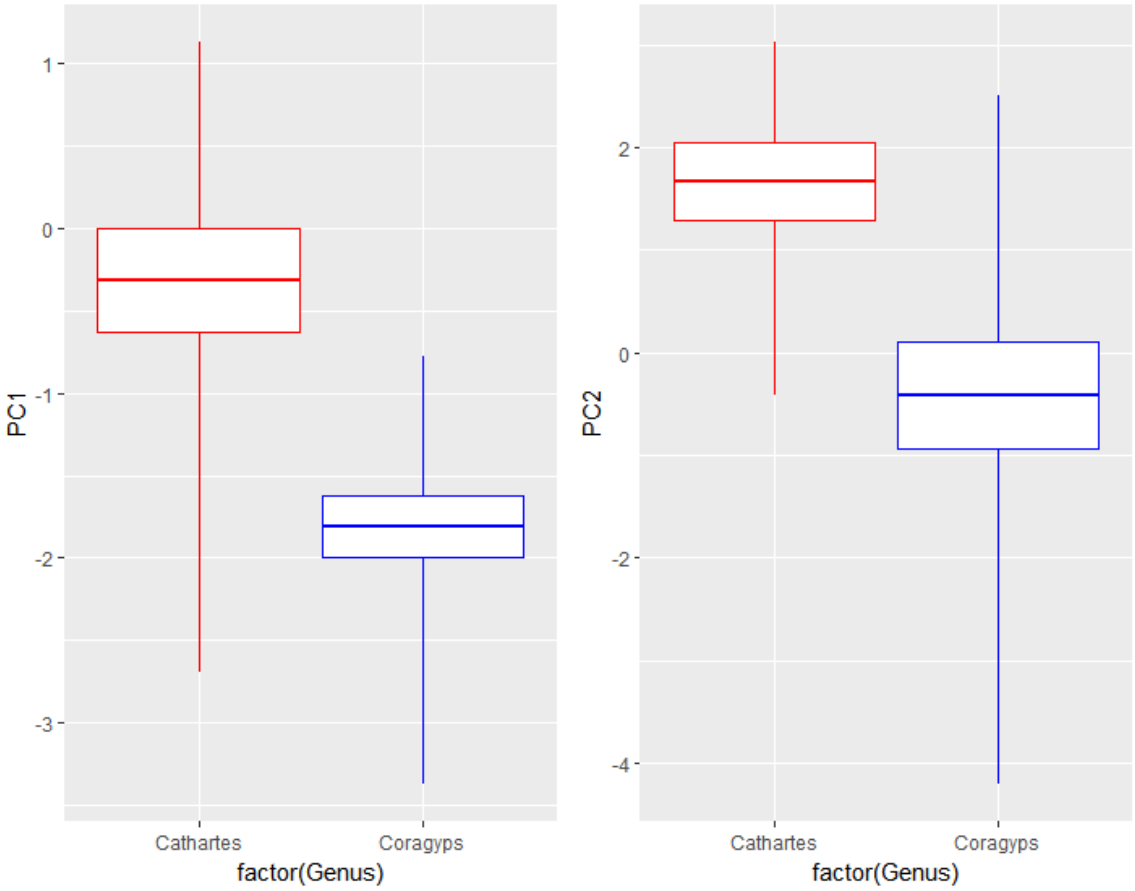

Figure 13: The separation of all vulture genera via principal components 1 (left) and 2 (right). Boxplots show mean (middle horizontal line), +1 standard error measurement (top horizontal line), -1 standard error measurement (bottom horizontal line), max value (top vertical line), min value (bottom vertical line). PC1 is negatively weighted with average nodes/barbule, width of nodes on the basal barbule, basal barbule nodal abundance, and basal barbule internodal distance; and positively weighted with barbule length of basal, mid and distal barbules. PC2 is positively weighted with nodal abundance of basal and mid barbules, subpennaceous length, and nodal abundance and nodal width on the distal barbule. *Cathartes aura* typically had longer basal, mid and distal barbules than *Coragyps atratus* but overlapping measurements were observed within these species.

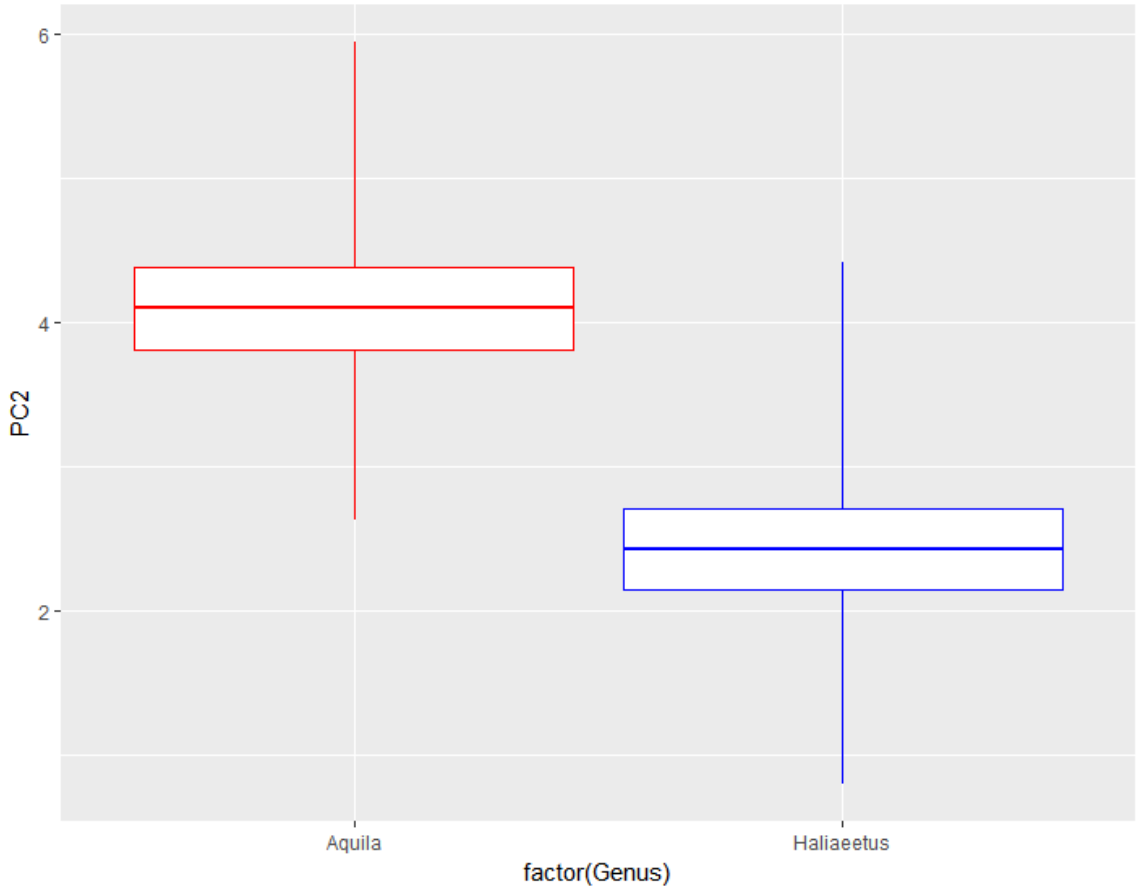

Figure 14: The separation of all eagle genera via principal component 2. Boxplots show mean (middle horizontal line), +1 standard error measurement (top horizontal line), -1 standard error measurement (bottom horizontal line), max value (top vertical line), min value (bottom vertical line). PC2 is positively weighted with nodal abundance of basal and mid barbules, subpennaceous length, and nodal abundance and nodal width on the distal barbule. *A. chrysaetos* had a higher nodal abundance on basal and mid barbules, and a longer subpennaceous length than *H. leucocephalus*. Overlap is noted in ranges of most measurements.

Quantitative Results: Falconiformes/Psittaciformes

The PCA for Falconiformes/Psittaciformes identified two PCs with eigenvalues greater than 1.0 that accounted for 56.2% of the observed interspecific variation (Table 5). Measurements with eigenvectors with weighting greater than 0.30 (Quinn and Keough 2002) were considered important. Both PCs were significant in separating various Falconiformes/Psittaciformes taxa via ANOVA tests, and significant comparisons were isolated with Tukey's honest significant difference test (Table 6). PC1 was positively weighted with nodal abundance of the mid and distal barbules, length of basal, mid and distal barbules, and nodal width of the distal barbule; and negatively weighted with subpennaceous length and average nodes/barbule (Table 5). PC2 was negatively weighted with nodal width of the basal and mid barbules, and average nodes/barbule length; and positively weighted with internodal distance of the mid and distal barbules and basal cell length of the basal, mid and distal barbules (Table 5).

Falconiformes/Psittaciformes ANOVA tests revealed both PC1 ($P < 0.001$, $F = 24.52$, $DF = 2$) and PC2 ($P < 0.001$, $F = 77.31$, $DF = 2$) significantly separated the means of measurements of Falconiformes/Psittaciformes genera (Figure 15). Tukey's honest significant difference test showed PC1 significantly separated *Caracara* from *Falco* ($P < 0.001$) and *Myiopsitta* ($P = 0.021$); and *Falco* from *Myiopsitta* ($P = 0.002$). PC2 significantly separated *Myiopsitta* from *Caracara* ($P < 0.001$) and *Falco* ($P < 0.001$); and *Falco* from *Caracara* ($P < 0.001$). Analyses between the different *Falco* species revealed both PC1 ($P < 0.001$, $F = 95.15$, $DF = 1$) and PC2 ($P < 0.001$, $F = 23.42$, $DF = 1$) significantly separated *F. peregrinus* from *F. sparverius* (Figure 16).

Table 5: Variable loadings onto each significant PC for Falconiformes/Psittaciformes. PC's are labeled with their eigenvalue and % of variance explained. Loadings are arranged in order of significance for the respective principle component and labeled with PC loading weight in bold.

PC1 – **34.3%** Eigenvalue: **3.15**	PC2 – **21.9%** Eigenvalue: **2.52**
Nodal Abundance (Mid) = **0.891** Barbule Length (Mid) = **0.857** Barbule Length (Distal) = **0.805** Nodal Abundance (Distal) = **0.786** Subpennaceous Length = **-0.760** Barbule Length (Base) = **0.720** Mid Internodal Distance (Distal) = **0.709** Distal Nodal Width (Mid) = **0.680** Basal Internodal Distance (Distal) = **0.644** Distal Nodal Width (Distal) = **0.622** Distal Nodal Width (Base) = **0.620** Mid Nodal Width (Distal) = **0.613** Nodal Abundance (Base) = **0.600** Mid Nodal Width (Mid) = **0.595** Average # Nodes/Barbule = **-0.588** Basal Nodal Width (Mid) = **0.577** Mid Nodal Width (Base) = **0.550** Basal Internodal Distance (Mid) = **0.541** Mid Internodal Distance (Mid) = **0.529** Basal Internodal Distance (Base) = **0.522** Mid Internodal Distance (Base) = **0.503** Basal Nodal Width (Base) = **0.476** Distal Internodal Distance (Distal) = **0.371** Basal Cell (Mid) = **-0.367**	Basal Nodal Width (Base) = **-0.776** Basal Nodal Width (Distal) = **-0.759** Distal Internodal Distance (Mid) = **0.733** Basal Nodal Width (Mid) = **-0.704** Distal Internodal Distance (Distal) = **0.616** Basal Cell (Distal) = **0.615** Mid Nodal Width (Base) = **-0.604** Average # Nodes/Barbule = **-0.557** Basal Cell (Mid) = **0.544** Basal Cell (Base) = **0.517** Mid Nodal Width (Mid) = **-0.517** Mid Internodal Distance (Mid) = **0.503** Distal Internodal Distance (Base) = **0.443** Mid Internodal Distance (Distal) = **0.440** Mid Nodal Width (Distal) = **-0.414** Subpennaceous Length = **0.396** Basal Internodal Distance (Mid) = **0.358** Barbule Length (Mid) = **0.345** Barbule Length (Distal) = **0.338** Barbule Length (Base) = **0.322**

Table 6: Falconiformes/Psittaciformes microstructure PCA ANOVA Results – P Values mark with * are significant (P < 0.05). P values are adjusted with a Holm-Bonferroni stat correction test. Tukey's test results show significant comparisons (P < 0.05) between all Falconiformes/Psittaciformes taxa with multiple groups and relevant principal components.

Group	Principal Component	Adjusted P Value	F Value	Degrees of Freedom	Comparison	Tukey's P Value
Falconiformes/Psittaciformes Genera	1	< 0.001*	24.52	2	Caracara-Falco	< 0.001*
					Caracara-Myiopsitta	0.021*
					Falco-Myiopsitta	0.002*
	2	< 0.001*	77.31	2	Caracara-Falco	< 0.001*
					Caracara-Myiopsitta	< 0.001*
					Falco-Myiopsitta	< 0.001*
Falco Genera	1	< 0.001*	95.15	1	NA	NA
	2	< 0.001*	23.42	1	NA	NA

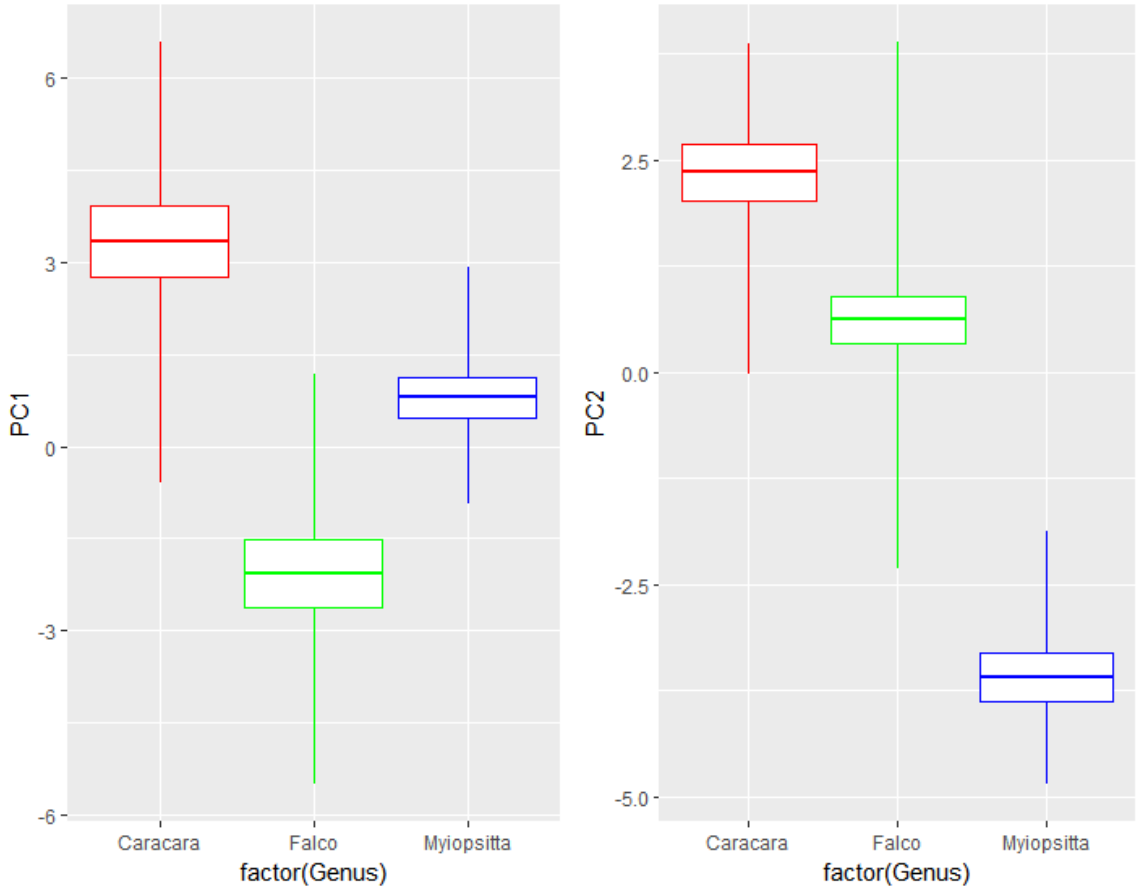

Figure 15: The separation of all Falconiformes/Psittaciformes studied via principal components 1 (left) and 2 (right). Boxplots show mean (middle horizontal line), +1 standard error measurement (top horizontal line), -1 standard error measurement (bottom horizontal line), max value (top vertical line), min value (bottom vertical line). PC1 is positively weighted with nodal abundance of the mid and distal barbules, length of basal, mid and distal barbules, and nodal width of the distal barbule; and negatively weighted with subpennaceous length and average nodes/barbule. PC2 was negatively weighted with nodal width of the basal and mid barbules, and average nodes/barbule length; and positively weighted with internodal distance of the mid and distal barbules and basal cell length of the basal, mid and distal barbules. *Caracara* has longer barbules and a higher nodal abundance than *Falco* and *Myiopsitta*. *Myiopsitta* has wider nodes in basal and mid barbules than *Falco* or *Caracara*. Overlap is noted in ranges of most measurements.

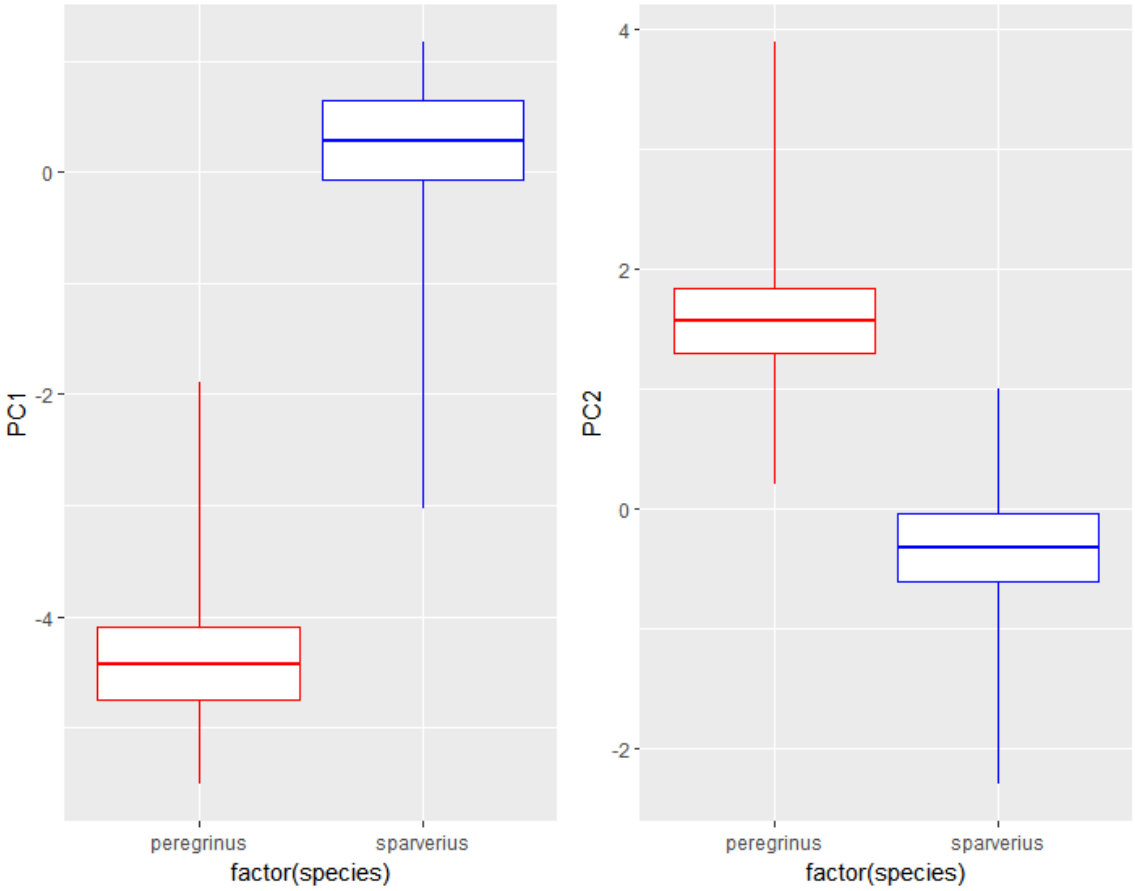

Figure 16: The separation of all *Falco* genera studied via principal components 1 (left) and 2 (right). Boxplots show mean (middle horizontal line), +1 standard error measurement (top horizontal line), -1 standard error measurement (bottom horizontal line), max value (top vertical line), min value (bottom vertical line). PC1 is positively weighted with nodal abundance of the mid and distal barbules, length of basal, mid and distal barbules, and nodal width of the distal barbule; and negatively weighted with subpennaceous length and average nodes/barbule. PC2 was negatively weighted with nodal width of the basal and mid barbules, and average nodes/barbule length; and positively weighted with internodal distance of the mid and distal barbules and basal cell length of the basal, mid and distal barbules. *F. sparverius* typically has longer barbules and a higher nodal abundance on all barbules than *F. peregrinus*. *F. sparverius* also had wider nodes at the basal and mid barbules than *F. peregrinus*. Overlap is noted in ranges of most measurements.

Qualitative Analysis

A qualitative survey of pigmentation patterns and intensity, and spine morphology revealed visible differences in the internodal pigment, pigment patterns, and intensity of pigment and spine distribution at nodes of the taxa studied. These visual characteristics can be of great assistance since measurements overlap in most of the closely related taxa studied here. Members of Accipitriformes typically have dense stippled internodal pigmentation compared to those of Falconiformes, which typically have dark concentrated nodal pigmentation with little or no internodal pigmentation. Pigment was present in most barbs of the majority of Accipitriformes species studied, with some exceptions having little or no pigment such as Swallow-tailed Kite (*Elanoides forficatus*). When present, pigment was usually heavily stippled and evenly distributed in the internode, and slightly less concentrated or absent within the node, often making the nodes appear clear. In contrast, Falconiformes and Psittaciformes species studied had very dark dense pigment that was well contained within the node or sometimes present just below the node, visually separating these orders from Accipitriformes. Spines were present at the nodes of barbules with varying abundance in all Accipitriformes species studied but were not present in Falconiformes or Psittaciformes. Falcons and parrots typically have small pointed structures at the pigmented nodes instead of longer spined nodes. The most common and characteristic pigmentation patterns and spine distributions in each species studied are summarized below and compared to closely related species with similar microstructure. Appendix 3 concisely summarizes these descriptions to facilitate direct comparison.

Vultures (*Cathartes, Coragyps*)

Turkey Vulture (*Cathartes aura*) (Figure 17A) – Heavy stippled internodal pigment is evenly distributed throughout the barb. Internodal pigment of barbules is light (intensity: 1) at the base of the barb and darkens (intensity: 2) towards the distal portion of the barb. Nodal pigment is usually absent or very lightly stippled (light; intensity 1) in barbules at the basal end of the barb and darkens and becomes more concentrated in barbules towards the mid (medium; intensity: 1) and distal (heavy; intensity: 2) regions of the barb. Pigment is evenly distributed along the entire barbule in all sections of the barb. Spines were present at nodes of all barbules, but sparsely distributed (spines: 1) and were not present on the distal section of barbules.

Black Vulture (*Coragyps atratus*) (Figure 17B) – Heavy stippled internodal pigment is evenly distributed throughout the barb. Internodal pigment is relatively dark (intensity: 2) in barbules at the base of the barb and becomes darker (intensity: 3) in the middle barbules of the barb and very dark (intensity: 4) barbules are noted towards the distal end. Nodal pigment is lightly stippled at the basal (intensity: 1) and mid (intensity: 1) barbules of barbs and darkens and becomes more concentrated in barbules towards the distal end of barbs (medium; (intensity: 2)). Pigment is evenly distributed along the entire barbule in all sections of the barb. The amount of internodal pigment and intensity of the pigment at the distal end of the barb is unique to this species and separates it from Turkey Vulture in the breast feathers studied here. Spines were present at nodes on all barbules, but sparsely distributed (spines: 1) and were not present on the distal portion of the barbule.

Cathartes aura and *Coragyps atratus* are distinguishable based on a multitude of microscopic characters examined in upper left breast feathers. *C. aura* has significantly longer barbules on average, longer average internodal distance and higher average nodes per barbule than *C. atratus*. *C. atratus* has significantly shorter barbules, but more nodes/barbule than *C. aura*. In addition, visual observations of the barbules of *C. aura* are long and wavy, whereas the barbules of *C. atratus* tend to be much more stiff and rigid. *C. atratus* can also be distinguished from *C. aura* by typically having much darker pigment in all regions of the barb (Figure 17). There is a large degree of overlap in the average range of microscopic measurements of the vulture and hawk species analyzed for this study, and measurements alone may not be diagnostic. However, vultures and hawks can generally be distinguished by pigment distribution. Vulture pigment in both species studied tends to be lighter at the base of the barb and gradually gets darker towards the distal end of the barb, whereas hawk pigment is generally darker at the base of the barb and gradually gets lighter towards the distal end of the barb.

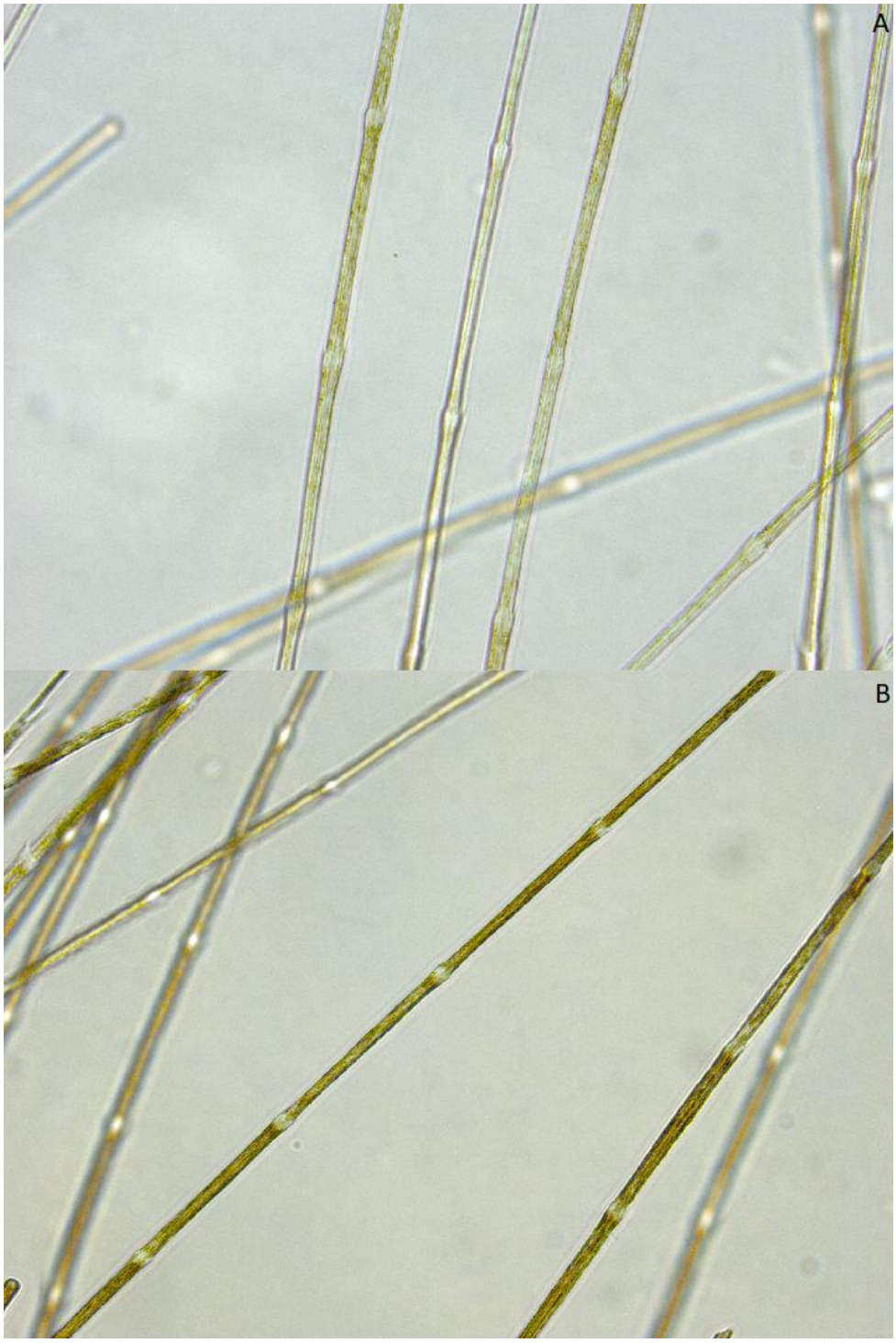

Figure 17: Comparison of barbules from the basal region of barb of Turkey Vulture (*Cathartes aura*) (A) and Black Vulture (*Coragyps atratus*) (B). Photomicrographs taken at 400x. Basal barb pigment intensity is generally much darker in Black Vulture than in Turkey Vulture (Photo by Charles Coddington).

Osprey (*Pandion haliaetus*)

Western Osprey (*Pandion haliaetus*) (Figure 18, Figure 19) – Stippled pigment is evenly distributed in barbules throughout the barb and stippling is heavy (intensity: 1) in the internode and medium (intensity: 1) within the node. Pigment is only present at the basal portion of barbules and disappears near the distal portion of the barbules. Spines at nodes are very abundant (spines: 4) in this species and are present in every barbule from basal to distal portions of barbules (Figure 18).

Harrier (*Circus cyaneus*)

Northern Harrier (*Circus cyaneus*) (Figure 19) – Internodal pigment is stippled on barbules at the base (medium; intensity: 1) and mid (medium; intensity: 1) sections of the barb and becomes lighter towards the distal (light; intensity: 1) section. Nodal pigment is lightly stippled (intensity: 1) in barbules and evenly distributed throughout the barb. Pigment is evenly distributed throughout barbules in all sections of the barb. Spines at nodes are present on all barbules, but sparsely distributed (spines: 1) and are not present in the distal portion of barbules.

Both Western Osprey (*P. haliaetus*) and Northern Harrier (*Circus cyaneus*) are distinguishable from all other species of Accipitriformes described in this study. The Western Osprey is the most unique species of Accipitriformes studied as it is the only species with spines at nodes present on more than 75% of each barbule from the base to distal portion of the barb (Figure 18) and the shortest barbules on average of any species

studied (Figure 19). Northern Harrier has the longest barbules on average of any Accipitriformes species studied, but also the lowest average number of nodes per barbule (Figure 19).

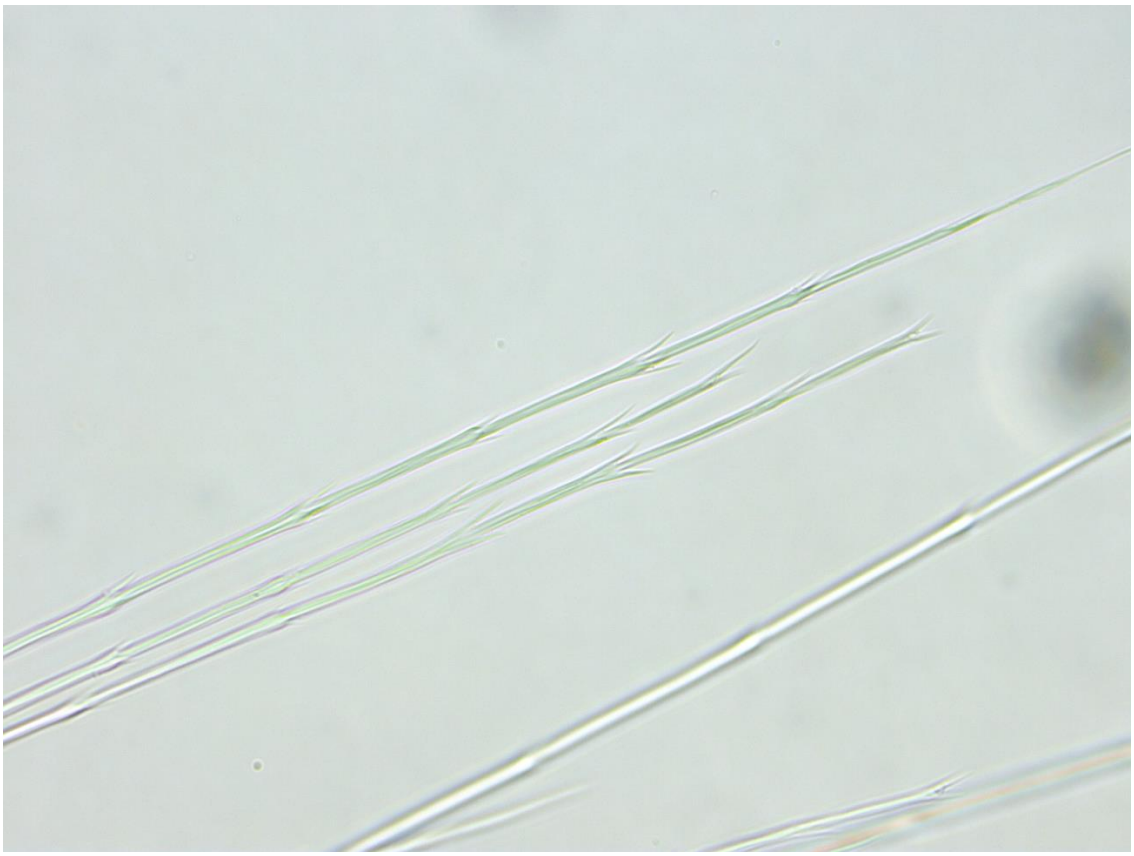

Figure 18: Distal portion of basal barbule of Osprey at 400x. Osprey are the only species studied with spines at nodes all along the barbules on all regions of the barb (Photo by Charles Coddington).

Figure 19: Comparison of barbule length of Osprey (*Pandion haliaetus*) (A) and Northern Harrier (*Circus cyaneus*) (B) at 50x. The Osprey has the shortest barbule lengths of any Accipitriformes species studied, and Northern Harrier the longest (Photo by Charles Coddington).

Hawks (*Buteo, Accipiter*)

Cooper's Hawk (*Accipiter cooperii*) (Figure 20A) – Internodal barbule pigment is stippled and concentrated in the basal (medium; intensity: 2) and mid (medium; intensity: 2) sections of the barb and becomes less concentrated towards the distal (light; intensity: 1) end of the barb. Nodal pigment is lightly stippled (intensity: 1) on barbules and evenly distributed throughout the barb. Pigment is evenly distributed throughout the barbule in all sections of the barb. Spines at nodes are present on all barbules, but sparsely distributed (spines: 1) and mainly concentrated on barbules the basal portion of the barb.

Sharp-shinned Hawk (*Accipiter striatus*) (Figure 20B) – Internodal pigment of barbules is heavily stippled at the basal (intensity: 3) and distal (intensity: 2) sections of the barb. Internodal pigment becomes lighter and less concentrated on barbules located in the mid region of the barb (light; intensity: 1). Nodal pigment is either absent or lightly stippled (intensity: 1) and pigment is evenly distributed throughout the barb. Pigment is evenly distributed throughout barbules in all sections along the barb. Spines at nodes are present at nodes on all barbules, but sparsely distributed (spines: 1) and when present, mainly concentrated on barbules at the basal section of the barb.

Accipiter hawks were visually distinguishable from all other hawk genera studied based on noticeably shorter barbules and higher average nodes/barbule. The *Accipiter* hawk species are likely indistinguishable based on microscopic measurements alone. Although *A. cooperii* has a longer subpennaceous region on average than *A. striatus,* this

measurement may be unreliable because subpennaceous region length depends on accurate removal of the entire section from the feather rachis during barb sampling. However, the *Accipiter* hawks can be distinguished visually by pigmentation pattern. *A. striatus* has much more abundant and darker pigment in the basal and distal regions of the barb than *A. cooperii* (Figure 20) in examination of feather characters from the upper left breast.

Figure 20: Comparison of basal barbule region of Cooper's Hawk (*Accipiter cooperii*) (A) and Sharp-shinned Hawk (*Accipiter striatus*) (B) at the basal region of barbs. Photomicrographs taken at 400x (Photo by Charles Coddington). Sharp-shinned hawks have darker pigment than Cooper's Hawks at the basal portion of barbs in feathers examined in this study.

Red-tailed Hawk (*Buteo jamaicensis*) (Figure 21A) – Internodal barbule pigment is heavily stippled at the base (intensity: 2) of the barb and decreases in both amount and intensity in the mid (medium; intensity: 1) and distal (light; intensity: 1) regions of the barb. Nodal pigment is stippled on basal barbules (medium; intensity: 2) and becomes less concentrated at the mid (light, intensity: 1) and distal (light, intensity: 1) regions of the barb. Pigment is evenly distributed throughout the barbules in all sections of the barb. Spines at nodes are present on all barbules along the barb, but sparsely distributed (spines: 1) and mainly concentrated at the basal portion of the barbules.

Swainson's Hawk (*Buteo swainsoni*) (Figure 21B) – Internodal pigment is heavily stippled on barbules at the base of the barb (intensity: 2) and decreases in amount (medium) but darkens on barbules (intensity: 3) in the mid region of the barb and decreases in amount and becomes lighter towards the distal end of the barb (light; intensity: 1). Nodal pigment of barbules is stippled at the base (light; intensity: 2) and becomes more concentrated (medium) and lighter (intensity: 1) in the mid-section of the barb, then becomes less concentrated (light) towards the distal end of the barb. Pigment is evenly distributed throughout the barbule in all sections of the barb. Spines at nodes are present on all barbules, but sparsely distributed (spines: 1) and mainly concentrated at the basal portion of the barbules.

The barbule length of *Buteo* hawks are indistinguishable from Common Black Hawk (*Buteogallus anthracinus*) and Harris's Hawk (*Parabuteo unicinctus*) based on

microstructure measurements alone. The average barbule length of *Buteo* hawks is significantly longer than the *Accipiter* hawks and significantly shorter than *Circus cyaneus*. The only difference in nodal abundance between *B. jamaicensis* and *B. swainsoni* occurs at basal barbules on the barb, so it is nearly impossible to distinguish the two species based on microstructure alone without a basal barbule in the feather type studied here. The pigment of *B. swainsoni* is visually slightly darker in the mid region of the barb than *B. jamaicensis*, but these species are likely indistinguishable unless the complete barb is present (Figure 21). *Buteogallus anthracinus* is visually distinguishable from the *Buteo* hawks based on much darker pigment throughout the barb. *Parabuteo unicinctus* has slightly darker pigment towards the distal end of the barb, and less pigmentation within the nodes, than the *Buteo* hawks, but these species are likely indistinguishable based on pigment alone unless a complete barbs are present and feather type is known.

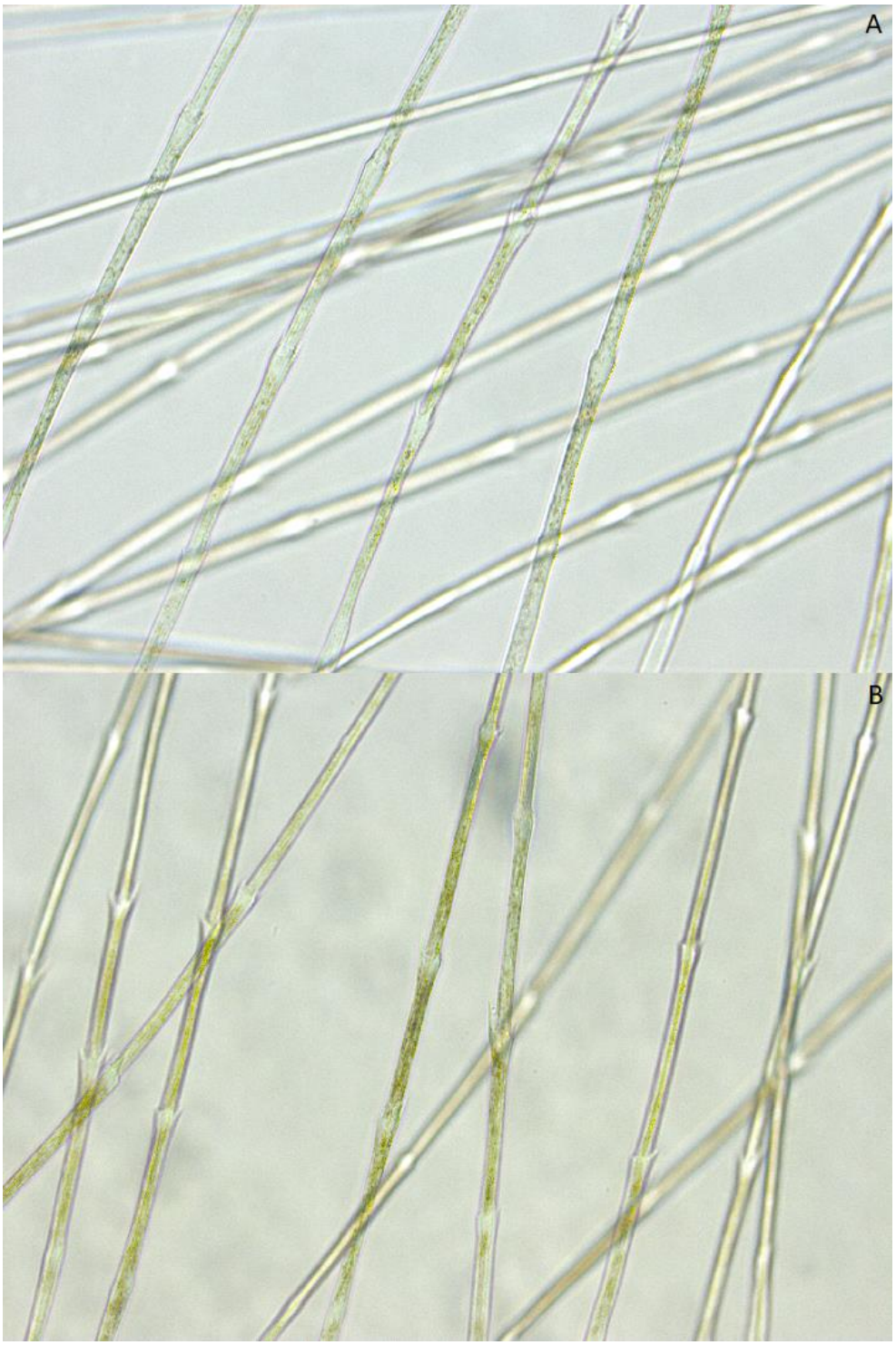

Figure 21: Comparison of mid region of Red-tailed Hawk (*Buteo jamaicensis*) (A) and Swainson's Hawk (*Buteo swainsoni*) (B). Pigment intensity is typically darker in Swainson's hawks in barbules of the mid region of the barb than in the same region of Red-tailed Hawks, but these two species are very similar microscopically. Photomicrographs taken at 400x (Photo by Charles Coddington).

Kites (*Ictinia, Elanoides, Elanus, Rostrhamus*)

Mississippi Kite (*Ictinia mississippiensis*) (Figure 22A) – Internodal pigment of barbules is heavily stippled at the base (intensity: 2) and mid (intensity: 2) regions of the barb and becomes lighter and less concentrated towards the distal (medium; intensity: 1) region of the barb. Nodal pigment is lightly stippled (intensity: 1) and evenly distributed on barbules throughout the barb. Internodal pigment is more concentrated towards the basal portion of barbules, and gradually decreases in amount towards the distal end. Spines at nodes are present on all barbules, but sparsely distributed (spines: 1) and mainly concentrated towards the basal portion of barbules.

Swallow-tailed Kite (*Elanoides forficatus*) (Figure 22B) – No pigment is present in this species on barbs of upper left breast feathers. Spines at nodes are present on all barbules, but sparsely distributed (spines: 1) and mainly concentrated towards the basal portion of barbules.

White-tailed Kite (*Elanus leucurus*) – (Figure 22C) Spotted pigment is dark and sparsely concentrated (light; intensity: 4) on barbules at the basal section of the barb and disappears in the mid and distal barb regions. Nodal pigment is absent on barbules in this species. Internodal pigment is concentrated towards the basal section of the barbule and disappears in the mid and distal regions. Spines at nodes are present on all barbules, but sparsely distributed (spines: 1) and mainly concentrated towards the basal section of barbules.

Snail Kite (*Rostrhamus sociabilis*) – (Figure 22D) Internodal pigment of barbules is heavily stippled and dark (intensity: 3) at the basal and mid (intensity: 3) sections of the barb and becomes darker distally (intensity: 4) on the barb. Nodal pigment of barbules is either absent or lightly stippled (intensity: 1) and evenly distributed on barbules throughout the barb. Pigment is evenly distributed throughout the barbule in all sections of the barb. Spines at nodes are present on all barbules, but sparsely distributed (spines: 1) and mainly concentrated towards the basal portion of barbules.

Elanus leucurus is the only species distinguishable from other kite species studied here based on microscopic measurements of barbule length, and lower average nodes/barbule. The difference in basal average internodal distance of *Ictinia mississippiensis* and *Rostrhamus sociabilis* is likely the reason for their significant separation by Tukey's test; but this is also probably not a good measurement to distinguish the two species because there is much overlap in the range of measurements. All kite species studied were distinguishable visually by pigment pattern. *E. leucurus* is easily distinguishable from all other Accipitriformes species studied by having unique spotted pigment in barbule internode regions at the basal portion of the barb (Figure 22). Some Falconiformes species studied also have spotted pigment in the internode, but pigment shape within the node in the falcons is oval in shape and is absent in *E. leucurus*. *I. mississippiensis* is the only species in this subgroup that completely lacks pigment in all barbules. However, identification based only on a lack of pigment is difficult, because many other species have unpigmented barbs that do not originate from the plumulaceous

region or originate from different feather types on a bird's body (Dove pers. comm.; pers. obs.). *R. sociabilis* is the only kite species examined in this study that has very dark heavy stippled pigment on barbules in all sections of the barb. However, *R. sociabilis* barbule pigment closely resembles that of *Buteogallus anthracinus* and *Coragyps atratus*, and therefore may be difficult to distinguish due to overlapping microstructure character measurements and pigmentation patterns in this feather type.

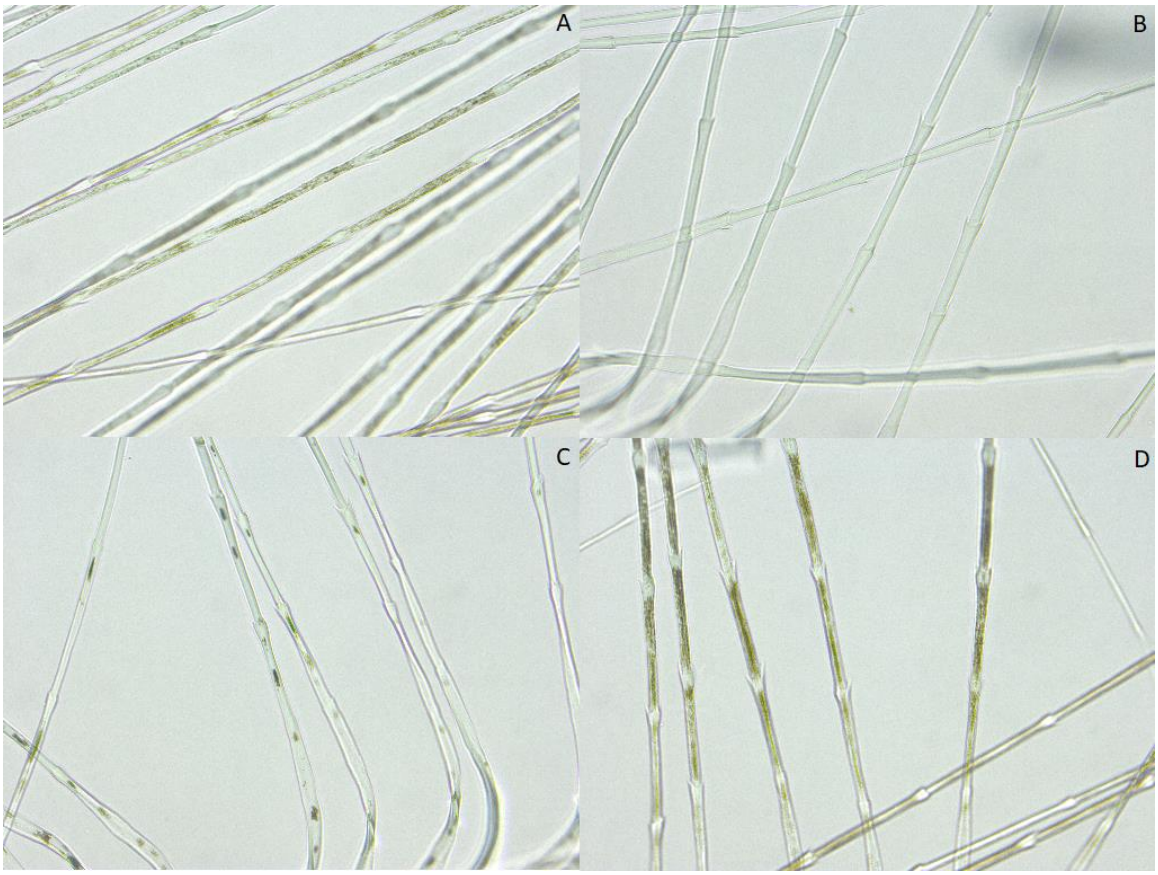

Figure 22: Pigment patterns of Kite species studied: Mississippi Kite (*Ictinia mississippiensis*) (A), Swallow-tailed Kite (*Elanoides forficatus*) (B), White-tailed Kite (*Elanus leucurus*) (C), and Snail Kite (*Rostrhamus sociabilis*) (D). Photomicrographs taken at 400x (Photo by Charles Coddington).

Eagles (*Haliaetus, Aquila*)

Bald Eagle (*Haliaetus leucocephalus*) (Figure 23A) – Internodal pigment of barbules is heavily stippled and dark (intensity: 3) at the base of the barb and becomes slightly lighter on barbules in the mid (intensity 2) and distal (intensity: 2) regions of the barb. Nodal pigment is evenly stippled (medium; intensity: 2) throughout all regions of the barb. Pigment (internodal and nodal) is evenly distributed throughout the barbule in all sections of the barb. Spines at nodes are more abundant and mainly concentrated at the basal portion of all barbules in this group and may distinguish them from all 'non-eagle' members of Accipitridae (spines: 2) in the feather type studied here.

Golden Eagle (*Aquila chrysaetos*) (Figure 23B) – Both nodal and internodal pigment of barbules are stippled (medium; intensity: 2) and evenly distributed through all sections of the barb and barbules. Spines at nodes are present on all barbules, concentrated at the basal section of barbules, and more abundant than all other non-eagle members of Accipitridae (spines: 2).

Both eagle species examined here have significantly higher basal nodal abundance on barbules and average nodal abundance than any other Accipitriformes species studied. *A. chrysaetos* has a significantly longer subpennaceous region than *H. leucocephalus*, but there is potential for overlap in this character due to barb removal from the feather. *H. leucocephalus* also has significantly darker pigment in the base of the barb than *A. chrysaetos* (Figure 23) in the upper left breast feathers examined in this study.

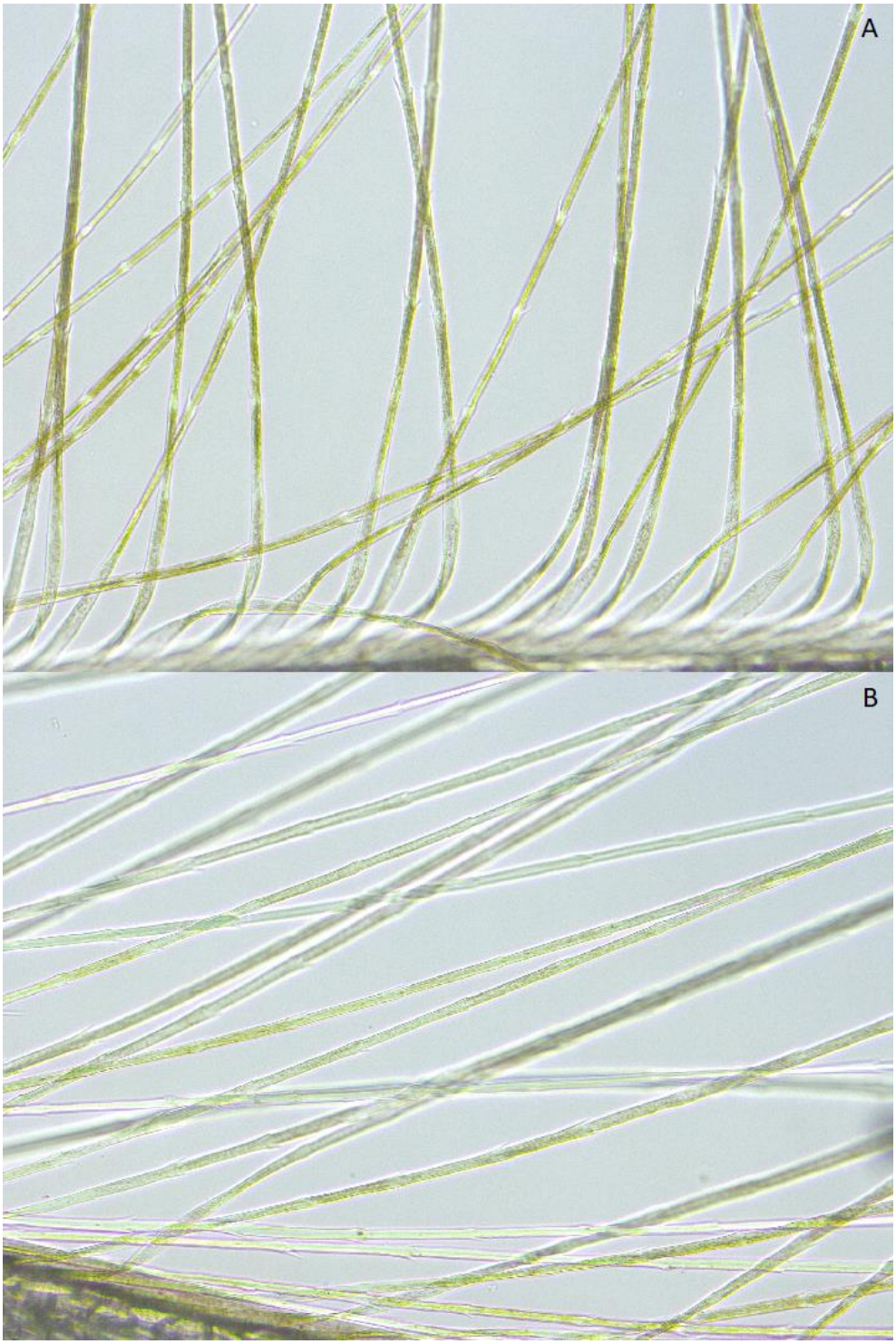

Figure 23: Comparison of basal barbule region of Bald Eagle (*Haliaetus leucocephalus*) (A) and Golden Eagle (*Aquila chrysaetos*) (B). Photomicrographs taken at 400x. Bald Eagle has visually darker internodal pigment in barbules located at the base of the barb in the feather type examined in this study (Photo by Charles Coddington).

Falcons (*Falco, Caracara*)

Peregrine Falcon (*Falco peregrinus*) (Figure 24A) – Nodal pigmentation is oval in shape and heavily concentrated and dark (intensity: 4) at nodes of barbules throughout the barb, and often extends slightly into the internode region. Internodal pigment of barbules is light and spotted at the base (intensity: 4) of the barb but lightens near the mid (intensity: 3) and distal (intensity: 3) regions of the barb. Pigment is evenly distributed at nodes throughout the barbule in all sections of barbs. Spines at nodes are not present in this species.

American Kestrel (*Falco sparverius*) (Figure 24B) – Nodal pigment of barbules is oval in shape and is heavy, dark (intensity: 4) and evenly distributed throughout barbs and barbules. Nodal pigment is well contained along the barbule and does not extend into the internode. Spines at nodes are not present in this species.

Crested Caracara (*Caracara cheriway*) (Figure 24C) – Nodal pigment is oval in shape and is heavy, dark (intensity: 4) and well contained within the node on barbules at the base of the barb. Nodal pigment is absent on barbules of the mid region of the barb, but is present again on distal (medium, intensity: 4) barbules of the barb where pigment extends into the internode (medium; intensity: 3). Internodal pigment of barbules is typically absent in the basal and mid regions of the barb. Spines at nodes are not present in this species.

Parakeet

Monk Parakeet (*Myiopsitta monachus*) (Figure 24D) – Nodal pigment of barbules is oval in shape and is medium in abundance, dark (intensity: 4), and evenly distributed throughout the barbule and barb. Internodal pigment of barbules is absent in the basal and mid regions of the barb but becomes light and spotted (intensity: 3) on barbules of the distal region of the barb. Spines at nodes are not present in this species.

Caracara cheriway is distinguishable from other Falconiformes species examined in this study by having long barbules in all regions of barbs. *Myiopsitta monachus* has significantly wider nodes at the basal and mid barbules of barbs than the *Falco* species studied but otherwise overall microstructure characters are very similar to the *Falco* species. *Falco sparverius* and *Falco peregrinus* are distinguishable with a multitude of microscopic characters. *F. sparverius* has significantly longer barbules, higher average nodal abundance, and higher average nodal width than *F. peregrinus.* The pigmentation pattern of all Falconiformes/Psittaciformes species studied were very different from each other (Figure 15). *F. sparverius* has the most well contained nodal pigment with no observable internodal pigment. The nodal pigment of barbules of *F. peregrinus* are messy in appearance overall and often has pigment granules extending into the internode area just below nodes. *C. cheriway* and *M. monachus* have very similar nodal pigment patterns to each other that appear well contained at barbules nodes at the base of the barb but extend to the internode section of barbules at the distal end of the barb creating a spotted

appearance. *C. cheriway* lacks pigment in the mid region of the barb where *M. monachus* had well contained nodal pigment in barbules of the mid region of the barb.

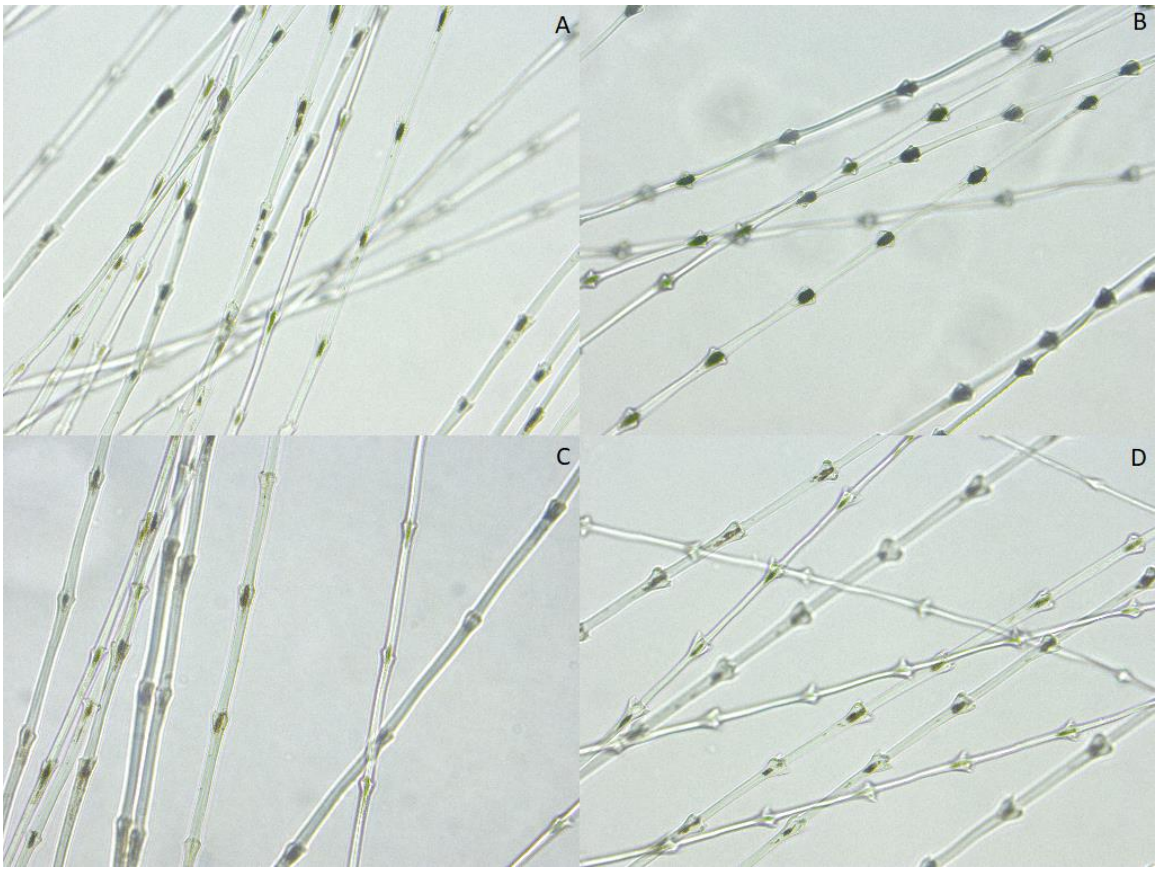

Figure 24: Pigment patterns of barbules at distal portions of barbs: Peregrine Falcon (*Falco peregrinus*) (A), American Kestrel (*Falco sparverius*) (B), Crested Caracara (*Caracara cheriway*) (C), and Monk Parakeet (*Myiopsitta monachus*) (D). Photos taken at 400x (Photo by Charles Coddington).

Discussion

This study of feather microstructure of Accipitriformes, Falconiformes and Psittaciformes is the first to examine in-depth variation of these minute characters among these groups of birds. Information regarding the use of plumulaceous feather characters for taxonomic identification of some Accipitriformes and Falconiformes examined in this study shows that distinctions may be determined between genera and some species at levels of specificity that was not previously described or well-known. Although there is overlap in the measurements of the microscopic characters of many of these species, combining measurements with qualitative assessment of pigment and spine morphology on barbules may allow for generic and even species designation within a limited set of genera.

The most important measurements for distinguishing the Accipitriformes taxa studied here were average number of nodes/barbule, basal, mid and distal barbule lengths, and the internodal distance and nodal abundance on the basal barbule. The Falconiformes taxa studied here were most easily distinguished by nodal abundance on mid and distal barbules, length of the mid and distal barbules, and nodal width of the basal and mid barbules.

A. cooperii and *A. striatus* did not have enough significant differences in microscopic measurements to be distinguished, but they were distinguishable based on internodal pigment intensity. Although some of the quantitative measurements showed significance differences in the means in some of the genera, because a specific feather type was selected for study, these results only reflect a very narrow subset of potential microscopic characters. Species level identifications based on microscopic characters

remains challenging and is an unrealistic goal in most identification cases that lack other supporting evidence.

This study did not attempt to suggest taxonomic hierarchies between species based on microscopic characters, but it is interesting to note that the differences in microscopic characters at the family level agreed with basic taxonomic placement within the order Accipitriformes (Hackett et al. 2008; Jarvis et al. 2014; Prum et al. 2015). This study described definitive familial differences between the plumulaceous microscopic characters of upper-left breast feathers in Cathartidae, Accipitridae, Pandionidae, Falconidae and Psittacidae. In most cases, plumulaceous characters were not useful for species-level identifications within the same genera in this study. However, *F. sparverius* and *F. peregrinus* were distinguishable microscopically in this study of upper-left breast feathers, based on their different barbule lengths and pigment distribution. The high degree of similarity in feather structure between Falconiformes and Psittaciformes studied here shows that feather microstructure in these groups is more similar to each other than to members of Accipitriformes and suggests a close relationship as reported by Hackett et al. (2008), Jarvis et al. (2014), and Prum et al. (2015).

The descriptive results of this study agree with previous basic descriptions of barbule structure and pigmentation of Accipitriformes and Falconiformes by Brom (1991), Shamoun (1994) and Chandler (1916), but provides a much more detailed analysis using a much broader group of species within these orders. Brom (1991) found that *F. peregrinus* had slightly longer barbules than *F. sparverius*. While there was some overlap in the barbule length of the *Falco* species in this study, *F. sparverius* had significantly longer

barbules on average than *F. peregrinus*. This discrepancy is likely due to several factors. Brom (1991) used microslide preparation techniques that did not include xylenes for barbule spreading prior to placing the coverslip on the sample, and it is probable that measurements of dry barbs differed slightly from measurements made on barbs that were mounted using liquid media with a similar refractive index to feathers. Brom (1991) also likely used an ocular micrometer, which is a challenging method of measurement for Accipitriformes and Falconiformes due to long barbules with predisposition to tangling. This problem was avoided in this study by using Leica Application Suite© measurement software to precisely measure barbule length by marking sections all along barbules which allows for accurate measurements despite tangling. It is also possible that discrepancies between the findings of Brom (1991) and this study are explained by differences in barb and barbule region, sample size, and feather type examined. Brom (1991) noted 'rings' at nodes of barbules on falcons which were not found on any of the barbules of species examined in this study.

The microscopic characters examined in this study were mostly useful in distinguishing family level differences of the species examined in this study. Many of these characters were based on those used by Dove (1997, 2000) and Heacker-Skeans (2002), and should continue to be used for plumulaceous microstructure studies, but variations of those characters were also tailored for this study and some characters were not useful for analysis in the Accipitriformes. For example, spine definition in this study differed from Dove (1997), and pigment descriptions in this study were made from qualitative observations of the entire group rather than measurements. According to statistical

analysis, average number of nodes/barbule and basal, mid and distal barbule lengths were the strongest characters found for separating these groups at the family and genus level. The basal barbule length and internodal distance of the basal barbule proved to be the most useful measurement when attempting to distinguish between species in the same genera but overlapping meristic values prohibit use of this technique alone for species identifications. This study was the first to use Leica Application Suite© measurement software to precisely measure plumulaceous feather characters in a taxonomic analysis. Future studies should use this precise measurement method rather than an ocular micrometer to achieve the most accurate measurements possible. Nodal pigment shape of all Falconiformes/Psittaciformes species studied here appeared to vary among species based on observable size, and future studies should consider following Dove's (1997, 2000) methods of measuring the length and width of the nodal pigment to further define the differences and similarities of falcons and parrots. In addition, the width of the internode was not measured in this study as it initially appeared to be insignificant in Accipitriformes, but *F. sparverius* appeared to have a much smaller internodal width than other members of Falconiformes and could potentially be a useful in future studies to distinguish these orders.

Only two species of each genera that occur in the United States were selected for this initial detailed study to keep the project manageable and predict differences in characters within these bird groups. Previous studies of the taxonomic implications of plumulaceous characters within a single order (Dove 1997, Dove 2000, Heacker-Skeans 2002) were unable to differentiate between species within the same genera based on

plumulaceous character measurements alone so a subset of taxa was used here. Because subtle differences in pigmentation were observed in Falconiformes, future studies of this group should include all *Falco* species to investigate whether other North American members of *Falco* overlap with species not included in this study. Accipitriformes and Falconiformes are relatively small clades of birds, and future phylogenetic analyses using plumulaceous feather characters including a representation of all species in these clades may refine the systematic application of these characters to morphological analysis and forensic identification of these bird species.

Overall, the combined quantitative and qualitative differences of these downy structures are very useful in identifying higher taxonomic levels, such as order (Accipitriformes, Falconiformes) and family (Accipitridae, Cathartidae, Pandionidae). This study agreed with previous plumulaceous feather structure studies (Chandler 1916, Brom 1991, Shamoun 1994, Dove 1997, Dove 2000, Heacker-Skeans 2002) in suggesting that these microscopic characters can be used to distinguish different avian taxonomic groups. However, feather characters often vary by feather type, barb location on the feather and barbule location on the barb (Gilroy 1987). It is very important to understand the variation among and within different groups of birds, and to use a multitude of distinguishing characters, in combination with all circumstantial evidence available to make accurate identifications rather than depending on certain diagnostic characters in isolation. It is also important to have a general idea of the type of feather being examined when attempting identifications based on plumulaceous barbules because variation in the plumulaceous microstructures within feather types (e.g. wing, breast, tail) of an individual

bird is known (Gilroy 1987). Thoroughly exploring the plumulaceous microstructure of other orders of birds is key in expanding our knowledge of the extent of the taxonomic implications of these morphological features. This study of plumulaceous microstructure of Accipitriformes and Falconiformes will enhance the knowledge available to those using the practical applications of forensic feather identification and provide a base for future study of these characters in other orders of birds.

CHAPTER TWO - SPECTROPHOTOMETRY

Introduction

Plumulaceous microscopic characters carry valid taxonomic implications that are applicable toward identification of higher-level groupings within Accipitriformes. However, these characters are rarely useful for distinguishing between congeneric species (Chapter 1). The fragmentary remains from birdstrikes and other identification-based studies may contain non-diagnostic pennaceous feathers that lack the diagnostic plumulaceous feather types studied in Chapter 1. Regardless, accurate identifications of species from fragmentary remains are still important in cases of birdstrikes to properly implement effective wildlife management strategies on airfields and reduce risks and damaging costs (Dove 2000). Flight and body feathers can be used to identify birdstrike remains when a nearly complete feather is available, but accurate identification is challenging with partial feather fragments (Dove et al. 2008). Therefore, it is important to explore new analytical methods as they become available to enhance feather identification techniques.

Spectrophotometry has recently been applied to bird studies (Hill et al. 2002; Quesada and Senar 2006; Delhey et al. 2010, Thomas et al. 2014) to quantitatively measure color variation and the wavelengths of light that are absorbed by bird plumages. Reflectance at the peak of the spectrum directly correlates to the brightness or intensity of

color displayed by bird feathers (Endler 1990). Spectrophotometry has mainly been applied to measure colorful carotenoid-based plumages that convey information about individual quality (Endler 1990, Hill et al. 2002, Quesada and Senar 2006, Delhey et al. 2010, Thomas et al. 2014), but has not been explored as a means for use in forensic-types of feather identification.

The majority of pigment in most Accipitriform flight feathers is melanin based, which makes visual comparisons challenging due to similar dark coloration between species. Additionally, barring patterns of Accipitriform flight feathers adds a new challenge as coloration and bar width is similar between congeneric species. Finally, many Accipitriformes exhibit a great deal of geographic variation making visual comparisons challenging. Spectrophotometry has rarely been used to analyze melanin-based pigments due to the tendency of this pigment to produce uniform reflectance profiles that lack the dramatic peaks of carotenoid-based plumage (Hill and McGraw 2006). The use of spectrophotometry for identification of melanin-based plumage has yet to be investigated. Chapter 2 of this thesis explores the use of spectrophotometry to analyze the reflectance profiles of visually similar Accipitriformes congeneric species pairs to determine if spectrophotometry can be a tool to aid in fragmentary feather identification.

Materials and Methods

Species were selected for spectrophotometry analysis based on overall plumage similarity, and because they were determined to have similar plumulaceous microscopic structures. Three species pairs were examined: Black Vulture (*Coragyps atrattus*) and Turkey Vulture (*Cathartes aura*) for degrees of brown and black plumage coloration; Red-tailed (*Buteo jamaicensis*) and Swainson's (*Buteo swainsoni*) hawks because plumage colorations of flight feathers exhibit similar dark and light banding patterns, and the Cooper's (*Accipiter cooperii*) and Sharp-shinned (*Accipiter striatus*)) hawks as their plumage coloration is visually indistinguishable. A minimum of 13 male specimens per species from the continental Unites States were selected for this spectrophotometry analysis in the Division of Birds, National Museum of Natural History, Smithsonian Institution (USNM) (Appendix 4).

Spectrophotometry reflectance spectra were measured with an Ocean Optics© S2000 (Ocean Optics Inc., Florida, USA) spectrophotometer provided by the Smithsonian Institution, with an AIS© Model DT 1000 (Analytical Instrument Systems, Inc. New Jersey, USA) fiber optic halogen light source. Reflectance spectra were quantified as a measurement of reflectance light intensity across the wavelengths of the visible light spectrum (λ/nm) and recorded using Ocean Optics Overture© software (version 1.0.1, 2011). The spectrophotometer probe was affixed inside a black housing box to standardize probe measurements at a 90° from a fixed distance (~1mm) on each feather. Prior to measuring, white and dark standard reflectance spectra measurements were stored by

measuring the intensity of a standard Ocean Optics© white and dark reference spectrum. White and dark reference spectra were recalibrated once per hour to ensure consistency between measurements, and to minimize variation due to the normal intensity drift of the spectrophotometer. Light intensity readings were taken at 3 standardized locations along primary feather 7, and secondary feather 3 of each specimen examined. For all hawk species (*Accipiter* and *Buteo*) examined, two sets of measurements were recorded for each feather: light colored feather bars and dark colored feather bars, for a total of 6 standardized locations along each feather. If the standardized primary 7 or secondary 3 feathers were missing or molting on a specimen, primary 6 or secondary 2 was used instead. Measurements were taken on the leading edge of the feather, where feather coloration is less variable.

Reflectance spectra were compared on reflectance intensity plots over the range of wavelengths of the visual light spectrum (λ/nm) (Figure 25). These plots detail the wavelengths of visible light that are reflected by the surface being measured. Intensity peaks on reflectance intensity plots summarize which color wavelengths are being reflected by the measured surface. Spectrophotometry studies of carotenoid-based plumage generally directly compare the intensity readings of each sample directly to each other (Hill et al. 2002; Quesada and Senar 2006; Delhey et al. 2010). Because the intensity of each reading was so variable with the natural drift of the spectrophotometer, intensity readings had to be adjusted in terms of change in intensity at certain wavelengths in this study. Changes in intensity for each species were calculated in 50nm increments from 200-

850nm. Readings below 200nm were not included because those wavelengths are below the lower limit of the light source and were not stable.

A Principal Component Analysis (PCA) was conducted on the change in intensity to determine if there were significant differences in changes in intensity between visually similar species pairs. The changes in intensity between each pair of species were tested for significance using an analysis of variance (ANOVA) test, with the principal component (PC) variables as the response variables. Measurements with eigenvectors weighting greater than 0.30 (Quinn and Keough 2002) were considered important. P values adjusted using a Holm-Bonferroni stat correction to reduce type 1 error. All statistics were carried out with statistical software package R© (R Foundation for Statistical Computing, Vienna, Austria).

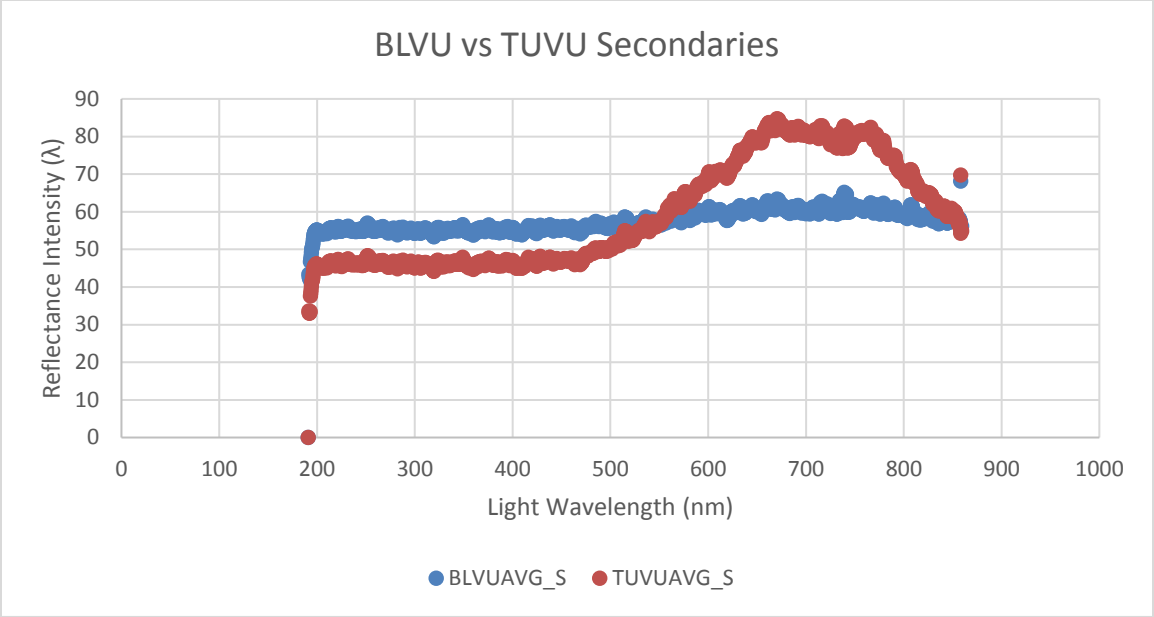

Figure 25: A comparison of average reflectance spectra of Black Vulture (*Coragyps atratus*) (BLVUAVG_S; blue) and Turkey Vulture (*Cathartes aura*) (TUVUAVG_S; red) secondary feathers. This plot details the maximum intensity of light being reflected at certain wavelengths on the visible light spectrum and provides a quantitative measurement of color. Turkey vulture secondary feathers have higher reflectance intensity between 600-800nm than Black Vulture.

Results

Vultures

The PCA for the vulture species studied identified one PC with eigenvalues greater than 1 that accounted for 51.56% of the observed interspecific variation (Table 7). PC1 was positively weighted with changes in the following wavelength ranges: 550-600nm, 750-800nm, 600-650nm, 500-550nm, 450-500nm, 650-700nm, and 300-350nm; and negatively weighted with: 800-850nm, 700-750nm, and 250-300nm. Only Turkey Vulture (*C. aura*) secondary feathers were significantly different from Black Vulture (*C. atratus*) secondary feathers ($P < 0.001$, $F = 86.07$, $DF = 1$) (Table 8; Figure 26) based on their higher reflectance intensity between 600-800nm.

Table 7: Variable loadings onto PC1 for Black and Turkey Vulture feathers, labeled with the eigenvalue and % of variance explained. Loadings are arranged in order of significance for the respective principle component and labeled with PC loading weight in bold.

PC1 – 51.58% Eigenvalue = 2.59
550-600nm = **0.984**
750-800nm = **0.982**
800-850nm = **-0.976**
600-650nm = **0.965**
500-550nm = **0.964**
450-500nm = **0.898**
700-750nm = **-0.774**
650-700nm = **0.481**
300-350nm = **0.363**
250-300nm = **-0.321**

Table 8: Vulture feather spectrophotometry ANOVA Results – P Values mark with * are significant (P < 0.05). P values are adjusted with a Holm-Bonferroni stat correction test.

Comparison	**Adjusted P Value**	**F Value**	**Degrees of Freedom**
Vulture Primaries PC1	0.384	2.442	1
Vulture Secondaries PC1	< 0.001*	86.07	1

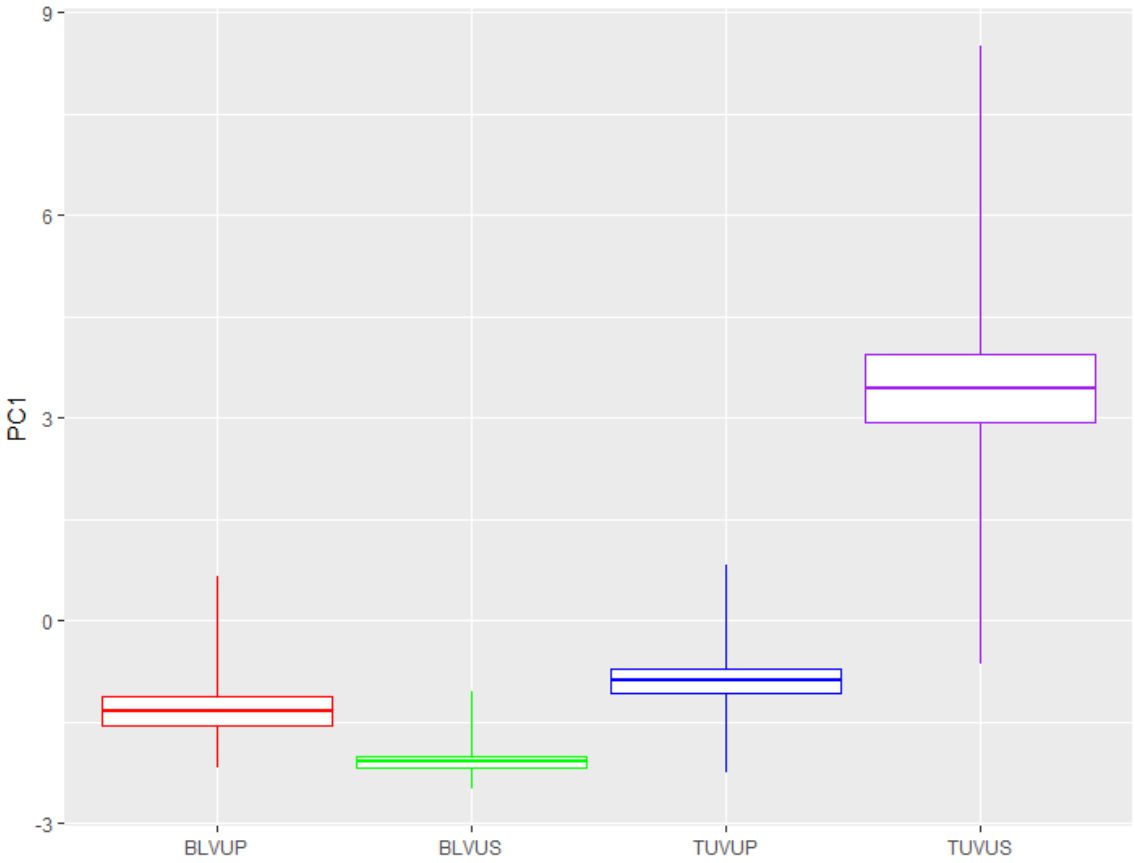

Figure 26: The separation of Black and Turkey Vulture feathers via principal component 1. Boxplots show mean (middle horizontal line), +1 standard error measurement (top horizontal line), -1 standard error measurement (bottom horizonal line), max value (top vertical line), min value (bottom vertical line). Abbreviations are as follows: BLVU = Black Vulture (*Coragyps atratus*), TUVU = Turkey Vulture (*Cathartes aura*), P = Primary feathers, S = Secondary Feathers. PC1 significantly separated the average reflectance profiles of Turkey Vulture and Black Vulture secondary feathers. Overlap is noted in the range of average reflectance profiles.

Buteo Hawks

The spectrophotometry PCA for the *Buteo* species identified one PC with eigenvalues greater than 1 that accounted for 52.79% of the observed interspecific variation (Table 9). PC1 was positively weighted with changes in the following wavelength ranges: 500-550nm, 550-600nm, 600-650nm, and 450-500nm; and negatively weighted with: 750-800nm, 800-850nm, and 700-750nm. Dark primaries ($P < 0.001$, $F = 19.56$, $DF=1$), light primaries ($P < 0.001$, $F = 65.76$, $DF=1$), dark secondaries ($P = 0.001$, $F = 15.26$, $DF=1$), and light secondaries ($P < 0.001$, $F = 71.27$, $DF=1$) were all significantly separated by PC1 (Table 10; Figure 27).

Table 9: Variable loadings onto PC1 for *Buteo* hawk feathers, labeled with the eigenvalue and % of variance explained. Loadings are arranged in order of significance for the respective principle component and labeled with PC loading weight in bold.

PC1 – 52.79% Eigenvalue = 2.61
500-550nm = **0.983**
750-800nm = **-0.980**
550-600nm = **0.970**
800-850nm = **-0.965**
600-650nm = **0.961**
450-500nm = **0.933**
700-750nm = **-0.912**
400-500nm = **0.607**

Table 10: *Buteo* hawk feather spectrophotometry ANOVA Results – P Values mark with * are significant (P < 0.05). P values are adjusted with a Holm-Bonferroni stat correction test.

Comparison	Adjusted P Value	F Value	Degrees of Freedom
Buteo Dark Primaries PC1	< 0.001*	19.56	1
Buteo Light Primaries PC1	< 0.001*	65.76	1
Buteo Dark Secondaries PC1	0.001*	15.26	1
Buteo Light Secondaries PC1	< 0.001*	71.27	1

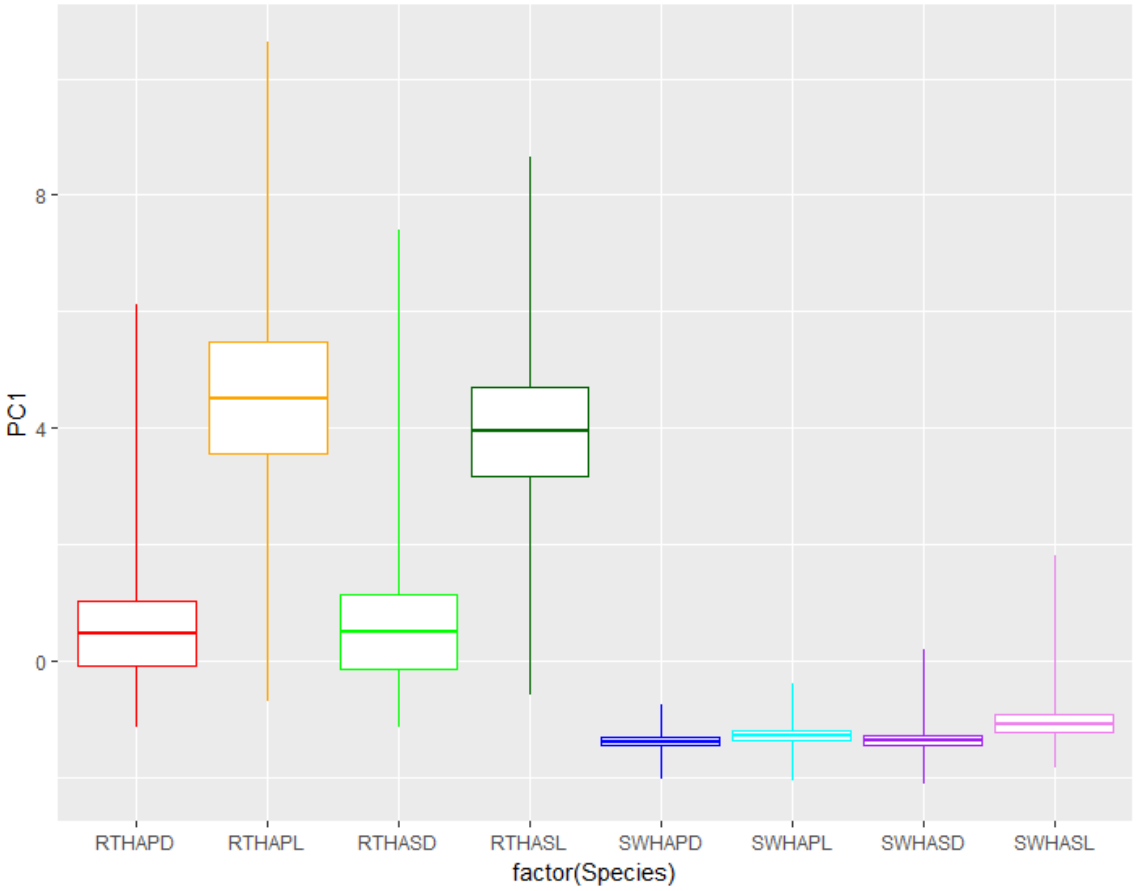

Figure 27: The separation of all *Buteo* hawk feathers studied via principal component 1. Boxplots show mean (middle horizontal line), +1 standard error measurement (top horizontal line), -1 standard error measurement (bottom horizonal line), max value (top vertical line), min value (bottom vertical line). Abbreviations are as follows: RTHA = Red-tailed Hawk (*Buteo jamaicensis*), SWHA = Swainson's Hawk (*Buteo swainsoni*), P = Primary feathers, S = Secondary Feathers, D = Dark, L = Light. PC1 significantly separated the average reflectance profiles of Red-tailed Hawk and Swainson's Hawk for all feathers. Overlap is noted in the range of average reflectance profiles.

Accipiter Hawks

The PCA for the *Accipiter* species identified one PC with eigenvalues greater than 1 that accounted for 59.16% of the observed interspecific variation (Table 11). PC1 was positively weighted with changes in the following wavelength ranges: 500-550nm, 450-500nm, 550-600nm, 600-650nm, and 400-450nm; and negatively weighted with: 750-800nm, 700-750nm, 800-850nm, and 650-700nm. Only the light primary feathers ($P = 0.023$, $F = 7.815$, $DF = 1$) were significantly separated by PC1 in the *Accipiter* hawks (Table 12; Figure 28).

Table 11: Variable loadings onto PC1 for *Accipiter* hawk feathers, labeled with the eigenvalue and % of variance explained. Significant loadings are arranged top to bottom in order of their loading significance and labeled with their PC loading weight in bold.

PC1 – 59.16% **Eigenvalue = 2.77**
500-550nm = **0.991**
750-800nm = **-0.972**
700-750nm = **-0.969**
450-500nm = **0.964**
550-600nm = **0.955**
800-850nm = **-0.916**
600-650nm = **0.894**
400-450nm = **0.836**
650-700nm = **-0.738**

Table 12: *Accipiter* hawk feather spectrophotometry ANOVA Results – P Values mark with * are significant (P < 0.05). P values are adjusted with a Holm-Bonferroni stat correction test.

Comparison	Adjusted P Value	F Value	Degrees of Freedom
Accipiter Dark Primaries PC1	1	0.061	1
Accipiter Light Primaries PC1	0.023*	7.815	1
Accipiter Dark Secondaries PC1	0.999	0.96	1
Accipiter Light Secondaries PC1	0.657	1.553	1

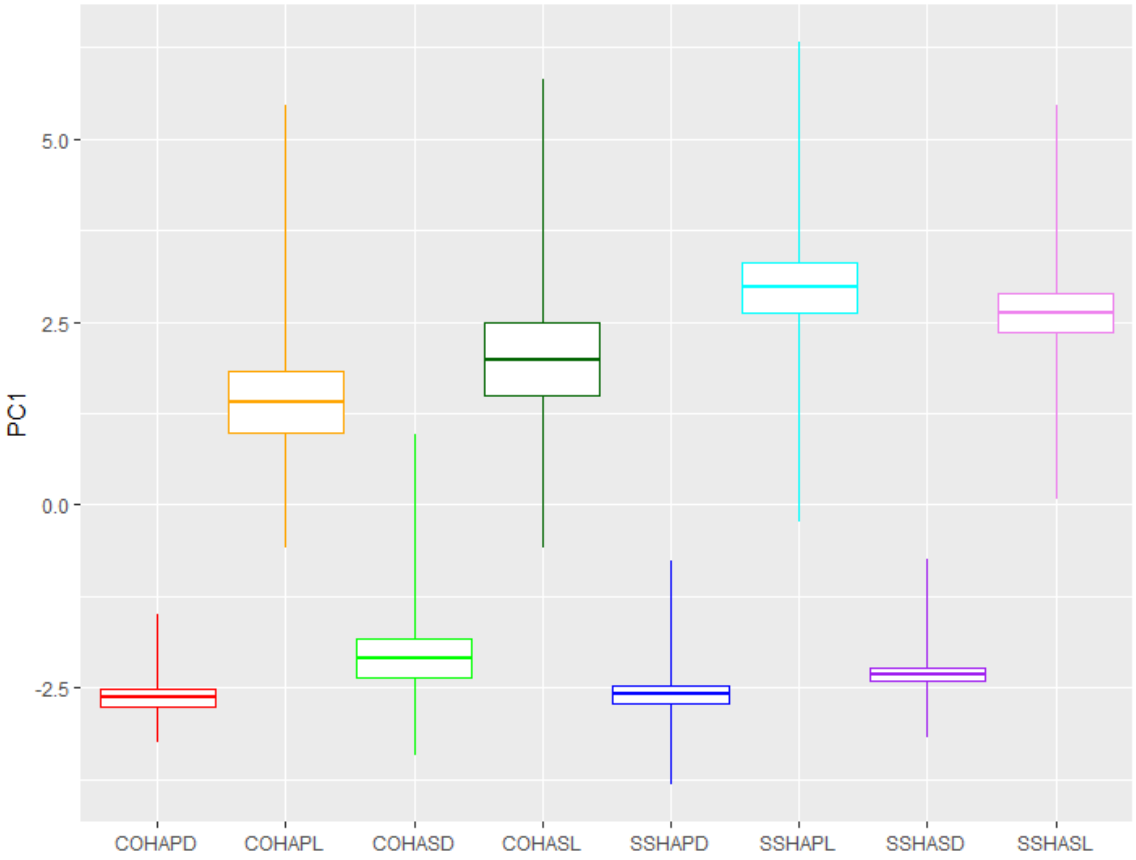

Figure 28: The separation of all *Accipiter* hawk feathers studied via principal component 1. Boxplots show mean (middle horizontal line), +1 standard error measurement (top horizontal line), -1 standard error measurement (bottom horizonal line), max value (top vertical line), min value (bottom vertical line). Abbreviations are as follows: COHA = Cooper's Hawk (*Accipiter cooperii*), SSHA = Sharp-shinned (*Accipiter striatus*), P = Primary feathers, S = Secondary Feathers, D = Dark, L = Light. There was no significant separation of any reflectance profiles for Cooper's Hawk and Sharp-shinned Hawk feathers. Overlap is noted in the range of reflectance profiles.

Discussion

The exploration of spectrophotometry as a technique to quantify differences in visually similar feathers of Accipitriformes examined in this study failed to adequately differentiate subtle colors differences among species. Although the reflectance peaks of Turkey Vulture (*C. aura*) secondary feathers were significantly different from those of Black Vulture (*C. atratus*), this observation is distinguishable visually without the use of spectrophotometry. The primary feathers of Black Vulture and Turkey Vulture are also visually distinguishable based on slight color and texture differences, but these comparisons did not show significantly different reflectance profiles, making the technique unreliable, especially for small fragments.

The *Buteo* hawk feathers were the most visually distinguishable of any species pair studied based on degree of darkness in primaries, and this was shown in reflectance profiles, as all reflectance profiles measured for this pair were significantly different. Only light morphs of *Buteo* hawks were used in this study; the coloration of dark morphs of these two species is very similar and likely isn't distinguishable with spectrophotometry. The *Accipiter* hawk light bands of primary feathers had significantly different reflectance profiles, but no other feather reflectance profiles showed significant differences. This may be due to the huge amount of variation in the coloration of the light primary feathers of the *Accipiter* species studied. While the spectrophotometry results were significant, excessive overlap in reflectance profiles makes it unlikely that these species can be distinguished confidently using this technique. In this study, it was not possible to control for geographic variation between species due to lack of available specimens and so the entire range of

plumage variation in each species was not examined. It is possible however, that there are differences in the reflectance profiles in geographically distinct morphs of a species.

Spectrophotometry has been successfully used to measured melanin levels in humans to detect early indicators of skin cancer (Dwyer et al. 1998). However, the melanin in the flight feathers of the Accipitriformes species studied here is likely too concentrated and produces reflectance profiles that are too flat and uniform to show any significant differences as predicted by Hill and McGraw (2006). The Vulture and *Buteo* hawk species pairs were visually distinguishable, and it is possible this method could confirm their identification in cases where the feather fragments are too small for confident identification. A more thorough study that encompasses the whole extent of plumage variation and geographic variation in these birds is warranted before spectrophotometry can be determined useful for identifications of melanin-based feathers.

The preliminary spectrophotometry methods tested in in this were limited in several ways. The Ocean Optics© S2000 (Ocean Optics Inc., Florida, USA) spectrophotometer and AIS© Model DT 1000 (Analytical Instrument Systems, Inc. New Jersey, USA) light source was somewhat outdated for use in this type of spectrophotometry. The model spectrophotometer used for this study had an expected drift of up to 0.05% max intensity per hour, which could significantly alter the uniform reflectance profiles of melanin-based surfaces. Future studies should use more advanced spectrophotometry technology to reduce the expected drift to 0.01% and yield more conclusive results. Additionally, the light source used for this study slightly deteriorated in intensity over time, making direct comparison of reflectance profiles impossible. This fault was adjusted for in this study by

comparing the change in reflectance at certain wavelengths, rather than directly comparing reflectance intensity. It is recommended to use newer light sources that do not lose intensity over time for future studies so intensity profiles can be directly compared among species. Nevertheless, based on the results of this study, it is unlikely that directly comparing the intensity profiles of plumages of visually similar species will succeed at identification of melanin-based feathers with spectrophotometry.

Overall, this preliminary analysis using a small subset of Accipitriformes revealed that spectrophotometry is likely not useful in identifying species based on melanin-based flight feathers. Because spectrophotometry has been successful in measuring differences in colorful carotenoid-based plumage (Hill et al. 2002; Quesada and Senar 2006; Delhey et al. 2010, Thomas et al. 2014), it may be possible to use this method for identifying species with carotenoid-based plumage. Many Anseriformes and Passeriformes species that are commonly involved in birdstrikes or used on anthropological artifacts have colorful carotenoid-based plumage, and spectrophotometry may be a tool to explore in these circumstances where species are expected to show more dramatic reflectance peaks. This preliminary study focused on a small number of taxa (Appendix 4), and future studies in species identification with spectrophotometry should consider capturing the entire color spectrum of variation within a species before attempting to make identifications with spectrophotometry alone. While this study of the use of spectrophotometry for identification of fragmentary feathers was unsuccessful, it added to the knowledge base of the limitations of this technology and provided a framework for which future studies of spectrophotometry-based feather identification can build upon.

APPENDICIES

Appendix 1: Complete list of specimens examined for the microstructure study (Chapter 1). Specimens are located in the Bird Division in the National Museum of Natural History, Smithsonian Institution (USNM), Washington, DC

Genus	Species	USNM Number	Drawer	Sex	State	Date Collected
Cathartes	aura	342071	K04C-5	Male	Florida	6-Apr-1937
Cathartes	aura	342072	K04C-5	Male	Florida	6-Apr-1937
Cathartes	aura	342073	K04C-5	Male	Florida	1-Apr-1937
Coragyps	atratus	175537	K04B-4	Male	Florida	14-Mar-1895
Coragyps	atratus	152126	K04B-3	Male	Florida	12-Feb-1896
Coragyps	atratus	150071	K04B-3	Male	Florida	13-Mar-1901
Pandion	haliaetus	599194	K07B-1	Male	Maryland	31-Mar-1978
Pandion	haliaetus	599206	K07B-1	Male	Maryland	9-Apr-1978
Pandion	haliaetus	599207	K07B-1	Male	Maryland	1-Apr-1978
Accipiter	cooperii	597044	K14B-1	Male	Maryland	1-Apr-1989
Accipiter	cooperii	600784	K14B-1	Male	Maryland	29-Apr-1998
Accipiter	cooperii	361786	K14B-1	Male	South Carolina	13-Apr-1940
Accipiter	striatus	596532	K15B-1	Male	Maryland	14-Jan-1988
Accipiter	striatus	576684	K15B-2	Male	Virginia	10-Jan-1979
Accipiter	striatus	599468	K15B-1	Male	Virginia	21-Feb-1980
Buteo	jamaicensis	307773	K18B-B	Male	New Jersey	28-Oct-1926
Buteo	jamaicensis	309394	K18B-B	Male	New Jersey	30-Oct-1927
Buteo	jamaicensis	309386	K18B-B	Male	New Jersey	2-Nov-1919
Buteo	swainsoni	597433	K23C-5	Male	Colorado	Fall 1987
Buteo	swainsoni	597434	K23C-6	Male	Colorado	Fall 1987
Buteo	swainsoni	600028	K23C-5	Male	Colorado	Fall 1987
Circus	cyaneus	309311	L15C-3	Male	New Jersey	11-Oct-1924
Circus	cyaneus	309308	L15C-3	Male	New York	22-Oct-1917
Circus	cyaneus	309310	L15C-3	Male	New York	2-Oct-1920
Elanoides	forficatus	176961	K08B-3	Male	Florida	18-Apr-1901
Elanoides	forficatus	293608	K08B-3	Male	Florida	10-Mar-1895
Elanoides	forficatus	414220	K08B-3	Male	Florida	24-Mar-1921
Ictina	mississippiensis	340292	K09C-1	Male	Louisiana	12-Aug-1935
Ictina	mississippiensis	480915	K09C-1	Male	Florida	7-Aug-1925
Ictina	mississippiensis	141087	K09C-1	Male	Oklahoma	5-Aug-1892
Elanus	leucurus	572474	K08A-8	Female	Texas	20-Mar-1986
Elanus	leucurus	532818	K08A-8	Male	Texas	16-Feb-1970
Elanus	leucurus	176881	K08A-8	Female	Florida	15-Apr-1901
Rostrhamus	sociabilis	287881	K10A-2	Male	Florida	11-May-1923
Rostrhamus	sociabilis	287882	K10A-2	Male	Florida	10-May-1923
Rostrhamus	sociabilis	298782	K10A-2	Male	Florida	13-May-1925
Buteogallus	anthracinus	163720	L02A-4	Male	Texas	13-Feb-1898
Buteogallus	anthracinus	588474	L02A-8	Female	Arizona	21-Mar-1933
Buteogallus	anthracinus	126925	L02A-8	Female	Texas	24-Apr-1891
Parabuteo	unicinctus	285800	L01A-8	Male	Texas	4-Feb-1899
Parabuteo	unicinctus	567410	L01A-8	Male	Texas	27-Mar-1970
Parabuteo	unicinctus	588470	L01A-8	Male	Texas	26-Mar-1933
Haliaeetus	leucocephalus	135627	L08C-4	Male	Alaska	10-Jun-1894
Haliaeetus	leucocephalus	151566	L08C-4	Male	Alaska	22-Jun-1895
Haliaeetus	leucocephalus	286534	L08C-5	Male	Alaska	14-May-1920
Aquila	chrysaetos	311742	L05C-4	Male	Virginia	1-Dec-1908
Aquila	chrysaetos	242089	L05C-4	Male	Virginia	28-Oct-1893
Aquila	chrysaetos	310595	L05C-3	Male	New Jersey	28-Sep-1928
Falco	peregrinus	366400	L22B-3	Male	Alaska	20-May-1936
Falco	peregrinus	366407	L22B-3	Male	Alaska	23-Jun-1937
Falco	peregrinus	366399	L22B-3	Male	Alaska	7-Jun-1936
Falco	sparverius	582627	L25C-4	Male	Maryland	8-Jan-1981
Falco	sparverius	598540	L25C-4	Male	Maryland	17-Jan-1968
Falco	sparverius	598536	L25C-4	Male	Maryland	15-Jan-1981
Caracara	cheriway	175542	L19B-2	Male	Florida	18-Mar-1901
Caracara	cheriway	176023	L19B-2	Male	Florida	21-Mar-1895
Caracara	cheriway	176758	L19B-2	Male	Florida	4-Apr-1901
Myiopsitta	monachus	626335	Q01B-11	Female	Florida	12-Apr-2001
Myiopsitta	monachus	622514	Q01B-11	Male	Florida	12-Apr-2001
Myiopsitta	monachus	626336	Q01B-11	Female	Florida	12-Apr-2001

Appendix 2: Summary statistics for all Accipitriformes/Falconiformes/Psittaciformes measurements.

Species	Stat	SPL (µm)	BLB (µm)	BCB (µm)	BIDB (µm)	BIDM (µm)	BIDD (µm)	NAB (µm)	BNWB (µm)	BNWM (µm)	BNWD (µm)	BLM (µm)	BCM (µm)	MIDB (µm)	MIDM (µm)	MIDD (µm)	NAM (µm)	MNWB (µm)	MNWM (µm)	MNWD (µm)	BLD (µm)	BCD (µm)	DIDB (µm)	DIDM (µm)	DIDD (µm)	NAD (µm)	DNWB (µm)	DNWM (µm)	DNWD (µm)	NABL (#/barbule)
TUVU																														
	x̄	4324.3	2491.1	144.8	81.6	95.2	87.7	23.6	6.7	5.8	4.9	2137.4	137.4	78.2	91	80.9	21.8	7.1	6.4	5.5	1476.5	127.1	73.9	79.1	69.6	16.8	6.4	6.4	4.8	10.2
	σ	2515.1	194.2	20	3.4	7.9	9.6	1.7	0.6	1	0.6	315.1	14.6	5.3	8.3	11.6	2.8	0.6	0.8	0.8	345.6	26.4	11.2	15.3	13.4	3.7	0.9	1.1	0.7	0.6
	R	8112.5	754.5	75.8	12.1	30.5	39.7	5	2.2	2.8	2.3	996.3	49.1	18.9	25.5	35.1	9	2.2	3	2.5	929.2	86.8	43.3	61.4	54.1	10	3.1	3.6	2.5	1.7
	CV	0.58	0.08	0.14	0.04	0.08	0.11	0.07	0.1	0.17	0.13	0.15	0.11	0.07	0.09	0.14	0.13	0.09	0.13	0.15	0.23	0.21	0.15	0.19	0.19	0.22	0.14	0.17	0.15	0.06
BLVU																														
	x̄	4136.1	1964.5	132.4	71	78.7	68.1	21.5	6.1	5.1	4.4	1707.2	126.8	69.7	71	59.2	21.3	6.5	5.5	4.9	1420.9	107.9	68.6	63.2	55.1	19.8	6.1	5.5	5.2	12.4
	σ	2762.5	419.7	28.9	7.9	7.8	8.1	3	1	1.2	0.8	281.9	29.3	5.2	7.2	6.2	3.3	1.1	0.6	0.7	187.7	18.5	7	4.8	5.5	1.9	1.4	1	0.7	0.9
	R	9416	1788.8	84.3	24.2	26	21.3	11	3.3	4.6	3.4	943.5	93.2	18.6	25.7	23.1	10	3.5	1.5	2.3	739.2	60.8	26.7	13.1	17.6	6	4.6	3.5	2.2	3.2
	CV	0.67	0.21	0.22	0.11	0.1	0.12	0.14	0.17	0.23	0.19	0.17	0.23	0.08	0.1	0.11	0.15	0.16	0.11	0.14	0.13	0.17	0.1	0.08	0.1	0.1	0.23	0.19	0.14	0.07
OSPR																														
	x̄	3046.7	1150.1	135.4	61.6	62.6	53.2	15.5	5.3	4.9	4.7	972.1	114.9	62.8	59.1	50.2	14.4	5.8	4.9	4.6	768.7	114.3	62	60.6	51.3	12.1	5.5	5.2	4.7	14.9
	σ	1575.5	128.8	22.2	6.5	5.5	6.8	1.4	0.7	0.7	0.8	285.6	16.1	5.7	5.5	5.6	1.1	0.4	0.6	0.8	226.8	20.5	6.5	4.5	6.8	1.3	0.9	0.8	1.1	2.7
	R	5224.1	440.3	78.3	24.5	17.5	22.2	4	2.4	2.5	2.1	1093.7	50	18.2	18.1	16.7	4	1.2	1.9	2.5	840.2	64.4	18	15.8	23.9	4	2.7	2.5	3.5	8.91
	CV	0.52	0.11	0.16	0.1	0.09	0.13	0.09	0.14	0.14	0.14	0.29	0.14	0.09	0.09	0.11	0.08	0.06	0.12	0.17	0.29	0.18	0.11	0.08	0.13	0.11	0.17	0.16	0.23	0.18
COHA																														
	x̄	5555.7	2184.8	128.3	68.7	90.4	74.8	24.3	6.6	5.1	4.1	2042	123.4	66.1	81.4	68.8	24.3	6.84	5.57	4.63	1510.4	133.6	69.7	71.7	61.8	19.5	6.6	5.9	4.2	12
	σ	2399.9	410	24.4	6.2	7.9	14.3	3.1	1.2	1	0.7	357.2	23.5	4.9	11.9	9.7	3.6	0.8	1.2	0.7	254.2	12.4	6.1	7.2	9.8	3	0.8	1.1	0.8	1.1
	R	7021.8	1331.8	92.9	19.5	24.9	54.2	12	3.9	3.3	2.2	1055	70.8	17.6	40	34.4	10	3	3.3	2.3	814.6	42	19.5	20.7	37.2	9	2.5	3.5	2.4	4.3
	CV	0.43	0.19	0.19	0.09	0.09	0.19	0.13	0.18	0.2	0.17	0.17	0.19	0.08	0.15	0.14	0.15	0.12	0.21	0.16	0.17	0.09	0.09	0.1	0.16	0.15	0.11	0.18	0.2	0.1
SSHA																														
	x̄	4266.2	2021.7	137	50.8	58.4	42.1	15.2	6.5	3.5	2.1	1664.7	130.5	50.5	73.5	48.4	20.8	6.9	5.3	3.7	1288.7	134.7	55.5	60.1	57.5	18.8	6.6	5.5	4.7	11.7
	σ	2042.1	679.7	14.6	5.1	38.7	33.3	6.9	0.9	2.5	1.8	486	23.6	5.6	16.3	16.9	3.7	1.1	1.3	1.5	257.1	13.8	7.9	7.1	5.8	3.7	1.1	1.2	1	3.2
	R	5731.8	2246.6	46.1	16.9	107.1	95.6	20	2.8	7.4	4.8	1562.9	69.1	19.7	52.2	66.6	10	3.2	3.5	6	859.3	39.8	26.7	26.6	17.8	11	3.1	3.9	3.3	9
	CV	0.48	0.34	0.11	0.1	0.66	0.79	0.46	0.14	0.73	0.82	0.29	0.18	0.11	0.22	0.35	0.18	0.16	0.24	0.4	0.2	0.1	0.14	0.12	0.1	0.2	0.16	0.22	0.21	0.27
RTHA																														
	x̄	5146.1	2851.1	122.7	72.5	108	95	19.6	7.4	5.3	4	2246.4	112.4	75.1	100.1	77.4	22.3	7.2	5.6	5.2	1745.4	125.9	71.2	77.9	60.7	21	6.6	6.5	5.1	9.5
	σ	3115.8	749.6	25.2	6.9	18	18.2	3.9	1	1.1	1	465.7	16.3	10.3	23	19.6	2.7	0.9	0.8	1.1	316.5	24.7	4.8	15.5	9.8	2	0.7	1.2	0.9	2.1
	R	11030.3	2091.7	63.1	19.8	59.5	59.4	13	3.6	3.3	3.3	1560.9	50.6	29.7	68.8	61.3	8	2.9	3	3.7	933.4	76.8	15.6	53.7	27.2	7	2.2	3.9	3.1	5.6
	CV	0.61	0.26	0.21	0.1	0.17	0.19	0.2	0.14	0.21	0.26	0.21	0.14	0.14	0.23	0.25	0.12	0.12	0.15	0.21	0.18	0.2	0.01	0.2	0.16	0.1	0.1	0.18	0.17	0.22
SWHA																														
	x̄	3690.3	2584.2	128.8	78.2	52.1	37.7	8.1	6.7	1.8	1.3	2656.2	119	73.2	118.1	86.5	21.4	7.7	5.5	4.3	1615.3	122	74.7	80.1	64	19.8	6.8	6.2	5.1	7.2
	σ	1573.2	597.4	15.4	10.2	64.6	56.1	5	0.9	2.4	2.1	349.2	21.7	8	13.5	16	4.4	1	1.3	0.9	148.2	18	6.8	9.6	10.2	2.4	0.6	1.4	1.5	1.2
	R	4975.8	2038.5	55.2	39.1	131.3	122.7	15	2.9	6.3	6.3	1199.1	74.4	26.9	43.6	49.3	13	2.9	4.7	2.6	492.8	48.5	24.9	31	31.3	9	1.8	5.1	5.2	4.1
	CV	0.43	0.23	0.12	0.13	1.2	1.5	0.62	0.13	1.3	1.6	0.13	0.18	0.11	0.11	0.18	0.21	0.13	0.23	0.2	0.1	0.12	0.16	0.12	0.09	0.23	0.29	0.17		
NOHA																														
	x̄	0	3469	118.8	77.6	0	0	4.7	6.5	0	0	2879.7	137.2	75.1	99.9	53	20.3	7.6	4.2	2.43	1849.1	135.2	76	82.1	64.8	21.8	6.1	5.5	4.1	5.8
	σ	0	652.2	18.4	7.3	0	0	1	0.8	0	0	548.9	18	12	38.2	32.4	7.5	1	1.8	1.5	294.3	20.5	11.7	10.6	12.2	2.2	0.5	1.1	1.1	1.3
	R	0	1813.9	60.3	22.6	0	0	3	2.5	0	0	1783.4	62.6	39.6	147	77.8	22	4.4	7.2	3.7	941.1	59.6	44.3	39.1	43.4	7	1.3	3.3	3.6	3.6
	CV	NA	0.19	0.16	0.1	NA	NA	0.21	0.12	NA	NA	0.19	0.13	0.16	0.38	0.61	0.37	0.14	0.44	0.61	0.16	0.15	0.15	0.13	0.19	0.1	0.08	0.2	0.27	0.22
STKI																														
	x̄	4568	1850.3	117.4	69.3	98.7	87.5	17.8	6.3	5.3	4.4	1627.6	119.4	71.9	80.5	59.5	19.9	6.6	5.4	4.6	1305.9	126.5	70.8	69.3	53.9	17.9	5.9	5.6	4.4	11.7
	σ	2099.8	355.9	29.6	10.6	16	18.6	3	0.7	1.3	1.2	168.6	17.8	9	13.5	8.9	3.4	1.1	0.7	0.5	163.5	29.9	6.8	10.3	8	2.4	1	0.9	0.7	1.5
	R	6505.4	1179.2	96.1	37.6	49.7	58.2	11	2.6	3.8	4	513.2	59.7	30.1	52	28.2	10	3.7	2.6	1.7	525.1	91.6	23.8	34.8	24.4	8	3.5	2.8	2.6	4.7
	CV	0.46	0.19	0.25	0.15	0.16	0.21	0.17	0.12	0.24	0.27	0.1	0.15	0.13	0.17	0.15	0.17	0.16	0.14	0.12	0.13	0.24	0.1	0.15	0.15	0.14	0.17	0.16	0.16	0.13
MIKI																														
	x̄	2291.3	2295.1	124.5	61.1	97.8	83.9	22.9	6	4.3	4	17.91.7	125.7	62.7	80.1	64.5	22.7	6.1	4.575	4	1514.5	118.1	68.2	67.7	50.9	21.3	6	4.9	4.5	12.11
	σ	1245.5	441.6	23.16	10.7	19.9	19.8	2.5	1	0.9	1	251.3	28	6.9	13.5	13.8	3	0.9	0.4	0.6	225.4	24.5	7.1	8.9	9.1	2.5	1	0.7	0.6	1.6
	R	4659.3	1368.6	67.6	35.9	66.5	68	7	3.6	3.4	3.5	791.3	81.7	21.6	51.8	50.5	11	2.4	1.5	2.1	639.5	84	27.8	33.1	34.5	7	3.3	2	2.2	5
	CV	0.54	0.19	0.19	0.18	0.2	0.24	0.11	0.16	0.22	0.25	0.14	0.22	0.11	0.17	0.21	0.13	0.14	0.1	0.16	0.15	0.21	0.1	0.13	0.18	0.12	0.17	0.14	0.14	0.13
WTKI																														
	x̄	821.8	2897.4	122.1	65.9	27.2	27.6	14.4	7.1	1.8	1.2	2426.4	128.9	64	82.5	73.9	28.3	7.3	4.9	3.8	1666.9	123.1	67.9	71.8	71.9	21.2	6.2	5.1	4	9.2
	σ	1393.8	432.2	26.6	6.5	40.4	40.9	9.1	0.8	2.7	1.7	414.7	28.1	7.6	11.6	10.6	2.8	0.8	0.81	0.81	236.6	25.5	6.3	6	10.2	3.2	0.5	0.8	0.6	1.7
	R	3847.2	1416.9	99.8	20.9	93.2	88.5	23	2.6	6.2	3.9	1550.8	112.5	24.2	40.1	30.1	9	2.5	2.5	2.6	961.8	77.3	19.2	23.3	40.1	11	1.7	2.7	1.8	5.3
	CV	1.7	0.15	0.22	0.1	1.5	1.5	0.63	0.1	1.5	1.5	0.17	0.22	0.12	0.14	0.14	0.1	0.11	0.17	0.21	0.14	0.21	0.092	0.083	0.14	0.15	0.084	0.16	0.14	0.18
SNKI																														
	x̄	2441	2234.5	97.6	68.1	114.1	100.4	19.3	6.4	4.1	4.1	1823.5	125	69.7	80.8	64.4	22.3	6.3	5.2	4.4	1339.1	122.3	67.7	69.7	57.3	18.2	5.9	5.4	4.4	11.2
	σ	1018.4	415.5	17.4	7.1	13.7	18.3	2.5	0.9	0.7	0.6	347.9	16.8	6.6	11.6	10.1	3.1	0.9	0.9	0.7	168.5	24.3	6.6	10.2	9.3	2.3	1.2	0.7	0.9	1.1
	R	3153.4	1405	48.4	25.9	48.6	57.3	9	2.7	2.2	1.8	1046.7	48.2	23.6	43.4	35	11	2.8	3.2	2.4	438.4	94.8	22.8	30.8	30.5	6	4.1	2.6	3.6	3.4
	CV	0.42	0.19	0.18	0.1	0.12	0.18	0.13	0.13	0.17	0.14	0.19	0.13	0.1	0.14	0.16	0.14	0.14	0.17	0.16	0.13	0.2	0.1	0.15	0.16	0.13	0.2	0.13	0.21	0.1
CBHA																														
	x̄	2712.7	2617.1	133.9	74.7	87.8	59.1	17	8.4	3.9	2.5	2658.4	126.8	78.3	108.8	90.8	25.2	7.5	5.3	4.6	1745.8	132.6	72.1	73.9	55.5	23.3	7.3	6	5.7	9.4
	σ	2270.8	467.7	28.1	12	57.4	54.9	9.3	1.6	2.6	2.3	319	25.9	8.9	20.6	21	3.7	1.5	1.3	1.1	206.3	26.3	7.3	11.2	9.6	3.2	1.2	1.3	1.4	2.2
	R	7232.5	1581.3	99.6	39.5	167.9	140	25	4.1	7.5	5.5	1091.1	70.7	36.8	68.3	58.2	13	5.5	3.8	3.9	728.8	90.8	23	40.9	27.8	10	4	4.6	5	5.7
	CV	0.84	0.18	0.21	0.16	0.65	0.93	0.55	0.19	0.66	0.92	0.12	0.2	0.11	0.19	0.23	0.15	0.19	0.25	0.24	0.12	0.2	0.1	0.15	0.17	0.14	0.17	0.21	0.24	0.23
HRSH																														
	x̄	3234	2652.1	128	60.1	62.2	53.6	15.6	6.7	2.5	1.9	2383	135.3	65.4	100.1	82.8	23.8	7	4.4	3.9	1858.6	128.7	67.4	76.9	67.1	22.7	7	5.5	4.8	9.1
	σ	1702.1	521.4	16.4	9.5	56.3	48.8	8.9	0.9	2.3	1.7	233.1	25.3	7	14.8	13.1	2.3	1.2	0.7	0.5	243.1	26.1	7.8	8.4	9.4	3.4	0.8	0.8	0.9	1.8
	R	4796.3	1686.5	53.4	26.7	132.5	117.1	21	2.9	5.1	3.9	837	89.7	21.2	48.1	43.4	6	4.3	2.2	1.7	973.2	100.8	29.1	24.8	27.9	10	2.3	2.7	2.7	5.2
	CV	0.53	0.2	0.13	0.16	0.9	0.91	0.57	0.14	0.9	0.89	0.1	0.19	0.11	0.15	0.16	0.1	0.17	0.17	0.13	0.13	0.2	0.12	0.11	0.14	0.15	0.11	0.14	0.19	0.2
BAEA																														
	x̄	9473	2380.5	164.1	73.6	84.9	70.3	28.9	7.3	5.5	4.4	2185.5	157	71	77.7	60.5	28.7	6.7	6.4	5.2	1633.8	137.2	72.1	65.3	49.8	23.9	6.4	5.8	4.9	13.2
	σ	2706.2	275	30.9	11.2	16.4	14.6	2.4	1.5	1.1	0.7	194.4	19	7.8	9.7	10	3	0.7	1	0.8	241.4	23.4	6.6	6.8	6.4	3.4	0.9	1	0.9	1
	R	9578	836.1	106.7	47.2	45.5	44.8	7	5.4	3.7	2.3	669.3	64.6	27.8	26.8	34.3	11	2.4	3.8	2.6	790.2	65.6	18.6	22.4	19.1	12	3.4	3.4	3	3.6
	CV	0.29	0.12	0.19	0.15	0.19	0.21	0.09	0.2	0.2	0.16	0.09	0.12	0.11	0.12	0.16	0.1	0.1	0.16	0.16	0.15	0.17	0.1	0.1	0.13	0.14	0.15	0.18	0.19	0.08
GOEA																														
	x̄	11474.8	2795.5	144.9	71.3	90.5	68.2	32.1	7.9	6.3	5.1	2506.9	141.3	75.6	81.9	58.7	33.3	7.7	6.4	5.8	1869.3	136.1	71.2	72.4	60.2	25.8	7.2	5.8	4.9	12.8
	σ	3599.2	591.6	22.3	9.3	15.9	11.7	3.4	1.4	1.4	1.3	298.9	24.2	9.8	9.5	8.2	3.4	1.4	1.1	1	276.3	33.2	4.8	7.9	8	2.2	1.3	1	1.1	1.2
	R	11753.1	1651.6	75.9	26.7	55	38.2	11	4.4	4.3	3.9	941.5	76.9	39.3	29.9	26.2	12	4.2	3.4	3.3	846.8	94.2	16.2	27.8	28.2	7	3.5	3.3	3.4	5
	CV	0.31	0.21	0.15	0.13	0.18	0.17	0.11	0.18	0.22	0.25	0.12	0.17	0.13	0.12	0.14	0.1	0.19	0.18	0.17	0.15	0.24	0.1	0.11	0.13	0.09	0.18	0.17	0.22	0.1
PEFA																														
	x̄	6109	1495.7	138.2	51.2	61.3	52.3	24.7	6.1	4.3	3.5	1316.7	136.3	50.4	56	41.1	24.5	6	4.46	3.56	1117.4	125.6	49.4	52.2	40.3	21.5	6	4.7	3.6	18.1
	σ	1840.9	193.3	24.2	6.8	12.2	8	2.5	0.8	0.7	0.7	130.9	17.5	9.7	8.1	7.1	1.7	1	1	0.6	141.2	25.8	4.9	5.8	3.9	2.1	1.1	0.9	0.7	1.3
	R	5880.4	633.4	78.8	22	42.1	28.1	10	2.8	2.1	2.4	394.6	59	37.4	28.3	24.4	6	3.3	3	1.8	446.7	78.5	15.8	21.3	13.7	7	3.5	3	2.3	4.1
	CV	0.3	0.12	0.18	0.13	0.2	0.15	0.1	0.12	0.16	0.2	0.1	0.13	0.19	0.15	0.17	0.07	0.16	0.21	0.16	0.13	0.21	0.1	0.11	0.1	0.1	0.18	0.18	0.2	0.07
AMKE																														
	x̄	938.7	2594.9	98.7	58.6	68	59	37.3	8.9	7.3	4.6	2040.2	101.2	54	55.2	43.5	36.8	8.4	6.38	4.4	1529.5	103.5	49.5	48.5	38.5	30.9	8.2	6.4	4.3	17
	σ	1456.1	433.7	32.6	6.9	7.3	11.7	6.1	1.3	1.4	0.7	266.4	31.4	6.6	9.2	10.3	3.9	1	0.7	0.8	180.4	22.3	5	5.3	6.6	5.3	1.4	0.9	0.8	1.6
	R	4738.6	1120	124.4	19.6	27.4	38.9	21	4.9	4	2.6	809.2	111.3	21	34.5	38	14	3.3	2	2.9	652	63.3	18.3	17.1	24.1	18	5.1	3	2.5	4.7
	CV	1.6	0.17	0.33	0.12	0.11	0.2	0.16	0.14	0.19	0.16	0.13	0.31	0.12	0.17	0.24	0.11	0.12	0.11	0.19	0.12	0.22	0.1	0.11	0.17	0.17	0.17	0.14	0.18	0.1
CRCA																														
	x̄	1857.5	2774	132.9	67.1	78.2	74.1	38.4	7.8	7.7	5.6	3324.8	117.7	59	67.7	64.8	46.4	8.6	7.4	5.6	1909.9	133.4	51.7	56.6	50.5	32.8	8	6.8	5.4	14.8
	σ	1142.6	739.9	20	9.9	11.2	9.6	11.1	1.3	1.3	1	869.6	20.4	5.9	10.9	7.4	8.5	1.3	1.1	0.9	521.8	24.7	6.7	6.9	7	9.5	1	0.8	1.2	1
	R	3262.6	2293.5	56.7	34.1	38.8	33.3	39	3.5	4.3	2.9	2701.6	66.4	17.8	40.8	25.4	28	4.3	3.1	3.4	19.6.5	82.9	26.2	21.8	23.5	38	3	2.7	3.9	3.2
	CV	0.62	0.27	0.15	0.15	0.14	0.13	0.29	0.17	0.16	0.18	0.26	0.17	0.1	0.16	0.11	0.18	0.15	0.15	0.16	0.27	0.19	0.13	0.12	0.14	0.29	0.13	0.11	0.22	0.07
MOPA																														
	x̄	770.9	1716.4	90.6	55.4	63	61.5	25.8	11.2	10.7	9.2	1898	84.4	54.1	54.9	46.9	33.5	10.6	8.6	6.3	1310.1	84.8	47.6	44.3	35.7	28.9	8.3	6.6	5.3	18
	σ	307.7	254.1	21.8	6.1	9.1	12	3.5	1.3	0.9	1.6	221.7	17.6	6.1	8	7.7	2.2	2	2	1	87.2	19.7	4.9	5.1	4.4	2.7	1.3	1.1	1.3	1.5
	R	1041.7	938.7	68.2	18.7	29.2	40	9	3.8	3.5	4.8	768.6	59.7	19	27.3	28.9	7	7.5	6.1	3.3	318.4	71.7	12.5	16.2	11.8	10	5.2	4.1	4.7	4.7
	CV	0.4	0.15	0.24	0.11	0.14	0.19	0.13	0.11	0.09	0.17	0.12	0.21	0.11	0.15	0.16	0.06	0.19	0.23	0.15	0.07	0.23	0.1	0.12	0.12	0.09	0.16	0.17	0.25	0.09

Appendix 3: Description of pigmentation pattern and intensity of all Accipitriformes, Falconiformes and Psittaciformes species studied in the basal, mid and distal sections of each barb. Amount of pigment was scored as light, medium or heavy. Intensity of pigment was described on a scale of 0-4. Pigment patterns were subjectively described and characterized as stippled, spotted or oval. Presence of spines along the length of each barbule was described on a scale of 0-4 (0= no spines, 1= spines on 0-25% of each barbule, 2= spines on 25-50% of each barbule, 3= spines on 50-75% of each barbule, 4= spines on 75-100% of each barbule). Descriptions of pigment distribution long the barbule are detailed in 'Notes' section.

Species		Basal				Mid				Distal				Notes
		Type	Amount	Intensity	Spines	Type	Amount	Intensity	Spines	Type	Amount	Intensity	Spines	
TUVU	Nodal	Stippled	Light	1	1	Stippled	Medium	1	1	Stippled	Heavy	2	1	Pigment evenly distributed throughout barbule, less concentrated within nodes at the basal and middle barbules. Pigment is 100% evenly distributed and leaks into the nodes at the distal end. Pigment is darker towards distal end of barb.
	Internodal	Stippled	Heavy	1	1	Stippled	Heavy	1	1	Stippled	Heavy	2	1	
BLVU	Nodal	Stippled	Light	1	1	Stippled	Light	1	1	Stippled	Medium	2	1	Evenly distributed throughout barbule, less concentrated within nodes. Pigment darker than TUVU. Pigment more concentrated towards distal end of barb.
	Internodal	Stippled	Heavy	2	1	Stippled	Heavy	3	1	Stippled	Heavy	4	1	
OSPR	Nodal	Stippled	Medium	1	4	Stippled	Medium	1	4	Stippled	Medium	1	4	Light stippled pigment evenly distributed throughout barbule, pigment dissapears towards distal end of barbule, present within node. Pigment evenly concentrated throughout barb.
	Internodal	Stippled	Heavy	1	4	Stippled	Heavy	1	4	Stippled	Heavy	1	4	
COHA	Nodal	Stippled	Light	1	1	Stippled	Light	1	1	Stippled	Light	1	1	Light stippled pigment evenly distributed throughout barbule, present within node. Pigment evenly concentrated throughout barb.
	Internodal	Stippled	Medium	2	1	Stippled	Medium	2	1	Stippled	Light	1	1	
SSHA	Nodal	Stippled	Light	1	1	Stippled	Light	1	1	Stippled	Light	1	1	Dark pigment concentrated in internode, less concentrated within node. Pigment less concentrated in mid region of barb, more concentrated towards basal and distal ends.
	Internodal	Stippled	Heavy	3	1	Stippled	Light	1	1	Stippled	Heavy	2	1	
RTHA	Nodal	Stippled	Medium	2	1	Stippled	Light	1	1	Stippled	Light	1	1	Lightly stippled pigment evenly distributed throughout barbule. Amount and intensity of pigment decreases towards the distal end of the barb.
	Internodal	Stippled	Heavy	2	1	Stippled	Medium	1	1	Stippled	Light	1	1	
SWHA	Nodal	Stippled	Light	2	1	Stippled	Medium	1	1	Stippled	Light	1	1	Lightly stippled pigment evenly distributed throughout barbule. Amount and intensity of pigment decreases towards the distal end of the barb. Pigment is slightly darker than RTHA
	Internodal	Stippled	Heavy	2	1	Stippled	Medium	3	1	Stippled	Light	1	1	
NOHA	Nodal	Stippled	Light	1	1	Stippled	Light	1	1	Stippled	Light	1	1	Light stippled pigment evenly distributed throughout barbule, present within node. Pigment more concentrated towards basal end of barb.
	Internodal	Stippled	Medium	1	1	Stippled	Medium	1	1	Stippled	Light	1	1	
STKI	Nodal	None	None	0	1	None	None	0	1	None	None	0	1	No pigment.
	Internodal	None	None	0	1	None	None	0	1	None	None	0	1	
MIKI	Nodal	Stippled	Light	1	1	Stippled	Light	1	1	Stippled	Light	1	1	Lightly stippled pigment concentrated in the internode. Pigment more concentrated towards the basal end of barbules. Pigment more concentrated towards basal end of barb.
	Internodal	Stippled	Heavy	2	1	Stippled	Heavy	2	1	Stippled	Medium	1	1	
WTKI	Nodal	None	None	0	1	None	None	0	1	None	None	0	1	Pigment scarce and randomly concentrated towards basal end of barbules. Pigment completely absent at mid and distal end of barb.
	Internodal	Spotted	Light	4	1	None	None	0	1	None	None	0	1	
SNKI	Nodal	Stippled	Light	1	1	Stippled	Light	1	1	Stippled	Light	1	1	Strong stippled pigment well contained within internode. Seldom leaks into node, evenly distributed along barb. Stippling becomes denser towards distal end of barb.
	Internodal	Stippled	Heavy	3	1	Stippled	Heavy	3	1	Stippled	Heavy	4	1	
CBHA	Nodal	Stippled	Light	1	1	Stippled	Light	1	1	Stippled	Light	1	1	Dark pigment concentrated in internode, less concentrated within node. Evenly distributed along barb. Pigment sometimes less concentrated toward distal end of barbule.
	Internodal	Stippled	Heavy	3	1	Stippled	Heavy	3	1	Stippled	Heavy	3	1	
HRSH	Nodal	Stippled	Light	1	1	Stippled	Medium	1	1	Stippled	Medium	2	1	Pigment concentrated in internode, less concentrated within node. Pigment mostly evenly concentrated within barb, more concentrated toward distal end of barb.
	Internodal	Stippled	Heavy	2	1	Stippled	Heavy	2	1	Stippled	Heavy	2	1	
BAEA	Nodal	Stippled	Medium	1	2	Stippled	Medium	1	2	Stippled	Medium	1	2	Pigment heavily stippled and evenly dtributed throughout barbules and barb.
	Internodal	Stippled	Heavy	3	2	Stippled	Heavy	2	2	Stippled	Heavy	2	2	
GOEA	Nodal	Stippled	Medium	2	2	Stippled	Medium	2	2	Stippled	Medium	2	2	Pigment lighter than BAEA, pigment evenly distributed throughout barbules and barb.
	Internodal	Stippled	Medium	2	2	Stippled	Medium	2	2	Stippled	Medium	2	2	
PEFA	Nodal	Spotted	Heavy	4	0	Spotted	Heavy	4	0	Spotted	Heavy	4	0	Pigment loosely contained within node, often leakes into internode. Pigment becomes less well contained towards distal end of barb.
	Internodal	Oval	Light	4	0	Oval	Light	3	0	Oval	Light	3	0	
AMKE	Nodal	Oval	Heavy	4	0	Oval	Heavy	4	0	Oval	Heavy	4	0	Pigment well contained within node, rarely leaks into internode.
	Internodal	None	None	0	0	None	None	0	0	None	None	0	0	
CRCA	Nodal	Oval	Medium	4	0	None	None	0	0	Oval	Medium	4	0	Pigment well contained within node at base, rarely leaks into internode. Pigment absent mid barb. Pigment reappears towards distal end, much messier, often leaks into internode
	Internodal	None	None	0	0	None	None	0	0	Spotted	Medium	3	0	
MOPA	Nodal	Oval	Medium	4	0	Oval	Medium	4	0	Oval	Medium	4	0	Pigment well contained within node, rarely leaks into internode. Similar to AMKE but pigment is not as heavy within the node
	Internodal	None	None	0	0	None	None	0	0	Spotted	Light	3	0	

Appendix 4: List of *Buteo* hawk specimens used for the spectrophotometry study (Chapter 2). Specimens are stored in the Bird Division and the National Museum of Natural History, Smithsonian Institution (USNM).

Common Name	Genus	Species	USNM Number	Sex	State	Date Collected
Red-tailed Hawk	Buteo	jamaicensis	309394	M	New Jersey	11/2/1919
Red-tailed Hawk	Buteo	jamaicensis	479256	M	Iowa	11/5/1932
Red-tailed Hawk	Buteo	jamaicensis	253756	M	Maryland	5/25/1917
Red-tailed Hawk	Buteo	jamaicensis	307773	M	New Jersey	10/28/1926
Red-tailed Hawk	Buteo	jamaicensis	270467	M	New Jersey	11/3/1919
Red-tailed Hawk	Buteo	jamaicensis	309386	M	New Jersey	10/30/1927
Red-tailed Hawk	Buteo	jamaicensis	311749	M	New Jersey	10/25/1924
Red-tailed Hawk	Buteo	jamaicensis	121479	M	New Jersey	3/21/1891
Red-tailed Hawk	Buteo	jamaicensis	272295	M	New Jersey	3/29/1919
Red-tailed Hawk	Buteo	jamaicensis	121480	M	Maryland	6/3/1888
Red-tailed Hawk	Buteo	jamaicensis	599470	M	Maryland	7/1/1980
Red-tailed Hawk	Buteo	jamaicensis	588419	M	Maryland	2/21/1947
Red-tailed Hawk	Buteo	jamaicensis	565392	M	Maryland	1/1/1987
Swainson's Hawk	Buteo	swainsoni	155529	M	Oregon	8/7/1896
Swainson's Hawk	Buteo	swainsoni	126053	M	California	NA
Swainson's Hawk	Buteo	swainsoni	169206	M	Iowa	5/1/1899
Swainson's Hawk	Buteo	swainsoni	588450	M	Colorado	5/25/1920
Swainson's Hawk	Buteo	swainsoni	588541	M	Oregon	8/8/1933
Swainson's Hawk	Buteo	swainsoni	89642	M	Oregon	8/30/1882
Swainson's Hawk	Buteo	swainsoni	204415	M	Washington	5/20/1907
Swainson's Hawk	Buteo	swainsoni	89640	M	Oregon	9/2/1882
Swainson's Hawk	Buteo	swainsoni	89645	M	Oregon	8/29/1882
Swainson's Hawk	Buteo	swainsoni	141130	M	Idaho	7/30/1893
Swainson's Hawk	Buteo	swainsoni	419346	M	Idaho	5/20/1951
Swainson's Hawk	Buteo	swainsoni	529602	M	Nebraska	4/26/1938
Swainson's Hawk	Buteo	swainsoni	588449	M	Oklahoma	10/22/1942
Swainson's Hawk	Buteo	swainsoni	258548	M	Arizona	6/30/1914
Swainson's Hawk	Buteo	swainsoni	99243	M	Arizona	5/13/1884
Swainson's Hawk	Buteo	swainsoni	479272	M	Iowa	4/23/1929
Swainson's Hawk	Buteo	swainsoni	84519	M	Utah	6/27/1869
Swainson's Hawk	Buteo	swainsoni	53205	M	Nevada	7/29/1867
Swainson's Hawk	Buteo	swainsoni	644389	M	Utah	2/28/2011
Swainson's Hawk	Buteo	swainsoni	644391	M	Utah	2/28/2011
Swainson's Hawk	Buteo	swainsoni	186736	M	Texas	7/22/1903
Swainson's Hawk	Buteo	swainsoni	163866	M	Colorado	8/11/1891
Swainson's Hawk	Buteo	swainsoni	600028	M	Colorado	9/1/1987
Swainson's Hawk	Buteo	swainsoni	597433	M	Colorado	9/1/1987

Appendix 4 Continued: A complete list of Vulture specimens used for the spectrophotometry study (Chapter 2). Specimens are stored in the Bird Division and the National Museum of Natural History, Smithsonian Institution (USNM).

Common Name	Genus	Species	USNM Number	Sex	State	Date Collected
Black Vulture	Coragyps	atratus	565379	M	Indiana	2/22/1987
Black Vulture	Coragyps	atratus	105459	M	Texas	1/10/1885
Black Vulture	Coragyps	atratus	299197	M	Virginia	1/27/1927
Black Vulture	Coragyps	atratus	362970	M	South Carolina	10/1/1940
Black Vulture	Coragyps	atratus	352246	M	Tennessee	10/12/1937
Black Vulture	Coragyps	atratus	601897	M	Maryland	2/10/1994
Black Vulture	Coragyps	atratus	602360	M	Virginia	7/13/2004
Black Vulture	Coragyps	atratus	152126	M	Florida	2/12/1896
Black Vulture	Coragyps	atratus	339175	M	South Carolina	3/2/1931
Black Vulture	Coragyps	atratus	596234	M	Maryland	11/10/1985
Black Vulture	Coragyps	atratus	150071	M	Florida	3/14/1895
Black Vulture	Coragyps	atratus	379034	M	Georgia	7/26/1939
Black Vulture	Coragyps	atratus	175537	M	Florida	3/13/1903
Black Vulture	Coragyps	atratus	176012	M	Florida	3/16/1895
Turkey Vulture	Cathartes	aura	356695	M	Kentucky	10/12/1938
Turkey Vulture	Cathartes	aura	404779	M	Kansas	9/28/1908
Turkey Vulture	Cathartes	aura	311785	M	Virginia	12/30/1905
Turkey Vulture	Cathartes	aura	212873	M	Virginia	5/19/1919
Turkey Vulture	Cathartes	aura	121455	M	District of Columbia	1/1/1889
Turkey Vulture	Cathartes	aura	176016	M	District of Columbia	12/25/1885
Turkey Vulture	Cathartes	aura	376968	M	Maryland	11/14/1943
Turkey Vulture	Cathartes	aura	414213	M	North Carolina	10/24/1917
Turkey Vulture	Cathartes	aura	312976	M	District of Columbia	9/12/1926
Turkey Vulture	Cathartes	aura	414216	M	Florida	4/20/1940
Turkey Vulture	Cathartes	aura	175274	M	Florida	1/31/1901
Turkey Vulture	Cathartes	aura	596233	M	Maryland	4/3/1981
Turkey Vulture	Cathartes	aura	298587	M	Louisiana	11/14/1925
Turkey Vulture	Cathartes	aura	342072	M	Florida	4/6/1932
Turkey Vulture	Cathartes	aura	365111	M	Florida	4/19/1937
Turkey Vulture	Cathartes	aura	340608	M	Florida	3/18/1937
Turkey Vulture	Cathartes	aura	340607	M	Florida	3/25/1937
Turkey Vulture	Cathartes	aura	342074	M	Florida	3/31/1937
Turkey Vulture	Cathartes	aura	365108	M	Florida	3/25/1937
Turkey Vulture	Cathartes	aura	342073	M	Florida	4/1/1937
Turkey Vulture	Cathartes	aura	342071	M	Florida	4/6/1937

Appendix 4 Concluded: A complete list of *Accipiter* hawk specimens used for the spectrophotometry study (Chapter 2). Specimens are stored in the Bird Division and the National Museum of Natural History, Smithsonian Institution (USNM).

Common Name	Genus	Species	USNM Number	Sex	State	Date Collected
Cooper's Hawk	Accipiter	cooperii	597044	M	Maryland	4/1/1989
Cooper's Hawk	Accipiter	cooperii	600437	M	Maryland	12/8/1992
Cooper's Hawk	Accipiter	cooperii	361786	M	South Carolina	4/13/1940
Cooper's Hawk	Accipiter	cooperii	309321	M	Virginia	12/26/1905
Cooper's Hawk	Accipiter	cooperii	602144	M	South Dakota	5/5/1992
Cooper's Hawk	Accipiter	cooperii	350729	M	Virginia	6/3/1937
Cooper's Hawk	Accipiter	cooperii	168436	M	Texas	7/11/1901
Cooper's Hawk	Accipiter	cooperii	367446	M	Washington	7/13/1942
Cooper's Hawk	Accipiter	cooperii	394601	M	Idaho	7/15/1947
Cooper's Hawk	Accipiter	cooperii	389303	M	Maryland	11/21/1946
Cooper's Hawk	Accipiter	cooperii	602253	M	Virginia	9/22/2004
Cooper's Hawk	Accipiter	cooperii	600784	M	Maryland	4/29/1988
Cooper's Hawk	Accipiter	cooperii	528992	M	California	6/17/1937
Cooper's Hawk	Accipiter	cooperii	313078	M	Maryland	10/5/1929
Cooper's Hawk	Accipiter	cooperii	309323	M	Virginia	7/16/1916
Sharp-shinned Hawk	Accipiter	striatus	596532	M	Maryland	1/14/1988
Sharp-shinned Hawk	Accipiter	striatus	141094	M	California	8/13/1889
Sharp-shinned Hawk	Accipiter	striatus	197926	M	District of Columbia	1/1/1906
Sharp-shinned Hawk	Accipiter	striatus	422113	M	Pennsylvania	10/15/1950
Sharp-shinned Hawk	Accipiter	striatus	358211	M	North Carolina	10/25/1939
Sharp-shinned Hawk	Accipiter	striatus	588406	M	Virginia	3/16/1940
Sharp-shinned Hawk	Accipiter	striatus	462570	M	District of Columbia	12/31/1923
Sharp-shinned Hawk	Accipiter	striatus	573529	M	Maryland	12/29/1971
Sharp-shinned Hawk	Accipiter	striatus	575655	M	Maryland	12/23/1987
Sharp-shinned Hawk	Accipiter	striatus	358212	M	North Carolina	11/1/1939
Sharp-shinned Hawk	Accipiter	striatus	329775	M	Maryland	11/21/1931
Sharp-shinned Hawk	Accipiter	striatus	241036	M	West Virginia	4/15/1893
Sharp-shinned Hawk	Accipiter	striatus	193444	M	New Mexico	10/13/1903
Sharp-shinned Hawk	Accipiter	striatus	599468	M	Virginia	2/21/1980
Sharp-shinned Hawk	Accipiter	striatus	421872	M	Pennsylvania	10/2/1949
Sharp-shinned Hawk	Accipiter	striatus	422114	M	Pennsylvania	10/15/1950
Sharp-shinned Hawk	Accipiter	striatus	120059	M	Maryland	4/13/1891
Sharp-shinned Hawk	Accipiter	striatus	176362	M	Florida	2/4/1896
Sharp-shinned Hawk	Accipiter	striatus	595977	M	Maryland	5/2/1986
Sharp-shinned Hawk	Accipiter	striatus	396896	M	Idaho	5/2/1949
Sharp-shinned Hawk	Accipiter	striatus	176361	M	Maryland	4/20/1889
Sharp-shinned Hawk	Accipiter	striatus	424061	M	California	11/15/1949
Sharp-shinned Hawk	Accipiter	striatus	261988	M	Washington	7/10/1918
Sharp-shinned Hawk	Accipiter	striatus	205613	M	New Mexico	6/22/1909
Sharp-shinned Hawk	Accipiter	striatus	195883	M	California	3/14/1905
Sharp-shinned Hawk	Accipiter	striatus	342104	M	Mississippi	11/5/1939
Sharp-shinned Hawk	Accipiter	striatus	479272	M	Iowa	9/27/1932
Sharp-shinned Hawk	Accipiter	striatus	576684	M	Virginia	1/10/1979
Sharp-shinned Hawk	Accipiter	striatus	599228	M	Maryland	3/17/1977
Sharp-shinned Hawk	Accipiter	striatus	309343	M	New York	11/1/1922

REFERENCES

Boonseub, S., Johnston, G. and Linacre, A., 2012. Identification of protected avian species using a single feather barb. *Journal of forensic sciences*, *57*(6), pp.1574-1577.

Brom, T.G., 1991. *The diagnostic and phylogenetic significance of feather structures* (Doctoral dissertation, University of Amsterdam).

Chandler, A.C., 1916. *A study of the structure of feathers: with reference to their taxonomic significance* (Vol. 13). University of California press.

Davies, A., 1970. Micromorphology of feathers using the scanning electron microscope. *Journal of the Forensic Science Society*, *10*(3), pp.165-174.

Day, M.G., 1966. Identification of hair and feather remains in the gut and faeces of stoats and weasels. *Journal of Zoology*, *148*(2), pp.201-217.

Delhey, K., Roberts, M.L. and Peters, A., 2010. The carotenoid-continuum: carotenoid-based plumage ranges from conspicuous to cryptic and back again. *BMC ecology*, *10*(1), p.13.

De Meo, A.M., 1994. Access to eagles and eagle parts: Environmental protection v. native American free exercise of religion. *Hastings Const. LQ*, *22*, p.771.

Dolbeer R.A., Anderson A.L., Begier M.J. and Weller J.R., 2016. Wildlife strikes to civil aircraft in the United States 1990-2015. U.S. Department of Transportation, Federal Aviation Administration, Office of Airport Safety and Standards, Serial Report No. 14, Washington, DC, USA, 121 pp.

Dove, C.J., 1997. Quantification of microscopic feather characters used in the identification of North American plovers. *Condor*, pp.47-57.

Dove, C.J., 2000. A descriptive and phylogenetic analysis of plumulaceous feather characters in Charadriiformes. *Ornithological Monographs*, pp.1-163.

Dove, C.J. and Agreda, A., 2007. Differences in plumulaceous feather characters of dabbling and diving ducks. *The Condor*, *109*(1), pp.192-199.

Dove, C.J. and Coddington, C.P., 2015. Forensic techniques identify the first record of snowy owl (Bubo scandiacus) feeding on a razorbill (Alca torda). *Wilson Journal of Ornithology*, *127*(3), pp.503-506.

Dove, C.J., Hare, P.G. and Heacker, M., 2005. Identification of ancient feather fragments found in melting alpine ice patches in southern Yukon. *Arctic*, pp.38-43.

Dove, C.J. and Koch, S.L., 2011. Microscopy of feathers: a practical guide for forensic feather identification. *Microscope-Chicago*, *59*(2), p.51.

Dove, C.J. and Peurach, S.C., 2002. Microscopic analysis of feather and hair fragments associated with human mummified remains from Kagamil Island, Alaska. *Ethnographical Series*, 20, pp.51-62.

Dove, C.J., Rotzel, N.C., Heacker, M. and Weigt, L.A., 2008. Using DNA barcodes to identify bird species involved in birdstrikes. *Journal of Wildlife Management*, *72*(5), pp.1231-1236.

Dove, C.J., Snow, R.W., Rochford, M.R. and Mazzotti, F.J., 2011. Birds consumed by the invasive Burmese python (Python molurus bivittatus) in Everglades National Park, Florida, USA. *The Wilson Journal of Ornithology*, *123*(1), pp.126-131.

Dove, C.J. and Wickler, S., 2016. Identification of Bird Species Used to Make a Viking Age Feather Pillow. *ARCTIC*, *69*(1), pp.29-36.

Dwyer, T., Muller, H.K., Blizzard, L., Ashbolt, R. and Phillips, G., 1998. The use of spectrophotometry to estimate melanin density in Caucasians. *Cancer Epidemiology and Prevention Biomarkers*, *7*(3), pp.203-206.

Endler, J.A., 1990. On the measurement and classification of colour in studies of animal colour patterns. *Biological Journal of the Linnean Society*, *41*(4), pp.315-352.

Gilbert, F.F. and Nancekivell, E.G., 1982. Food habits of mink (Mustela vison) and otter (Lutra canadensis) in northeastern Alberta. *Canadian Journal of Zoology*, *60*(6), pp.1282-1288.

Gilroy, B.A. 1987, *Microscopic variation in plumulaceous barbules of the rock dove, Columba livia (Aves: Columbidae)* (Unpublished Master's Thesis, George Mason University)

Griffin, C.R., Baskett, T.S. and Sparrowe, R.D., 1982. *Ecology of bald eagles wintering near a waterfowl concentration* (No. 247). US Fish and Wildlife Service.

Hackett, S.J., Kimball, R.T., Reddy, S., Bowie, R.C., Braun, E.L., Braun, M.J., Chojnowski, J.L., Cox, W.A., Han, K.L., Harshman, J. and Huddleston, C.J., 2008. A phylogenomic study of birds reveals their evolutionary history. *Science*, *320*(5884), pp.1763-1768.

Heacker-Skeans, M.A. 2002, *A quantitative and phylogenetic study of the plumulaceous feather characters of the waterfowl (Aves: Anseriformes)* (Unpublished Master's Thesis, George Mason University)

Hill, G.E. and McGraw, K.J. eds., 2006. *Bird coloration: mechanisms and measurements* (Vol. 1). Harvard University Press.

Hill, G.E., Inouye, C.Y. and Montgomerie, R., 2002. Dietary carotenoids predict plumage coloration in wild house finches. *Proceedings of the Royal Society of London B: Biological Sciences*, *269*(1496), pp.1119-1124.

Jarvis, E.D., Mirarab, S., Aberer, A.J., Li, B., Houde, P., Li, C., Ho, S.Y., Faircloth, B.C., Nabholz, B., Howard, J.T. and Suh, A., 2014. Whole-genome analyses resolve early branches in the tree of life of modern birds. *Science*, *346*(6215), pp.1320-1331.

Laybourne, R.C., 1974. Collision between a vulture and an aircraft at an altitude of 37,000 feet. *The Wilson Bulletin*, *86*(4), pp.461-462.

Laybourne, R.C., Deedrick, D.W. and Hueber, F.M., 1994. Feather in amber is earliest New World fossil of Picidae. *The Wilson Bulletin*, pp.18-25.

Lucas, A.M. & Stettenheim, P.R. 1972, "Avian anatomy: integument. i-ii", *USDA Agr Handb*.

Manville, R.H., 1963. Altitude record for mallard. *The Wilson Bulletin*, *75*(1), p.92.

Messinger, N.G., 1965. Methods used for identification of feather remains from Wetherill Mesa. *Memoirs of the Society for American Archaeology*, pp.206-215.

Olsen, A.R., 1981. Distinguishing common food-contaminating bat hairs from certain feather barbules. *Journal-Association of Official Analytical Chemists*, *64*(4), pp.786-791.

Prum, R.O., Berv, J.S., Dornburg, A., Field, D.J., Townsend, J.P., Lemmon, E.M. and Lemmon, A.R., 2015. A comprehensive phylogeny of birds (Aves) using targeted next-generation DNA sequencing. *Nature*.

Quesada, J. and Senar, J.C., 2006. Comparing plumage colour measurements obtained directly from live birds and from collected feathers: the case of the great tit Parus major. *Journal of Avian Biology*, *37*(6), pp.609-616.

Quinn, G.P. and Keough, M.J., 2002. *Experimental design and data analysis for biologists*. Cambridge University Press.

R Core Team (2018). R: A language and environment for statistical computing. R Foundation for Statistical Computing, Vienna, Austria. URL https://www.R-project.org/.

Robertson, G.R., 2002. Birds of a feather stick: Microscopic feather residues on stone artifacts from Deep Creek Shelter, New South Wales. In *2001 Australian Archaeological Association Annual Conference* (Vol. 7, pp. 175-187). Anthropology Museum, The University of Queensland.

Rogers, J.D., Dove, C.J., Heacker, M. and Graves, G.R., 2002. Identification of feathers in textiles from the Craig Mound at Spiro, Oklahoma. *Southeastern Archaeology*, pp.245-251.

Trail, P.W., 2003. Identification of eagle feathers and feet. *Identification Guides for Wildlife Law Enforcement*, (3).

Sibley, D.A., 2014. The Sibley guide to birds (Second Edition). New York, NY: Alfred A Knopf, pp.120-329.

Sweeney, C.B. 2016, 'The Feather Detective', *Audubon Magazine*, 5 December, pp. 28-31, 50.

Thomas, D.B., McGraw, K.J., Butler, M.W., Carrano, M.T., Madden, O. and James, H.F., 2014. Ancient origins and multiple appearances of carotenoid-pigmented feathers in birds. *Proceedings of the Royal Society of London B: Biological Sciences*, *281*(1788), p.20140806.

Thomas, D.B., Nascimbene, P.C., Dove, C.J., Grimaldi, D.A. and James, H.F., 2014. Seeking carotenoid pigments in amber-preserved fossil feathers. *Scientific reports*, *4*, p.5226.

United States Air Force, 2015. Top 50 USAF Wildlife Strikes by Cost FY1995-FY2014, accessed 3 May 2017. http://www.safety.af.mil/Divisions/Aviation-Safety-Division/BASH

Ward, F.P. and Laybourne, R.C., 1985. A difference in prey selection by adult and immature peregrine falcons during autumn migration. *Conservation studies on raptors. Page Brothers, Norwich, England,* pp.303-309.

BIOGRAPHY

Charles Coddington was born in New York. He graduated from Irvington High School, Irvington, NY in 2009. He received his Bachelor of Arts degree in Biology from Connecticut College, New London, CT in 2013. He has been associated with the Feather Identification Laboratory, Division of Birds, USNM, Smithsonian Institution, Washington, D.C. since September 2014.